Characterization of the RIFIN protein family of the malaria parasite *Plasmodium falciparum* (Welch, 1897)

Dissertation

Submitted in partial fulfilment of the requirements for the doctoral degree

- Dr. rer. nat. -

Department of Biology,

Faculty of Mathematics, Informatics and Natural Sciences

University of Hamburg, Germany

by

Michaela Petter

from Freiburg

Hamburg 2007

Genehmigt vom Department Biologie
der Fakultät für Mathematik, Informatik und Naturwissenschaften
an der Universität Hamburg
auf Antrag von Frau Priv.-Doz. Mo KLINKERT
Weiterer Gutachter der Dissertation:
Frau Professor Dr. I. BRUCHHAUS
Tag der Disputation: 28. September 2007

Hamburg, den 11. September 2007

Professor Dr. Reinhard Lieberei
Leiter des Departments Biologie

TABLE OF CONTENTS

SUMMARY

Plasmodium falciparum, responsible for the most severe form of human malaria, replicates asexually in erythrocytes. The capacity to express and switch antigenically variant proteins on the surface of the host cell allows the parasite to evade host immune responses and contributes to its success in establishing long lasting and relapsing infections. An insight into the physiology of variant antigens may lead to better control measures against severe disease, ideally aiding in the generation of anti-malaria vaccines. The *rif* (repetitive interspersed family) gene family constitutes the largest of these variant antigen families and is encoded by more than 150 gene copies per haploid genome. In this thesis, different aspects of RIFIN biology were investigated.

In the first part, I analyzed membrane association and topology of RIFINs using antisera directed against semiconserved regions of these proteins. Sequential extraction of proteins from infected erythrocytes indicated that RIFINs are membrane-spanning and anchored in a fashion similar to the major virulence protein of *Plasmodium,* PfEMP1. Results from protease protection assays revealed protein anchorage by one transmembrane domain, in contrast to the widely accepted model predicting a two-transmembrane topology. Moreover, with respect to domain exposure there appeared to be two topologically distinct pools of RIFIN proteins.

In view of this variability between RIFIN proteins, I focused on classification and characterization of distinct RIFIN subgroups in the second and third parts of my thesis. Based mainly on the presence or absence of a 25 amino acid peptide, two structurally distinct families were evident. Immunofluorescence analysis of asexual and sexual blood stages showed that members of the larger and more diverse A-type RIFIN family were exported into the host cell and associated with host membranes, while variants of the smaller and more conserved B-type RIFIN subgroup displayed a parasite-restricted pattern. Most probably, this intriguing disparity in sub-compartmentalization reflects differences in protein functions. Importantly, it was demonstrated experimentally for the first time that RIFINs are associated with both the invasive stages and sexual forms of *P. falciparum*, identifying them as multistage antigens, thereby corroborating their biological significance in the parasite.

Since A-type variants were shown to be differentially regulated throughout development, I investigated the upstream non-coding regions of *rif* genes thought to encode regulatory motifs. Phylogenetic analysis led to the definition of five major *rif* gene supgroups, members of which were found to share similar genomic organizations and protein features.

Subclassification in such a way has previously allowed a correlation of PfEMP1 subgroups with disease phenotypes, and may now pave the way for a similar assignment of RIFIN subtypes.

In conclusion, RIFINs were identified as a highly diverse family of structurally distinct members, likely to play different roles in malaria disease. The classification of RIFINs into subgroups now provides a solid foundation for gaining a better understanding of the physiological roles inherent to these variant antigens.

ABBREVIATIONS

Ab	antibody
AMA1	apical membrane protein 1
APS	ammonium persulfate
ATP	adenosinetriphosphate
ATS	acidic terminal segment
bp	base pairs
BSA	bovine serum albumin
CD	cluster of differentiation
cDNA	copy DNA
chr	chromosome
CIDR	cysteine-rich interdomain region
CSA	chondroitin sulfate A
CSS	conservation shifting sites
DAPI	4’,6-Diamidin-2’-phenylindol- dihydrochlorid
DBL	Duffy-binding like
DNA	deoxyribonucleic acid
dNTP	deoxy-nucleotide-triphosphate
DTT	dithiothreitol
EDTA	ethylene diamine tetraacetic acid
EtBr	ethidium bromide
Exp	exported protein
FCS	fetal calf serum
Fig.	figure
g	gravity
gDNA	genomic DNA
GFP	green fluorescent protein
GlcNAc	N-acetyl-D-glucosamine
h	hour
HRP	horseradish peroxidase
HT	host targeting
ICAM-1	intracellular adhesion molecule 1
IE	infected erythrocyte
IFA	immunofluorescence analysis
IEM	immunoelectron microscopy
KAHRP	knob-associated histidine rich protein
kDa	kilodalton
kb	kilobase
l	liter
LB	Luria-Bertani
M	molar
MACS	magnetic activated cell sorting
MC	Maurer’s clefts
min	minute/ minutes
ml	milliliter
mM	millimolar
MP	Maximum Parsimony
MSP	merozoite surface protein

NJ	Neighbor Joining
NTS	N-terminal segment
ORF	open reading frame
PAM	pregnancy associated malaria
PBS	phosphate buffered saline
PCR	polymerase chain reaction
PEXEL/HT	*P. falciparum* export element
PfEMP1	*P. falciparum* erythrocyte membrane protein 1
p.i.	post-invasion
pir	*Plasmodium* interspersed repeats
PP5	protein phosphatase 5
PV	parasitophorous vacuole
PVM	parasitophorous vacuole membrane
RBC	red blood cell
RESA	ring-infected erythrocyte surface antigen
rif	repetitive interspersed family
RNA	ribonucleic acid
RSS	rate shifting sites
RT-PCR	reverse transcriptase PCR
rups	*rif* upstream
s	second
SBP1	skeleton binding protein 1
SDS	sodium dodecyl sulphate
SLO	streptolysin O
stevor	subtelomeric open reading frame
STIC	sexual-stage intraerythrocytic tubular compartment
taq	*Thermophilus aquaticus*
TBS	tris buffered saline
TEMED	N,N,N`,N`-tetramethylethylenediamin
Tris	tris-hydroxymethyl-aminoethane
TSP	thrombospondin
U	unit
UNICEF	United Nations International Children's Emergency Fund
ups	upstream
UTR	untranslated region
UV	ultraviolet
V	volt
vir	*vivax* interspersed repeats
VSA	variant surface antigens
WHO	World Health Organization
X-Gal	5-bromo-4-chloro-3-indolyl-b-D-galactoside
µl	microlitre
µM	micromolar

IUPAC ambiguity code for nucleic acids:

A	Adenine
C	Cytosine
G	Guanine
T	Thymine
U	Uracil
R	puRine (A or G)
Y	pYrimidine (C or T/U)
K	Keto (G or T/U)
M	aMino (A or C)
S	Strong (C or G)
W	Weak (A or T)
B	not A (C or G or T/U)
D	not C (A or G or T/U)
H	not G (A or C or T/U)
V	not T/U (A or C or G)
N	aNy (A or C or G or T/U)

1 INTRODUCTION

1.1 Malaria Disease

Malaria is caused by infection with protozoan parasites of the genus *Plasmodium* and is transmitted by the bite of a female *Anopheles* mosquito. According to the first World Malaria Report released by the WHO and the UNICEF within the frame of the Roll Back Malaria Partnership in the year 2005, presently 3.2 billion people (40 % of the world's population) in 107 countries live at risk of malaria infection. Up to 500 million annual clinical episodes have been recorded, more than 1 million of which take a fatal course. Although globally many tropical and subtropical regions are affected, the greater part of the burden rests on the sub-Saharan African countries, where 80 % of the malaria deaths occur (WHO 2005).

Four species of *Plasmodium* have been described to infect humans: *P. falciparum, P. vivax, P. ovale and P. malariae*. Of these, *P. falciparum* is responsible for most of the malaria associated morbidity and mortality. Although the majority of infections take a mild course associated with fever, headache, muscle pain and other influenza-like symptoms, a substantial number of the patients suffer from complications potentially leading to fatality (WHO 2000). Mainly children under the age of five and pregnant women are affected by severe disease.

In children, the syndrome of severe malaria includes different clinical pictures such as cerebral malaria, severe anaemia, severe respiratory distress, renal failure, hypoglycaemia and pulmonary oedema, appearing alone or in combinations. After repeated infections with *P. falciparum*, individuals in malaria-endemic regions gradually develop semi-immunity, resulting in protection from clinical symptoms in adults (Bull et al. 1998; Marsh et al. 1989). However, women become highly susceptible to the disease again when they get pregnant, especially in first- or second-time pregnancies. Malaria substantially contributes to maternal death, stillbirth and miscarriage, as well as to complications like maternal anaemia and low birth weight babies (Rogerson et al. 2007).

1.2 The Life Cycle of the Malaria Parasite

Plasmodium parasites exhibit a complicated life cycle consisting of a sexual and an asexual phase (Fig. 1). The infection begins with a bite by an infected female *Anopheles* mosquito. Together with the insect's saliva, *Plasmodium* sporozoites are injected into the subcutaneous tissues of the human host. The initial steps during infection have recently been documented impressively in animal models by in vivo imaging techniques using transgenic fluorescent parasites (revied in (Heussler and Doerig 2006)). Upon injection, sporozoites first breach the blood vessels to access the circulation from where they are rapidly transported to the liver (Amino et al. 2006). Here, sporozoites first transmigrate through Kupffer cells and several hepatocytes before they finally infect a hepatocyte and build up a parasitophorous vacuole (PV) (Mota et al. 2002). The developing hepatic schizont differentiates into thousands of merozoites, which travel to the liver sinusoids in vesicles extruding from the infected hepatocyte, called merosomes (Sturm et al. 2006). It is presently unclear how merozoites are finally released from these structures, however once freed into the blood stream they rapidly invade erythrocytes (Sturm and Heussler 2007). Within 48 hours, *P. falciparum* parasites multiply asexually through schizogony, giving rise to a new generation of merozoites. Upon release from the host cell, these initiate repeated cycles of red blood cell (RBC) infection that is responsible for the acute symptoms of the disease.

Occasionally, some of the merozoites invading new RBCs differentiate into sexual forms which are called gametocytes. These are the transmissive stages, which after ingestion by a blood-feeding mosquito develop into female macrogametocytes and male microgametocytes. In the stomach of the insect, male and female gametes form and fuse to build a motile diploid zygote called ookinete. The ookinete penetrates the mosquito midgut wall and differentiates into an oocyst. When mature, this gives rise to a number of sporozoites capable of migrating into the salivary gland (Frischknecht et al. 2004), from which they are discharged into another unfortunate human host during a blood meal.

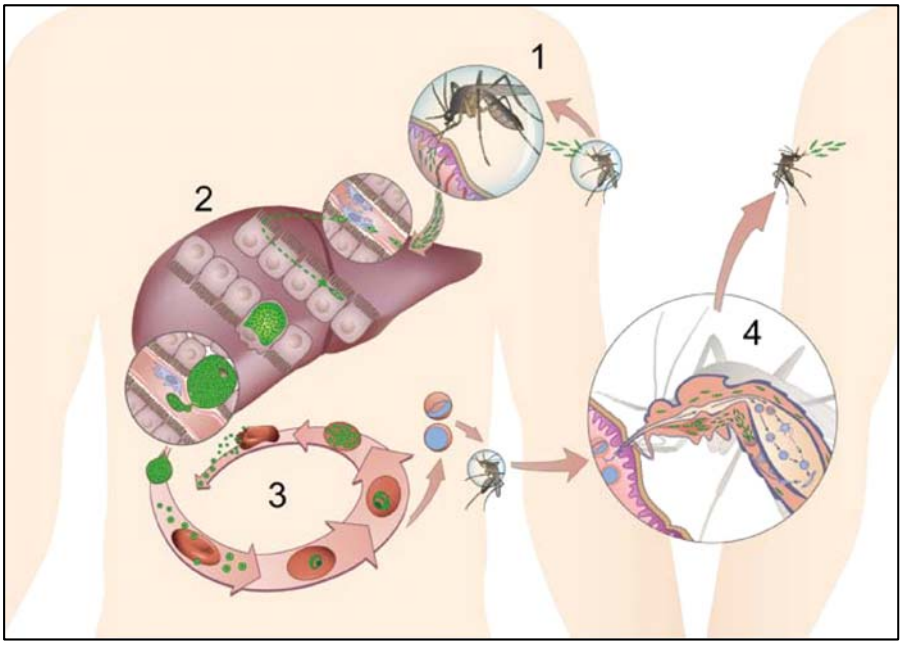

Fig. 1 Life cycle of *Plasmodium* species
1 Inoculation of *Plasmodium* sporozoites during blood meal of an infected *Anopheles* mosquito. **2** Sporozoites reach the liver with the blood stream and glide along sinusoidal endothelia. They transmigrate through Kupffer cells and several hepatocytes before finally developing into liver schizonts within an hepatocyte. Upon merozoite formation, merosomes are extruded into liver sinusoids. **3** Liver-derived merozoites are liberated and infect red blood cells. Repeated infection cycles occur with some parasites developing into gametocytes. **4** Fertilisation in the mosquito gut and development to infective sporozoites in the salivary glands. Picture courtesy of Angelika Sturm

1.3 Physiology of the Blood Stages of *P. falciparum*

Understanding the molecular processes of parasite survival within the human host represents an important step towards developing effective weapons to defeat malaria. The completion of the genomic sequence has opened new routes for the analysis of the molecular biology of *Plasmodium* parasites, unraveling a multitude of potential new drug targets and vaccine candidates (Gardner et al. 2002). Meaningful evaluation of target proteins requires a fundamental comprehension of the physiological and morphological makeup of the different parasite stages in the complex life cycle.

1.3.1 Merozoites

Plasmodium parasites are classified as members of the phylum Apicomplexa because their invasive stages, including merozoites, sporozoites and ookinetes, are hallmarked by a unique collection of organelles found at their anterior end. In merozoites, these include a pair of pear-shaped membrane-bound rhoptries, several smaller micronemes which are attached to the

rhoptry duct, and a number of vesicles described as dense granules that are distributed in the cytoplasm (Fig. 2A, B) (Preiser et al. 2000).

This apical complex plays a pivotal role during host cell invasion during which the contents are sequentially released. The initial contact with a RBC is mediated by merozoite surface proteins (MSPs) covering the membrane of the merozoite as a dense coat (Gaur et al. 2004). The best characterized, MSP-1, undergoes extensive proteolytic processing around the time of merozoite release (McBride and Heidrich 1987). The products, including a 42 kDa GPI-anchored fragment, build a complex together with other MSPs (Heidrich et al. 1983; McBride and Heidrich 1987). Since so far no host receptor for MSP attachment has been identified, the molecular mechanisms of this initial contact still remain unclear.

Rhoptry and microneme proteins are discharged early during invasion and appear to be responsible for several processes, including reorientation, formation of a tight junction, membrane invagination and formation of the PV (Cowman and Crabb 2006; Gaur et al. 2004; Kats et al. 2006; Preiser et al. 2000). Known micronemal proteins implicated in these processes through interaction with host cell receptors and other parasite proteins are the apical membrane antigen 1 (AMA-1) as well as a number of paralogous proteins belonging to the Duffy-binding protein family (EBA-175, EBA-181, EBA-140) (Cowman and Crabb 2006). Several rhoptry proteins, among them PfRh, RhopH and RAP family proteins have also been characterized and some of them, like micronemal proteins, seem to engage erythrocyte surface receptors (Galinski et al. 1992; Rayner et al. 2000). Expressing such a large array of erythrotropic proteins is thought to equip the parasite with the ability to quickly switch the invasion strategy by accommodating to polymorphisms in invasion receptors such as blood group antigens in different host individuals (Cowman and Crabb 2006).

Once the merozoite has entered the host, dense granules move to the pellicle, release their contents into the PV and move into finger-like channels of the parasitophorous vacuolar membrane (PVM) (Torii et al. 1989). Two dense granule proteins have so far been identified to localize to the erythrocyte membrane shortly after invasion (Aikawa et al. 1990; Trager et al. 1992). Recent evidence demonstrates that one of them, the ring infected erythrocyte surface protein (RESA), is responsible for the increased rigidity of the infected erythrocyte (IE) at febrile temperatures by interaction with spectrin at the membrane cytoskeleton, and moreover suppresses further invasion (Foley et al. 1991; Mills et al. 2007; Pei et al. 2007). Dense granule proteins thus appear to be crucial in the early events of installing the parasite in its host cell.

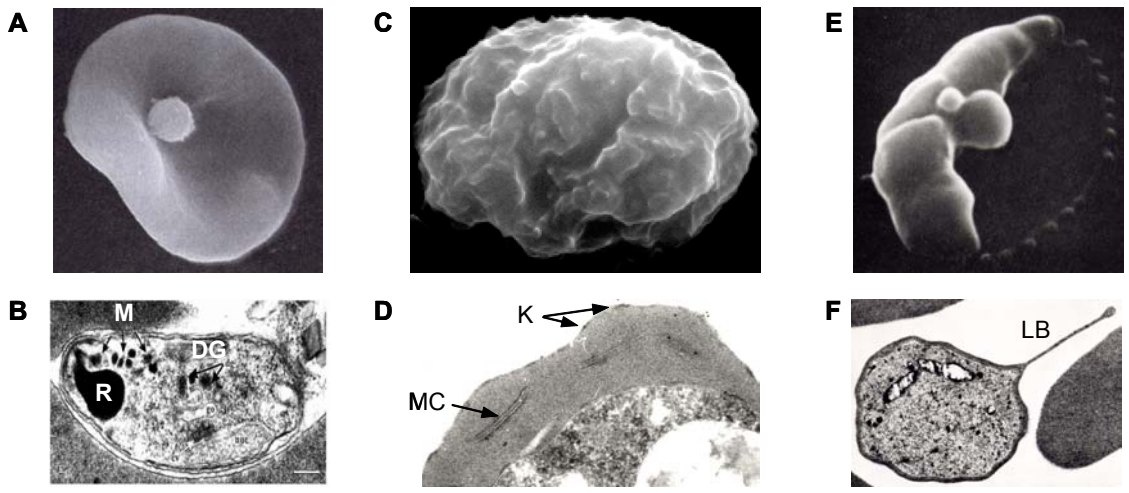

Fig. 2 Electronmicrographs of *P. falciparum* life cycle stages
A: Merozoite invading RBC. **B:** Merozoite. (R) rhoptry, (M) micronemes, (DG) dense granules. **C:** Infected erythrocyte with knobby surface. **D:** Trophozoite infected erythrocyte. (MC) Maurer's clefts, (K) knob. **E:** Gametocyte encolsed in hemoglobin depleted erythrocyte membrane, designated Laveran's bib. **F:** Cross section of gametocyte. (LB) Laveran's bib.

1.3.2 Asexual intra-parasitic stages

After invasion of RBC, the parasite develops within 48 hours from the initial ring stage to a trophozoite and subsequently to the schizont stage, which harbors approximately 16-32 progeny merozoites. During the ring stage, which lasts about 24 hours, the parasite shows no significant change in size or morphology and is still found in the circulation (Bannister et al. 2000; Bannister et al. 2004). The rather inconspicuous ring stage is thought to serve as a lag phase during which host cell modifications are installed that are necessary for the export and surface expression of parasite proteins involved in immune evasion, reshaping the interface between the infected cell and the host (Spielmann et al. 2006). These proteins mediate the possibly most remarkable feature discerning trophozoites and schizonts from the circulating ring stages, namely their ability to sequester in the microvasculature of various organs.

1.3.2.1 Erythrocyte remodelling by malaria parasites

The PVM in which the parasite becomes engulfed during invasion of an erythrocyte originates from the erythrocyte membrane, but is modified by the pathogen (Ward et al. 1993). Major erythrocyte proteins such as band 3, glycophorin A or cytoskeletal proteins are absent from the PVM while detergent resistant membrane raft proteins are recruited to the vacuole (Atkinson et al. 1988; Lauer et al. 2000; Murphy et al. 2004; Nagao et al. 2002). Moreover, parasite proteins such as early transcribed membrane proteins (ETRAMPs) or exported protein 1 and 2 (Exp1 and Exp2) are inserted (Fischer et al. 1998; Gunther et al.

1991; Spielmann et al. 2003). From the PVM, a network of tubular structures designated tubovesicular network extrudes into the erythrocyte cytoplasm (Elmendorf and Haldar 1993; Elmendorf and Haldar 1994). While this network is proposed to serve the parasite for nutrient uptake (Lauer et al. 2000; Lauer et al. 1997), a second system apparent as cisternae-shaped membranous vesicles, called Maurer's clefts (MC) was described to constitute a secretory organelle shuttling proteins from the parasite to the host erythrocyte surface (Fig. 2D) (Haeggstrom et al. 2004; Hinterberg et al. 1994; Wickert et al. 2003; Winter et al. 2005). Whether the two systems are actually constituents of the same or of different membrane assemblies remains controversal (Lanzer et al. 2006; Marti et al. 2005).

There is evidence suggesting that MC are anchored to the host erythrocyte skeleton, since these structures stay associated with the host cell ghost after schizont rupture and merozoite release. One component thought to be mediating this interaction is the *P. falciparum* skeleton binding protein 1 (PfSBP1) binding to the host protein lantibiotic synthetase component C-like protein (LANCL1) (Blisnick et al. 2000; Blisnick et al. 2005). However, IE morphology changed little when PfSBP1 was knocked out, challenging its role as a structural protein. More importantly, the knock-out parasites exhibited a significant constraint in their ability to cytoadhere, identifying PfSBP1 as an important player involved in virulence mechanisms of the malaria parasite (Cooke et al. 2006).

During the second half of intraerythrocytic maturation, hundreds of electron dense cup like structures begin decorating the IE surface (Fig. 2C, D) (Gruenberg et al. 1983). The main proteinaceous component of these so-called knobs is knob-associated histidine-rich protein (KAHRP) which interacts with the host cell cytoskeleton component spectrin (Pei et al. 2005). The knobs represent contact points between the IE and other cells they adhere to (Oh et al. 2000; Rug et al. 2006; Waller et al. 1999; Wickham et al. 2001). Chromosomal truncation or targeted gene deletion of KAHRP leads to knobless parasitized cells and a marked reduction in cytoadherence (Biggs et al. 1989; Crabb et al. 1997; Pologe and Ravetch 1986). Similar results were obtained after targeted deletion of a second major knob component, termed P*lasmodium falciparum* erythrocyte membrane protein 3 (PfEMP3) (Waterkeyn et al. 2000).

1.3.2.2 Signals and mechanisms involved in protein trafficking of surface proteins

Living inside a PV within a metabolically silent cell poses a dilemma to the malaria parasite. It cannot hitchhike on any existing protein transport machinery present in the host cell, as other pathogens do, but needs to install its own trafficking machinery (Haldar et al.

2006). It is known that hydrophobic NH_2-terminal or recessed signal peptides present in many of the proteins encoded in the plasmodial genome can mediate secretion over the parasite membrane into the PV, but the passage of proteins beyond the PVM into the erythrocyte cytoplasm and to the erythrocyte membrane is still ill-defined (Cooke et al. 2004). Recently, two studies have independently reported the presence of a functional motif that is required for the export of proteins across the PVM, designated *Plasmodium* export element (PEXEL) (Marti et al. 2004) or host targeting (HT) signal (Hiller et al. 2004) with the consensus sequence R/KxLxQ/E. The consequently predicted "exportome" embraces both soluble proteins present in the erythrocyte cytosol as well as membrane-bound proteins associated with the MC and the erythrocyte membrane (Marti et al. 2005).

How membrane-associated proteins are transported through the erythrocyte cytoplasm remains controversial. Two major models currently exist. The first proposes lateral diffusion of membrane proteins along a continuous MC network (Wickert et al. 2004; Wickert et al. 2003). The other model favours a vesicular pathway, dividing the intraerythrocytic membrane compartment into functionally distinct modules allowing the assembly, for example, of the cytoadherence complex consisting of PfEMP1 and KAHRP at certain sites (Haeggstrom et al. 2004; Wickham et al. 2001). In support of this, *Plasmodium* homologues of several components of the vesicle-mediated eukaryotic export machinery such as elements of the COPII complex have recently been found in association with the MC, showing parallels between mechanisms involved in protein trafficking between endoplasmic reticulum and Golgi apparatus and trafficking in the erythrocyte cytoplasm (Adisa et al. 2001; Albano et al. 1999), (reviewed in (Lanzer et al. 2006)).

1.3.3 Gametocytes

Gametocytes are responsible for the transmission of the malaria parasite to the mosquito vector and onwards to other human hosts, reflecting their vital importance for the maintenance of the *Plasmodium* population. Gametocytes may be present as male or female parasites, referred to as micro- and macrogametocytes, respectively. All merozoites originating from one schizont develop to gametocytes of the same sex, indicating that commitment already occurs in the developing trophozoite of the preceding generation (Bruce et al. 1990; Silvestrini et al. 2000; Smith et al. 2000b). Gametocytogenesis takes about 10 days in vitro from the invasion of a sexually committed merozoite till the presence of fertilization competent gametocytes (Fivelman et al. 2007).

During their maturation, gametocytes undergo massive ultrastructural changes. Carter and Miller described five major phenotypically distinct stages, but it should be kept in mind that gametocyte differentiation is a continuous process (Carter and Miller 1979). According to this nomenclature, stage I gametocytes have a similar shape as trophozoites and are thus difficult to distinguish, although they display a smoother appearance upon Giemsa staining and the hemozoin crystals are less condensed than in the asexual parasite. In stage II, the parasite becomes slightly elongated in shape, appearing like a drop or a half-moon. In stage III, the haemoglobin from the erythrocyte is almost completely metabolized, leaving the erythrocyte membrane as an empty sheath looking like a distorted, flattened apron extending at one side from the elongated parasite and referred to as "Laveran's bib" (Fig. 2E, F) (Kass et al. 1971). The parasite is now featured by rounded ends, sometimes giving it the appearance of a bowler hat. It continues to grow in length, reaching its maximal size in stage IV, where the parasite exhibits rather pointed ends along a straight axis. In stage V, mature female and male gametocytes can be distinguished. While the cytoplasm of the female macrogametocyte stains blue and hemozoin crystals accumulate in the centre of the now sausage shaped parasite, male microgametocytes appear pink and pigment is rather scattered.

1.4 Immunity and Immune Evasion

Severe malaria is mainly a disease of young children and pregnant women. The protection of elder children and adults in holoendemic areas is commonly understood as the result of slowly acquired immunity, which first shields from susceptibility to severe symptoms, and following continued exposure in time mediates protection from clinical disease (Bruce-Chwatt 1963; McGregor 1974).

Clinical immunity to malaria is developed only after repeated infections, because the parasite has evolved mechanisms to efficiently evade the host immune response. One remarkable strategy is the expression of variable antigens at the surface of the different life cycle stages which are under immune pressure, allowing the pathogen to change its phenotypical appearance. Two mechanisms contribute to antigenic diversity: (1) the presence of polymorphic alleles in the parasite population and (2) the presence of multi-copy gene families encoding variant surface antigens (VSA) (Ferreira et al. 2004). In *P. falciparum*, the three largest multi-copy gene families encode the *var* genes, *stevor* genes (subtelomeric open reading frame) and *rif* genes (repetitive interspersed family) (Gardner et al. 2002), the latter being the subject of this thesis. Gene products of the *var* and *rif* families, termed *Plasmodium*

falciparum erythrocyte membrane protein 1 (PfEMP1) and RIFIN, respectively have been implicated in a second important immune evasion strategy, which is the capacity of asexual parasites to cytoadhere and thereby sequester in the microvasculature of various organs, allowing the parasite to leave the circulation and to avoid immune clearance during passage through the spleen (Chen et al. 2000; Newbold et al. 1999). In the following paragraphs, some immune evasion strategies employed by the different blood stages will be discussed.

1.4.1 Immune evasion strategies of merozoites

Antibodies to several merozoite proteins have been shown to interfere with invasion and to protect from disease, thus making these antigens promising vaccine candidates (Collins et al. 1994; Holder et al. 1999). It is puzzling, though, how the parasite goes through several rounds of reinvasion without being cleared by neutralizing antibodies elicited in preceding infections. One possible mechanism is the extremely short reinvasion time, estimated to be less than 60 seconds (Cowman and Crabb 2006). Another explanation might be that many merozoite proteins such as the MSPs or Duffy-binding proteins exist in several alleles or copies in the genome, showing a certain degree of polymorphism (Holder et al. 1999; Khan et al. 2001). Recently, a multigene family coding for proteins termed SURFINs was discovered and implicated with antigenic variation of *P. falciparum* merozoites. However, the functional relevance of these proteins in merozoites remains elusive (Winter et al. 2005).

1.4.2 Sequestration of trophozoites

P. falciparum is the only human malaria parasite which has the capacity to leave the circulation by adhering to the vascular endothelium or the intervillous space in the placenta (Chen et al. 2000; Newbold et al. 1999). Other cytoadhesive phenomena described for the parasite include the formation of rosettes together with uninfected erythrocytes, or autoagglutination with other parasitized RBCs, bridged by platelets (Carlson et al. 1990; Pain et al. 2001; Roberts et al. 2000; Rowe et al. 1995; Udomsangpetch et al. 1989). It is generally accepted that the main physiological function of sequestration, rosetting and autoagglutination is the avoidance of splenic clearance, although these phenomena also significantly contribute to the pathology of the disease (Bray and Sinden 1979; Fremount and Rossan 1974; Langreth and Peterson 1985; Miller 1969).

Much debate has been spent on the relationship between the binding capacity of an infecting parasite to certain receptors such as CD36, ICAM-1, TSP, P-selectin or CD31 and the development and type of severe disease (Chen et al. 2000; Rasti et al. 2004). In pregnancy

associated malaria (PAM), chondroitin sulfate A (CSA) has been shown to act as the main receptor (Fried et al. 2006; Fried and Duffy 1996), but the exact role of other receptors remains largely controversial (Chen et al. 2000).

As the principle parasite ligand mediating interactions with the host cell tissue, many studies identified PfEMP1 (reviewed in (Sherman et al. 2003)). RIFINs (Fernandez et al. 1999; Helmby et al. 1993) and the giant protein Pf332 (Moll et al. 2007) have also been suggested to be involved in rosette formation. Yet, the exact role of these latter molecules in cytoadherence remains elusive.

1.4.3 Sequestration of gametocytes

Despite their crucial position in the *Plasmodium* life cycle, research on gametocytes is scarce and how these stages evade the immune system, despite being present in the infected human for several days, is unknown. Similar to asexual parasites, immature stage I to IV gametocytes can leave the circulation and sequester at various sites in the human body such as the bone marrow and the spleen (Smalley et al. 1981; Thomson and Robertson 1935). It is unclear how this is achieved, as knob structures associated with cytoadherence of asexual parasites are only present in very young sexual parasites at stages I and II, but absent later during maturation (Day et al. 1998; Sinden 1982). CD36 has been suggested to act as a receptor for adhesion of early gametocytes based on experiments on C32 melanoma cells, and PfEMP1 as well as modified band 3 were independently indicated as ligands on the surface of gametocyte IE (Hayward et al. 1999; Rogers et al. 1996b). However, CD36 dependent cytoadhesion does not continue in later stages. Using stromal bone marrow cells as a model more suitable to reflect the situation in vivo, Rogers and colleagues proposed ICAM-1, CD49c, CD166 and CD164 to serve as gametocyte receptors at stages III and IV, as binding of gametocytes could be inhibited by monoclonal antibodies against these receptors (Rogers et al. 1996a; Rogers et al. 2000). Still, the parasite ligands mediating these interactions are not yet identified.

1.5 Multigene Families and Antigenic Variation

Antigenic variation describes the process of changing the proteins exposed to and recognized by the host immune system, helping the parasite to evade immune clearance and to establish long lasting infections. This is achieved by switching the expression from one multigene family member to another during the course of an infection. Thus, the host is

confronted with an ever-changing opponent, explaining why sterile immunity against malaria is rarely acquired (Dzikowski et al. 2006b). Their significant implication in the successful establishment of long lasting and relapsing infections, accompanied by their contribution to the development of host immunity against malaria has thus made gene products of multigene families important candidate antigens for the development of an anti-malaria vaccine (Bolad and Berzins 2000; Chen 2007; Hviid 2007).

1.5.1 The *var* gene family

The *var* gene family is the best characterized of the *P. falciparum* multigene families and consists of about 60 copies in each parasite genome, each organized in two exons (Baruch et al. 1995; Gardner et al. 2002; Su et al. 1995). The *var* gene products PfEMP1 are about 200 to 350 kDa in size and are displayed in knobs at the surface of the IE (Baruch et al. 1995). The first exon encodes the large and highly diverse extracellular portion of the protein, which is composed of a varying number of domains (Smith et al. 2000a). A short N-terminal segment (NTS) is present in all *var* genes followed by a diverse combination of several Duffy binding like (DBL) domains and cysteine rich interdomain regions (CIDR), which have been implicated in mediating cytoadhesion via host cell receptors. The second exon encodes the conserved acidic terminal segment (ATS) protruding into the erythrocyte cytoplasm.

The majority of the *var* genes is located in subtelomeric regions of the 14 chromosomes, whereas a minority is found in the central regions. Depending on their 5' upstream regions *var* genes have been classified into the groups upsA, upsB, upsC, upsD and upsE as well as into the phylogenetically intermediate groups upsAB and upsBC (Gardner et al. 2002; Kraemer and Smith 2003; Lavstsen et al. 2003; Vazquez-Macias et al. 2002; Voss et al. 2000). UpsA and upsE associated *var* genes are subtelomerically located and are transcribed towards the telomeres, while upsB *var* genes, also mainly subtelomeric, are directed towards the centromere. In contrast, upsC *var* genes are located in central regions of the chromosomes (Gardner et al. 2002; Kraemer and Smith 2003; Lavstsen et al. 2003).

1.5.1.1 Relationship between var gene expression and disease

A number of studies have in the recent years addressed the question whether certain *var* genes are differentially implicated in the severity of disease. The best established correlation between the expression of certain *var* genes and a disease phenotype is known for pregnancy associated malaria. Many studies have independently characterized several DBL3γ domains present in *var* genes, collectively designated *var*PAM, as ligands of CSA in the placenta

(Buffet et al. 1999; Fried and Duffy 2002; Khattab et al. 2003; Khattab et al. 2001; Reeder et al. 1999; Vazquez-Macias et al. 2002). However, recent work has shifted attention to the upsE related *var2CSA* gene as a main player in placental malaria, as it was shown that disruption of this gene leads to the loss of the CSA binding capacity (Viebig et al. 2005), while disruption of the CSA binding *var1CSA* gene did not (Andrews et al. 2003). *Var2CSA*, as well as *var*PAM, are relatively conserved over different strains of *P. falciparum*, reflecting the importance of their functional conservation (Khattab et al. 2003; Salanti et al. 2003).

Other studies have investigated correlations between *var* types and mild or severe disease syndromes (Bull et al. 2005; Jensen et al. 2004; Kaestli et al. 2006; Kyriacou et al. 2006; Rottmann et al. 2006). The classification of different disease syndromes under investigation, the geographic provenance of the patients, as well as the techniques used for analysis of the samples and assignment of *var* gene groups varied significantly between the different studies, making it difficult to draw a general conclusion. However, studies conducted in Africa noted a more or less pronounced association between upsA *var* genes and severe disease (Bull et al. 2005; Jensen et al. 2004; Kyriacou et al. 2006; Rottmann et al. 2006), while one performed in Papua New Guinea found that mainly upsB *var* genes were associated with symptomatic infections (Kaestli et al. 2006). Although not yet comprehensive, these data underline the importance of identifying and characterizing subfamilies within the *P. falciparum* multigene families, in order to gain a better understanding of malaria pathology.

1.5.1.2 Sexual stage specific var gene expression

A recent study addressed *var* gene transcription in gametocytes by performing quantitative real time PCR experiments (Sharp et al. 2006). The peak level of transcription in gametocytes was only 3.8 % of that in asexual ring stage parasites and occurred on day 4 after induction of gametocytogenesis. Certain *var* genes were found to be dominantly expressed in trophozoites but not in gametocytes and vice versa. Independently of the binding phenotype and the *var* gene upregulated in the asexual culture, mainly those classified as type C (Lavstsen et al. 2003) were present after induction of gametocytogenesis.

1.5.2 The *Plasmodium* interspersed repeats families

The *rif* and *stevor* gene families are mainly found in the subtelomeric regions of all 14 *P. falciparum* chromosomes. Here, they are clustered together with the *var* genes and occur either in repeats of several equally orientated genes or are organized in opposing direction (Fig. 3A) (Gardner et al. 2002). The gene products, designated RIFINs and STEVORs, share

a common architecture. They are organized in two exons, the first of which is predicted to code for a signal peptide, while the second represents the main body of the protein, consisting of semiconserved as well as highly variable parts (Cheng et al. 1998; Kyes et al. 1999). Most STEVORs and many RIFINs are predicted to contain two transmembrane domains, which flank the polymorphic middle section and separate it from a semiconserved N-terminal and a short highly charged and highly conserved C-terminal region (Fig. 3B). According to this organization, RIFINs and STEVORs are thought to assume a membrane topology in which the hypervariable region forms a loop exposed at the IE surface, while the semiconserved N- and C-terminal domains point into the erythrocyte lumen (Cheng et al. 1998). However, this model remains to be confirmed experimentally.

Based on their similar organization, RIFINs and STEVORs are postulated to belong to a larger superfamily, extending over species boundaries (Cheng et al. 1998; Janssen et al. 2004). Thus, a superfamily of *Plasmodium* interspersed repeats (*pir*) was defined embracing similarly organized protein families present in many other *Plasmodium* species, for example in *P. vivax* (*vir*), as well as in several rodent and primate malaria parasites (*kir, bir*, *cir*, *yir*). Homology between the different members of this super-family is based on topographic conservation as well as on the presence of several short conserved motifs, indicating a common evolutionary ancestry (Janssen et al. 2004).

Both RIFINs and STEVORs contain a PEXEL/HT motif (Hiller et al. 2004; Marti et al. 2004), which labels them as exported proteins. This characteristic as well as their large number and hypervariability support their suggested role in antigenic variation. In contrast to PfEMP1, the functional relevance of STEVORs and RIFINs is however not well established, and their link to disease is not yet known.

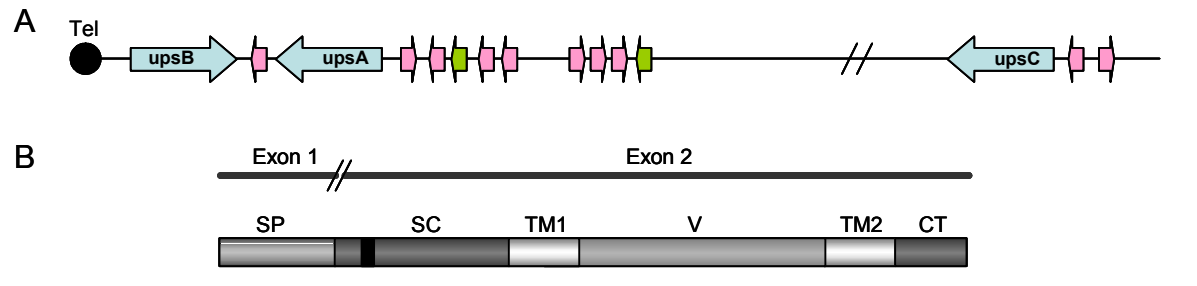

Fig. 3 Organization of *rif* and *stevor* genes and gene products
A: The chromosomal organization of *var* (blue), *rif* (pink) and *stevor* (green) genes in the *P. falciparum* genome is exemplified for chromosome 4. Tel: telomere. Arrows indicate the transcriptional direction. **B:** Gene and protein organization of RIFIN and STEVOR proteins. SP: signal peptide, SC: semiconserved domain, TM: predicted transmembrane domain, V: hypervariable domain, CT: conserved C-terminus.

1.5.2.1 RIFINs

The first report on *rif* genes dates back to the year 1988, when Weber and colleagues identified a repetitive interspersed element in the *P. falciparum* genome, which they first thought to be a transposable element (Weber 1988). Later, elucidation of the genome sequence revealed a total of 149 gene copies in *P. falciparum*, coding for proteins with a predicted molacular weight of 30 to 45 kDa (Gardner et al. 2002). Northern blot analyses showed that *rif* transcription peaks around 18-24 hours post invasion in asexual parasites, coincident with the decrease of *var* gene transcription (Kyes et al. 2000; Kyes et al. 1999). Being similar in size to a previously reported panel of proteins identified in strongly rosetting parasite strains, RIFINs were first referred to as rosettins (Helmby et al. 1993). However, surface trypsinization experiments and the identification of PfEMP1 as the parasite ligand challenged a direct involvement of RIFINs in rosette formation (Fernandez et al. 1999; Kyes et al. 1999; Rowe et al. 1997), although they were reported to be expressed at higher levels on the surface of rosetting parasites than on non-rosetting ones (Fernandez et al. 1999). The same study showed that RIFINs are expressed in an isolate specific fashion and are subject to switches in gene expression. Together with the finding that RIFINs are exported in the same compartment as PfEMP1 proteins, namely the MC (Haeggstrom et al. 2007; Haeggstrom et al. 2004), these data support the proposed role in antigenic variation.

Several studies have documented anti-RIFIN immune responses, showing that anti-RIFIN antibodies are associated with a stable response over time and with rapid clearance of parasites from the circulation (Abdel-Latif et al. 2003; Abdel-Latif et al. 2002). Dissection of the immune response according to IgG subclasses revealed that anti-RIFIN IgG2 antibodies occur predominantly in cerebral malaria patients, indicative of important functions in malaria pathology (Schreiber et al. 2006). Until recently, RIFINs were only considered antigens of asexual blood stage parasites. Several proteomic and transcriptomic studies over the entire *P. falciparum* life cycle have now unexpectedly uncovered highly complex patterns of *rif* gene expression, the majority of peptides and transcripts being detected in merozoites, gametocytes and sporozoites (Florens et al. 2002; Le Roch et al. 2003), thereby opening a completely new perspective for RIFINs as multistage antigens deserving further investigation.

1.6 Aims

Multigene families have been the focus of intense research owing to their fundamental relevance in anti-malaria immunity. Implicated as a vaccine candidate to prevent severe disease phenotypes such as cerebral malaria or placental malaria, PfEMP1 is the most thoroughly investigated parasite molecule amongst the VSAs. In contrast, much less attention has been paid to RIFINs, possibly due to their high copy number and seemingly limitless variability. Some open questions to be resolved as important steps towards elucidating the biological roles of RIFINs in the cell are how these molecules are displayed at the erythrocyte surface and whether subsets of RIFINs are preferentially expressed in certain developmental stages of the *P. falciparum* life cycle. In my thesis, I aimed

(1) to analyze the membrane association and surface topology of RIFINs, in order to understand which purpose the different protein domains might serve,
(2) to characterize two RIFIN subgroups with respect to their developmental expression profile throughout the asexual life cycle of the parasite,
(3) to establish and investigate RIFIN expression during sexual development of *P. falciparum* at the RNA and protein levels in order to evaluate them as candidate proteins involved in immune evasion of gametocytes and
(4) to classify RIFINs into further subgroups based on features in the protein-coding and the non-coding untranslated regions, to allow analysis of subtype specific expression patterns.

2 MATERIALS AND METHODS

2.1 Materials

2.1.1 Chemicals

Accudenz	Accurate Chemicals
Albumax	Gibco BRL Life Technologies
Albumin Bovine Fractin V (BSA)	Serva
Dithiotreitol (DTT)	BIOMOL GmbH
dNTPs	Fermentas
Ficoll-Paque™ PLUS	Amersham Biosciences
Gentamycin	Ratiopharm
Human serum AB^+	PAA
MOWIOL® 4-88	Calbiochem
N-Aceytl-D-Glucosamine	Serva
Ni-NTA Superflow	QIAGEN
Protease Inhibitor Mix HP	Serva
Protein G Sepharose 4 Fast Flow	GE Healthcare
RPMI 1640 powder	Biochrome AG
RPMI 1640 medium	PAA
SeaKem® LE Agarose	Cambrex
Streptolysin O (SLO)	S. Bhakdi (Bhakdi et al. 1985)
Triton® X-100	Serva
5-bromo-4-chloro-3-indolyl-b-D-galactoside (X-Gal)	Appligene Oncor

All chemicals whose supplier is not specified in this section were derived from Sigma-Aldrich Chemie GmbH (Munich, Germany), Carl Roth (Karlsruhe, Germany) or Merck (Darmstadt, Germany).

2.1.2 Kits and Reagents

NucleoSpin® Plasmid	Macherey-Nagel
NucleoSpin® Extract II	Macherey-Nagel
QIAGEN® Plasmid Maxi Kit	QIAGEN
RNeasy® Mini Kit	QIAGEN
QIAamp® DNA Blood Mini Kit	QIAGEN
SuperScript™ First Strand Synthesis System	Invitrogen
TOPO TA Cloning® Kit	Invitrogen
pTrcHis2 TOPO® TA Expression Kit	Invitrogen
Prime-a-Gene® Labeling Kit	Promega

ECL™ Western Blotting Detection Reagent	GE Healthcare
SuperSignal® West Pico chemiluminescent substrate	Pierce
ULTRAHyb™	Ambion
PeqGOLD TriFast™	Peqlab

2.1.3 Miscellaneous

Nitocellulose membrane Optitran BA-S 83	Schleicher & Schüll
Nitrocellulose membrane 0,2µm	Schleicher & Schüll
Hybond™ Nylon membrane	Amersham Bioscience
Whatman® chromatography paper	Whatman
Tissue culture flasks	Greiner
Petri-dishes	Sarstedt
MACS columns CS	Miltenyi Biotec
MicroSpin™ S-300 HR columns	Amersham Bioscience
X-ray film blue sensitive	CEA
Kodak BioMax MR	Sigma-Aldrich

2.1.4 Instruments

Primus PCR machine	MWG
Personal Cycler PCR machine	Biometra
Eppendorf centrifuge 5415D	Eppendorf
Beckmann JA12 centrifuge	Beckmann
Olympus CX31 microscope	Olympus
Leica DRMB fluorescence microscope	Leica
Mini Protean II gel electrophoresis chamber	Bio-Rad
Vario MACS™	Miltenyi Biotec

2.1.5 Enzymes

T4 DNA ligase	Fermentas
Taq polymerase	Fermentas
RNase-free DNase Set	QIAGEN

2.1.6 Recombinant Proteins

Overview over recombinant proteins used in this study

Name	Tag	Purification Conditions	Gene accession number	Reference
RIF29	N-ter 6x His	Native	AF483817	(Abdel-Latif et al. 2002)
RIF40	N-ter 6x His	Denaturing	AF483820	(Abdel-Latif et al. 2002)
RIF44	N-ter 6x His	Denaturing	AF48381	(Abdel-Latif et al. 2002)
RIF50	C-ter 6x His	native	AF483822	(Abdel-Latif et al. 2002)
RIFΔNC	C-ter 6x His	Native	PFI0050c	(Khattab et al. 2006)
ATS	C-ter 6x His	Native	PFD0625c	unpublished
482-DBLγ	N-ter 6x His	Native	AF334803	(Chia et al. 2005)
Stevor O1	C-ter 6x His	Denaturing	PFA0750w	(Schreiber et al. submitted)

2.1.7 Antibodies

Primary antibodies produced in the laboratory and their working dilutions:

	Western Blot	IFA
rat anti-RIF29	1:2000	1:100
rat anti-RIF40	1:2000	1:100
rat anti-RIF50	1:2000	1:100
rat anti-RIF44	1:2000	1:100
mouse anti-RIFΔNC	1:1000	1:100
mouse anti-ATS	1:333	1:50
rabbit anti-PP5	1:2000	1:100
mouse anti-Stevor O1	1:2000	1:500

Primary antibodies received from others and their working dilutions:

	WB	IFA	
rabbit anti-565 rabbit anti-562	1:500 1:500	1:50 1:50	M. Wahlgren, Karolinska Institutet, Stockholm, Sweden
rabbit anti-Exp1	-	1:50	K. Lingelbach, Universität Marburg
mouse anti-SBP1 N-ter (B28) mouse anti-SBP1 C-ter (BR5)	1:4000 1:4000	1:200 1:200	C. Braun-Breton, Institute Pasteur, Paris, France
rabbit anti-Eba181	-	1:100	T. W. Gilberger, BNI, Hamburg
rabbit anti-RhopH2 mouse anti-$MSP1_{42}$ mAb1E1	- 1:2000	1:100 1:200	A. A. Holder, National Institute of Medical Research, London, UK
mouse anti-AMA1	-	1:100	A. W. Thomas, Primate Biomedical Research Centre, Rijswik, Netherlands
rabbit anti-Pfg27	1:4000	1:200	P. Alano, Istiuto Superiore di Sanita, Rome, Italy
mouse anti-CCP1	-	1:100	G. Pradel, Universität Würzburg
mouse anti-RAP1	-	1:100	A. Saul, National Institute of Health, Rockville, USA

Secondary antibodies and working dilutions:

Molecular Probes	rabbit anti-rat and donkey anti-rat IgG Alexa488 (1:400)
	goat anti-mouse IgG Alexa594 cross adsorbed (1:400)
	goat anti-mouse IgG Alexa594 (1:400)
	goat anti-mouse IgG Alexa488 (1:400)
Dianova	goat anti-rabbit IgG Cy™3
	goat anti-rabbit IgG Cy™2 affinity purified (1:400)
	goat anti-rabbit and goat anti-rat IgG HRP (1:10.000)
Pierce	goat anti-mouse IgG HRP (1:10.000)
Dako Cytomation	rabbit anti-rat IgG (1:200)

Human immune antisera
The serum samples originated from a study performed in 2001-2002 in Thadiaye, Senegal. Ten highly reactive antisera were selected and combined as a positive control for FACS analysis. The samples were provided by the courtesy of P. Deloron, Université Paris Descartes, Paris.

2.1.8 Plasmids and Oligonucleotides

Plasmids: pCR2.1 (Invitrogen)

Oligonucleotides: All oligonucleotides were synthesized by MWG or Operon (QIAGEN) and stored at a concentration of 100 pmol/µl. Working concentrations were 10 pmol/µl. A list of all oligonucleotides used in this study is shown below.

Name	Sequence	Use
RIF-A For	5'- TGTAAAGAWMAATGYGAHAARGA	RT-PCR, Northern Probe
RIF-A Rev	5'- TTCGCAAAYRCAWGTDGGWAT	RT-PCR, Northern Probe
RIF-B For	5'- CGACAARCNTCACAAMGWTT	RT-PCR, Northern Probe
RIF-B Rev	5'- CACYTCCTARHSCAMACCCACA	RT-PCR, Northern Probe
Rif-For	5'-ATGAAARTCCAYTRYTATAAYATATTATTRTTT	RT-PCR
Rif-Rev	5'- YTTYTTACGWCGRTAWCGYAA	RT-PCR
Actin For	5'- GTTGTTGACAACGGATCAGG	RT-PCR
Actin Rev	5'- AACCTCCTATCCAGACTGAG	RT-PCR
RESA For	5'- GTTGTGTTCTAAACGTGGTGTTC	RT-PCR
RESA Rev	5'- CAGCATATGGGTTTACTGGC	RT-PCR
Pfs16 For	5'- TTCTTCGCTTTTGCAAACCTGG	RT-PCR, Northern Probe
Pfs16 Rev	5'- TTTATCATCATCTGCGTTCTTCG	RT-PCR, Northern Probe
PFI0020w For	5'- TTAAGCTTATGAAAATCCATTATACTAATATA TTATTGTTTCCTCTAAAA	RT-PCR
PFD1240w For	5'- TTAAGCTTATGAAAGTCCATTATATTAATATA TTATTGTTTGAGCTTCCA	RT-PCR
PFD1240w/ PFI0020w Rev	5'- TTCCGCGGTTCTTCTAATAATTTGAT	RT-PCR
PFA0740w For	5'- GGCAGCTGCTAAGGAATTTG	RT-PCR
PFA0740w Rev	5'- TATCCGCACACTTCGCACTA	RT-PCR
PFE1630w For	5'- TTAAGCTTATGAAAGTCCACTGCTATAACATA TTATTATTTTCTCTTCTA	RT-PCR
PFE1630w Rev	5'- TTCCGCGGTTGATTTAATAATTTTGT	RT-PCR
PFA0710c For	5'- GGCTATGGCTGAGGCTACTG	RT-PCR
PFA0710c Rev	5'- CTTTCGCGCACAATAATTCA	RT-PCR

2.1.9 DNA and Protein Standards

100 bp DNA Ladder	Roth
1 kb DNA Ladder Gene Ruler™	Fermentas
Roti®Mark prestained protein marker	Roth
Molecular Weight Marker	BioRad

2.1.10 Culture Media and Supplements

LB medium
10 g Tryptone
5 g Yeast extract
10 g NaCl
ad 1 l H_2O, pH 7.0
Sterilize by autoclaving

LB agar for agar plates
10 g Tryptone
5 g Yeast Extract
10 g NaCl
15 g Agar
ad 1 l H_2O, pH 7.0
Sterilize by autoclaving

SOB^{++} medium
20g Tryptone
5g Yeast extract
8.5 mM NaCl
2.5 mM KCl
ad 1 l H_2O, pH 7.0
Sterilize by autoclaving, then add
10 mM $MgCl_2$
10 mM $MgSO_4$

TB buffer
10 mM HEPES pH 6.7
15 mM $CaCl_2$
55 mM $MnCl_2$
250 mM KCl
Sterilize using a 0.22 µm filter

10x Albumax (500 ml, pH 7.2)
5.2 g RPMI-1640 powder
2.98 g HEPES
1.67 g Sodium bicarbonate
1 g Glucose
0.1 g Hypoxanthine
25 g Albumax II
50 µg/ml Gentamycin
Sterilize using 0.22 µm filter

RPMI-1640 complete medium
500 ml RPMI-1640 (PAA)
50 ml 10x Albumax
10 ml Human serum AB+ (PAA)
50 µg/ml Gentamycin
25 mM HEPES pH 7.2

Glycerolyte freezing solution (100 ml)
57 % Glycerol
1.6 g Na-lactate
30 mg KCl
2.5 mM sodium phosphate buffer (pH 6.8)

Thawing solution
12 % and 1.6 % sterile NaCl
Sterilize by autoclaving

Binding medium (500 ml, pH 6.8)
5.2 g RPMI powder
1.44 g Glucose
3.75 g HEPES
2.5 g BSA

2.1.11 Buffers and Solutions

10x PBS
1.37 M NaCl
26.8 mM KCl
80.6 mM Na_2HPO_4
14.7 mM KH_2PO_4
pH 7.4, sterilize by autoclaving

10x TBS
0.5 M Tris-HCl pH 7.5
1.5 M NaCl
Sterilize by autoclaving
→ For TBS-Tween add 0.05 % Tween20 to 1 l 1x TBS

50x TAE
2 M Tris
50 mM Na_2EDTA
5.71 % Glacial acetic acid

10x TBE
892 mM Tris
890 mM Boric acid
20 mM Na_2EDTA pH 8.0

20x SSC (pH 8.0)
175.3 g NaCl
88.2 g Sodium citrate-$2H_2O$
Ad 1 l H_2O, sterilize by autoclaving

10x SDS-PAGE running buffer
1 % SDS
250 mM Tris
1.92 M Glycine

6x DNA loading dye
0.25 % Bromphenol blue
0.25 % Xylene cyanol
50 mM Tris pH 7.6
60 % Glycerol

2x Protein loading buffer
100 mM Tris
100 mM DTT
4 % SDS
20 % Glycerol
0.02 % Bromphenol blue

5x Transfer buffer for wet blot
960 mM Glycine
0.187 % SDS
125 mM Tris pH 8.3
→ For 1x transfer buffer add 20 % Methanol

BSN Transfer buffer for semi-dry blot
(pH 9.0-9.4)
47.5 mM Tris
39 mM Glycine
0.375 % SDS
20 % Methanol

Ponceau S solution
0.5 % Ponceau S
1 % Acetic acid

Stripping buffer
200 mM Glycine-HCl pH 2.5
0.05 % Tween20
50 mM DTT

Salt extraction buffer
10 mM HEPES pH 7.2
0.6 M KCl
3 mM $MgCl_2$
5mM DTT

Carbonate extraction buffer
0.1 M $NaHCO_3/Na_2CO_3$ pH 11
1 mM EDTA

2.1.12 Bacterial strains

One-shot™ TOP10 E. coli	Invitrogen

2.1.13 *P. falciparum* strains

3D7, NF54 and FCR3	L. Hviid, University of Copenhagen
FCR3S1.2	M. Wahlgren, Karolinska Institutet, Stockholm
Placental isolate Gb337	(Khattab et al. 2004)
Placental isolateVIP43	(Diouf et al. 2004)
Cerebral malaria isolate Chc03	(Lindenthal et al. 2003)

2.2 Molecular Biology Methods

2.2.1 Extraction of genomic DNA from *P. falciparum*

For the extraction of genomic DNA, a mixed *P. falciparum* culture was harvested at >10 % parasitemia by centrifugation at 800 x g for 5 min. The pellet was stored at -20 °C until use. Genomic DNA was obtained by applying the *QIAamp® DNA Blood Mini Kit* (QIAGEN) according to the manufacturer's instructions with slight modifications. Briefly, 200 µl of the culture pellet were added to a tube containing 20 µl of protease (QIAGEN). The cells were lysed by the addition of 200 µl of AL buffer and incubation at 56 °C for 10 min. After addition of 200 µl 100 % ethanol, the lysate was applied to a QIAamp spin column and centrifuged for 1 min at 6.000 x g. The sample was washed sequentially with 500 µl AW1 and AW2 buffer and centrifuged each time for 1 min at 6.000 x g. To eliminate possible carryover of any buffer, the column was centrifuged again for 1 min at 12.000 x g prior to the elution step. Finally, DNA was eluted with 100 µl of H_2O. To optimize DNA elution, the sample was incubated for 5 min at room temperature before centrifugation for 1 min at 6.000 x g, and the eluate was reloaded onto the column and centrifuged again to maximize the yield. The DNA concentration was determined photometrically and the samples were stored at -20 °C.

2.2.2 Extraction of RNA from *P. falciparum*

Total RNA was extracted from *P. falciparum* IE essentially according to the protocol described by Kyes et al. (Kyes et al. 2000) with some modifications. In brief, *P. falciparum* cultures were harvested by centrifugation at 800 x g for 5 min. Ring stage and gametocyte IE were lysed in 10x pellet volume, trophozoite stages in 20 x pellet volume of pre-warmed

TriFast™ and incubated for 5 min at 37 °C to allow dissociation of nucleoprotein complexes. The samples were stored at -20 °C until further preparation.

For RNA purification, 0.2 ml of chloroform was added per 1 ml of *TriFast™* reagent and the samples were shaken vigorously followed by incubation at room temperature for 5 min. Then, the samples were centrifuged at 4.000 x g for 60 min at 4 °C. The aqueous phase was rescued, avoiding any carryover of material from the organic phase which contains genomic DNA and protein, and transferred into a new tube. RNA was precipitated by the addition of 500 µl of isopropanol per 1 ml of *TriFast™* reagent and incubation on ice for 2 h. Thereafter the samples were centrifuged at 4.000 x g for 60 min at 4 °C and the pellets washed once with 75 % ethanol and briefly air dried. The RNA was resolved in H_2O for cDNA synthesis or in formamide for northern blot analysis. Nuclei acid concentration was determined photometrically and the samples were stored at -70 °C.

2.2.3 RNA cleanup

In order to minimize the risk of DNA contamination in RNA samples applied for cDNA synthesis and RT-PCR, an additional purification step using the *RNeasy Mini Kit* (QIAGEN) was conducted. The protocol was performed according to the instructions given by the manufacturer including the optional on-column DNA digestion step. RNA was eluted in 30 µl RNase free H_2O and the eluate reloaded once to increase the final RNA concentration. The final concentration was determined photometrically and the samples were stored at -70°C.

2.2.4 Preparation of plasmid DNA

For small scale isolation of plasmid DNA from overnight cultures of single colonies prior to sequencing or restriction analysis, the *NucleoSpin® Plasmid* kit (Macherey-Nagel) was applied according to the manufacturer's instructions.

Large scale DNA preparation of clones was performed with the *Plasmid Maxi Kit* (QIAGEN) with some modifications. Briefly, a 200 ml overnight culture was inoculated by adding 200 µl of the starter culture. The bacteria pellet was harvested by centrifugation at 4.000 x g for 15 min at 4 °C. The pellet was first resuspended in 10 ml of buffer P1, then 10 ml of buffer P2 were added and the sample was carefully mixed to avoid shearing of the DNA. After incubation at room temperature for 5 min, 10 ml of chilled buffer P3 were added and the sample gently mixed and placed on ice for 15 min. Afterwards the sample was cleared by filtration through pieces of gauze placed in a funnel, and the filtrate was loaded onto the equilibrated column. The column was washed twice with 30 ml of buffer QC. The DNA was

eluted from the column with 15 ml of buffer QF and the eluate immediately mixed with 10.5 ml of isopropanol to precipitate the DNA. After centrifugation at 12.000 x g for 30 min at 4 °C, the pellet was resuspended in 1 ml of 70 % ethanol and transferred to a small tube. The sample was centrifuged at 14.000 x g for 15 min and the pellet left to air dry. Finally, plasmid DNA was resuspended in 100 µl of endotoxin-free TE buffer (QIAGEN). The concentration was determined photometrically and adjusted to 1 µg/µl. Plasmid DNA was stored at -20°C.

2.2.5 Generation of chemically competent bacteria

Treatment of bacteria with divalent metal ions renders them competent for taking up foreign DNA with high efficiency. Here, chemically competent bacteria of the *E. coli* strain TOP10 were generated. For this purpose, 3 ml of LB medium were inoculated with *OneShot™ TOP10 cells* (Invitrogen) and incubated overnight at 37 °C. The overnight culture was added to 500 ml of SOB^{++} medium and the culture incubated at RT on a shaker for 5-6 h until an OD_{600} of 0.4 - 0.6. The culture was then divided into 50 ml aliquots and chilled on ice for 10 min. The cells were pelleted by centrifugation at 4.000 x g for 10 min at 4 °C. Each bacteria pellet was resuspended in 10 ml of ice-cold TB buffer and the suspension incubated again for 10 min on ice. After centrifugation at 4.000 x g for 10 min at 4 °C, the pellets were pooled and resuspended in 18.6 ml ice-cold TB buffer and 1.4 ml DMSO. The suspension was incubated for 10 min on wet ice and finally distributed into aliquots of 250 µl or 500 µl. The aliquots were shock-frozen in liquid nitrogen and stored at -80°C.

2.2.6 Transformation of chemically competent bacteria

Chemically competent TOP10 *E. coli* cells were transformed by the heat shock method. The cells were slowly thawed on ice and 4-10 µl of a ligation reaction added. After incubation for 30 min on ice, the bacteria were subjected to a heat shock at 42 °C in a water bath for 60 s. After a short incubation period on ice, 600 µl of LB medium were added and the cells incubated at 37 °C for 45 min. The cells were pelleted, resuspended in 50 µl of LB medium and plated on LB agar plates containing the appropriate selective antibiotic. For blue-white colony screening, the plates were before treated with 40 µl of 2 % of X-Gal. The plates were incubated overnight at 37 °C.

2.2.7 Polymerase chain reaction (PCR) amplification

PCR amplification is a method that is used to amplify DNA sequences from a template by priming with sequence specific oligonucleotides. The reaction consists of three steps which are repeated in several cycles. In the first step, the template DNA is denatured at high temperatures to yield single stranded molecules. In the second step, single stranded sense or antisense oligonucleotide primers are allowed to hybridize with their target sequences in the template DNA molecules. In the third step, the DNA polymerase complements the hybrid to a double stranded DNA molecule by extending the oligonucleotide primers.

The reaction was performed in different volumes depending on the application. Cloning PCR amplifications, generating probes for radioactive labelling and RT-PCR amplifications were performed in 50 µl, while colony screening reactions were performed in 20 µl. Volumes and concentrations of individual components were employed as indicated below.

	Probe PCR RT-PCR	Colony PCR	
Component	Volume	Volume	Final concentration/ amount
dNTP (0.5 mM each)	5 µl	2 µl	50 nM each
10x PCR buffer (QIAGEN)	5 µl	2 µl	1x
Taq polymerase	0.2 µl	0.2 µl	1 U
Forward primer (10 pmol/µl)	2 µl	1 µl	0.4 pmol/µl 0.5 pmol/µl
Reverse primer (10 pmol/µl)	2 µl	1 µl	0.4 pmol/µl 0.5 pmol/µl
$MgCl_2$ (25 mM)	0-4 µl	-	0-8 mM
DNA	variable	-	variable
H_2O	variable	13.8 µl	
Final	50 µl	20 µl	

Cycling conditions were also dependent on the application and are summarized below. In order to optimize reaction conditions for the use of degenerate oligonucleotide primers, a protocol was applied in which the annealing temperature was decreased in two steps. Because of the high adenine-thymidine (A/T) content of the *Plasmodium* genome, the extension temperature was generally chosen to be 68 °C. For the amplification of the extremely A/T rich *Plasmodium* upstream sequences, the extension temperature was lowered to 60 °C (Su et al. 1996).

	Cloning and Colony PCR	RT-PCR of coding regions	RT-PCR of ups regions	
Step	Temperature and Time			Cycles
Denaturation	94 °C 120 s	94 °C 120 s	94 °C 120 s	1
Denaturation	94 °C 30 s	94 °C 30 s	94 °C 30 s	5
Annealing	55 °C 30 s	55 °C 30 s	50 °C 30 s	
Extension	68 °C 150 s	68 °C 150 s	60 °C 60 s	
Denaturation	94 °C 30 s	94 °C 30 s	94 °C 30 s	5
Annealing	50 °C 30 s	50 °C 30 s	45 °C 30 s	
Extension	68 °C 150 s	68 °C 150 s	60 °C 60 s	
Denaturation	94 °C 30 s	94 °C 30 s	94 °C 30 s	25
Annealing	45 °C 30 s	45 °C 30 s	40 °C 30 s	
Extension	68 °C 150 s	68 °C 150 s	60 °C 60 s	
Extension	68 °C 600 s	68 °C 600 s	60 °C 600 s	1
Cooling	∞	∞	∞	1

2.2.8 Reverse transcription of mRNA into cDNA

Equal amounts of total RNA of different stages were reverse transcribed with the *SuperScript™ II First-Strand Synthesis System* (Invitrogen) according to the manufacturer's instructions using random hexamer primers. For each RNA sample, one reaction was prepared which included *SuperScript™ II reverse transcriptase* (+RT), and one in which the enzyme was omitted (-RT). After reverse transcription and a final step of RNaseH treatment to destroy the RNA template, the cDNA samples were stored at -20°C until further analysis.

2.2.9 Separation of DNA by agarose gel electrophoresis

Separation of nucleic acids according to size was conducted for analytical as well as preparative purposes. Agarose concentrations varied between 1 and 2 % in TAE buffer, depending on the expected size of the fragments. The gels were supplemented with 0.1 µg/ml EtBr to allow visualization of the nucleic acids. The samples were supplemented with 6 x DNA loading dye and size standards indicated above were loaded in parallel for size estimation. The gels were run at 120 V until the separation of the fragments was sufficient. Documentation was done by photography of the bands as visualized on a UV transilluminator.

2.2.10 Restriction digestion

Restriction analysis was used for the characterization, identification and isolation of DNA molecules. Enzymes were derived from Fermentas and New England Biolabs (NEB) and used

according to the manufacturers instructions. Incubation periods ranged between 2 hours to overnight, usually at 37 °C in an incubator.

2.2.11 Purification of DNA by agarose gel extraction

Prior to ligation of PCR products into a vector backbone, both PCR fragments and linearized plasmids were purified by agarose gel extraction using the *NucleoSpin® Extract II* kit (Macherey-Nagel) according to the manufacturer's instructions in order to eliminate primers, undesired side products or undigested plasmid molecules.

2.2.12 Ligation of DNA fragments into vector DNA

For the ligation of PCR amplified DNA fragments into cloning vectors, the T4 DNA ligase system was applied. Molar ratios between vector DNA and insert DNA were 1:4 in a 20 µl reaction volume and approximately 200 ng vector DNA were used. T4 DNA ligase (2-5 U) was employed in each reaction. The reaction was incubated for 2 hours at 25 °C.

2.2.13 Cloning into TOPO-TA vectors

RT-PCR and genomic DNA PCR fragments were ligated into the *pCR2.1®TOPO®* vector (Invitrogen) according to the manufacturer's instructions. Briefly, 4 µl of purified PCR product, 1 µl of salt solution and 1 µl of vector were incubated for 20 min at 22 °C. 3 µl of the TOPO® cloning reaction was added to a vial of One Shot® chemically competent *E. coli*, mixed gently and incubated for 30 min on ice. After a heat shock treatment at 42 °C in a water bath for 1 min, 250 µl of SOC medium was added and the cells incubated at 37 °C for 1 h under agitation. The samples were then centrifuged at 6.000 x g for 5 min and 200 µl of the supernatant discarded. The bacteria were resuspended in the remaining medium and spread on LB agar plates (pretreated with 40 µl of 40 µg/ml X-gal in DMF) containing 50 µg/ml ampicillin. Blue / white colony screening was performed after overnight incubation at 37°C and white colonies picked and cultivated for further analysis.

2.2.14 Sequencing

Sequencing of plasmid DNA or PCR products was conducted by the ValueRead sequencing service offered at MWG Biotech.

2.2.15 NorthernBlot Analysis

For Northern blot analysis, RNA supplemented with EtBr was heated for 10 min at 60 °C, briefly chilled on ice and loaded on 1 % agarose gels containing 5 mM guanidinium thiocyanate in TBE buffer. Gel electrophoresis was performed at 110 V for 15 min and then switched to 80 V until sufficient separation was achieved. Equal loading and RNA quality were controlled and documented under UV light. Before transfer, the gel was soaked in 10x SSC for 30 min. Transfer of the separated RNA to *Hybond™* nylon membranes (Amersham Biosciences) was achieved by capillary transfer in 10x SSC containing 10 mM NaOH overnight. Efficient transfer was checked by UV illumination and the RNA was crosslinked by exposure to UV (1200 kJ, UV Stratalinker™ 1800).

2.2.16 Radioactive labeling of DNA probes

Templates for specific DNA probes were amplified by PCR on 3D7 genomic DNA. After purification, PCR products were labeled using the *Prime-a-Gene® Labeling System* (Promega) according to the instructions provided. The probes were purified by gel filtration using *MicroSpin S 300* columns (GE healthcare). Before use, the probes were boiled for 5 min at 95 °C.

2.2.17 Hybridization of a radioactively labeled DNA probe

Hybridization was carried out in *ULTRAhyb®* hybridization buffer (Ambion). Prehybridization was done for 30 min at 42 °C. After addition of the radioactively labeled probe, the blots were hybridized overnight at 42 °C. Nylon membranes were washed 3 times with 2x SSC / 0.1 % SDS at 50 °C for 15 min and shrink-wrapped. Depending on the intensity of the signal, X-ray films were exposed from 1 h to 7 days at -70 °C prior to development.

2.2.18 SDS-PAGE

For the separation of proteins by SDS-PAGE, 6 %, 12 % or 15 % polyacrylamide gels were prepared. The composition of stacking and resolving gels are given below. Samples were prepared in 2x protein loading buffer and heated for 5 min at 95 °C before loading. The proteins were separated in 1x SDS-PAGE running buffer for approximately 20 min at 90 V until the dye front had passed through the stacking gel and entered the resolving gel. Then the voltage was switched to 120 V. Estimation of protein sizes was done by comparison to the size standards given in 2.1.9.

	Resolving gel			Stacking gel
	6 %	12 %	15 %	5 %
H_2O (ml)	2.1625	1.6	1.325	1.5
40 % Acrylamide-Bis 19:1 (ml)	0.5625	1.125	1.4	0.25
1.5 M Tris pH 8.8 (ml)	0.95	0.95	0.95	-
1 M Tris pH 6.8 (ml)	-	-	-	0.25
10 % SDS (µl)	37.5	37.5	37.5	40
10 % APS (µl)	37.5	37.5	37.5	40
Temed (µl)	1.5	1.5	1.5	4
	3.75 ml	3.75 ml	3.75 ml	2 ml

2.2.19 Western Blot Analysis

Proteins separated by SDS-PAGE were transferred to nitrocellulose membranes by semi-dry blotting in 1x BSN transfer buffer. The transfer was performed for 1 h 20 min at 1.5 mA/cm^2. Efficient protein transfer was controlled for by staining with Ponceau S solution for 1 min at room temperature and extensive rinsing with H_2O. The membranes were then put into 1x TBS to wash off excess staining solution. Blocking of free protein binding sites was done with 5 % blotting grade milk powder in TBS for 30 min at room temperature on an orbital shaker. Primary antibodies were added and incubated overnight at 4 °C on a rocker. After washing 3 times with TBS-Tween for 20 min at room temperature, the membranes were again blocked for 30 min with 5 % blotting grade milk powder in TBS. HRP coupled secondary antibodies were added and incubated for 2 h at room temperature. After three washing steps with TBS-Tween for 20 min, the blots were incubated with the substrate solution for 5 min and the chemiluminescent signal subsequently visualized by exposure of X-ray films.

To reanalyze the same samples with different antibodies, the membranes were incubated in stripping buffer at 55 °C for 1 h and extensively washed with TBS.

2.2.20 Crossreactivity assay

To analyze the ability of anti-A_{RIF29} and anti-$B_{RIF\Delta NC}$ antisera to recognize a panel of recombinantly expressed RIFIN proteins, 150 ng of each recombinant protein were loaded on a 12 % gel and analyzed by SDS-PAGE and western blotting with the two antisera. To avoid crossreactivity due to vector derived epitopes, the anti-RIFIN antisera were pre-adsorbed by addition of 1 µM of irrelevant recombinant proteins expressed from the same vector backbone.

2.3 Cell Biology Methods

2.3.1 Culture of *P. falciparum* parasites

P. falciparum cultures were cultivated at 5 % hematocrit in 25 cm^2 or 75 cm^2 tissue culture flasks (Greiner) in a volume of 5 or 20 ml, respectively. As culture medium, RPMI-1640 complete medium was used. The parasites were propagated in erythrocytes of blood group 0^+ in a gas environment of 5 % O_2, 5 % CO_2 and 90 % N_2 at 37 °C. The medium was exchanged after three days when the starting parasitemia was below 0.5 %, and every day if the starting parasitemia was above 0.5 %. To estimate the parasitemia, thin smears were prepared and left to air dry, then fixed in methanol for 1 min and stained in Giemsa solution (1:10 diluted stock solution) for approximately 20 min. When the parasitemia reached roughly 10 %, the cultures were diluted.

2.3.2 Freezing and thawing of *P. falciparum* cultures

To prepare frozen stocks of *P. falciparum* parasites for long term storage, cultures were harvested at ring stage with a parasitemia of approximately 10 % by centrifugation at 800 x g. The supernatant was removed and the volume of the packed cell pellet was determined. A total of 0.33 ml of glycerolyte per ml cell pellet was slowly added and the tubes left to stand for 5 min at room temperature. Then, 1.33 ml of glycerolyte per ml cell pellet was added and the cells gently mixed. The samples were distributed to cryotubes which were placed inside a styrofoam box at -70 °C to allow slow and continuous freezing. For long term storage, the vials were transferred to liquid nitrogen.

To thaw and recultivate *P. falciparum*, a vial was quickly thawed and the volume of infected RBC measured. Per ml RBC suspension, 0.1 ml of 12 % NaCl solution was slowly added while shaking the tube. After an incubation period at room temperature of 5 min, 10 ml 1.6 % NaCl per ml RBC suspension was added dropwise. The samples were centrifuged at 800 x g for 5 min at room temperature and the supernatant discarded. The cells were washed once with RPMI-1640 complete medium and cultivated as described above.

2.3.3 Synchronization of *P. falciparum* cultures with 5 % sorbitol

Synchronization was performed on cultures containing mainly young ring stage parasites. The culture was centrifuged at 800 x g for 5 min at room temperature and the supernatant was discarded. The cell pellet was resuspended in 5 ml of sterile 5 % sorbitol in H_2O and the

suspension incubated for 10 min at 37 °C. Thereafter, the cells were centrifuged at 800 x g for 5 min at room temperature and the supernatant removed. The cells were washed once with RPMI-1640 complete medium and cultivation continued, as described above. The procedure was repeated once after 4 h.

2.3.4 Synchronization of *P. falciparum* cultures by Magnetic-activated cell sorting (MACS) selection

In order to achieve a very stringent synchronization, a second strategy was applied. Late stage parasites consisting of a high proportion of segmented schizonts were enriched by MACS. Fresh red blood cells were added to the resulting cell pellet of late stage parasites and the cells were cultivated for 2 to 4 h at 5 % hematocrit. The culture was then treated with 5 % sorbitol as described above. This procedure resulted in a highly synchronous parasite population differing no more than 2 to 4 h in age.

2.3.5 Culture of *P. falciparum* gametocytes

A modified version of the protocol described by Fivelman et al. was used for gametocyte cultivation (Fivelman et al. 2007). An overview is given in the table below. Prior to induction of gametocytogenesis, parasites of the NF54 strain were synchronized by treatment with 5 % sorbitol at ring stage as described above and cultivated at a parasitemia of about 1 % under standard conditions. Two days later, synchronized sexual development was stimulated by starving the fast-growing ring-stage culture at 6-8 % parasitemia in the presence of partially spent medium. To do so, only one third of the medium was removed and replaced by fresh medium. Parasites were kept in culture for 32 h without further medium exchange. The culture was then split into four flasks and fresh medium and blood was added to obtain a hematocrit of 5 %. The following day during which the cultures consisted mainly of ring-stage parasites was considered day 0 of gametocytogenesis. The spent medium was removed and replaced by fresh medium containing 50 mM N-Acetyl-D-Glucosamine. Afterwards, the medium was exchanged every second day and parasites harvested at various time points during gametocytogenesis. The scheme below summarizes the schedule for the procedures and the development of sexual-stage parasites during gametocyte culture. Purification of gametocytes was achieved by MACS preparation or by centrifugation through a discontinuous Accudenz gradient.

Day	Procedure	Stage
-4	Synchronization	Ring 1 % P
-2	Replace 1/3 of spent medium with fresh medium	Ring 6-8 % P
-1	Distribute culture into four flasks at 5% hematocrit	Trophozoite
0	Add 50 mM N-Acetyl-D-Glucosamine	Ring
2	Change medium + 50mM N-Acetyl-D-Glucosamine	Stage I
4	Change medium + 50mM N-Acetyl-D-Glucosamine	Stage I and II
6	Change medium + 50mM N-Acetyl-D-Glucosamine	Stage II and III
8	Change medium + 50mM N-Acetyl-D-Glucosamine	Stage III and IV
10	Change medium + 50mM N-Acetyl-D-Glucosamine	Stage IV and V

2.3.6 Isolation of free *P. falciparum* merozoites

To prepare naturally released merozoites, 44-48 (p.i.) hour schizonts were purified by MACS and placed back into culture at 1 % hematocrit in RPMI-1640 complete medium. Every 90 min the culture was examined by microscopy for schizont rupture and merozoite release. When the majority of schizonts had ruptured, free hemozoin, intact schizonts and uninfected erythrocytes were removed by four times centrifugation for 4 min at 600 x g at room temperature followed by a single step of purification by passage through the MACS column. Finally, merozoites were pelleted from the flow through by centrifugation for 15 min at 2880 x g and 4 °C, and washed several times in PBS.

2.3.7 MACS enrichment of pigmented parasite stages

During their intracellular development, malaria parasites digest erythrocyte hemoglobin, leaving insoluble high-spin oxidized heme products, which polymerize into a pigmented substance, called hemozoin (Francis et al. 1997). In contrast to hemoglobin, hemozoin has paramagnetic properties that allow the purification of IE which exhibit hemozoin deposits by magnetic separation (Uhlemann et al. 2000). Here, a *Vario MACS*™ magnetic separator (Miltenyi) was used. First, the equipment was assembled by connecting a MACS CS-column via a three-way valve to a 20 ml syringe as well as a 0.8 mm needle, and attaching this construction to the magnet. The column was equilibrated by careful injection of PBS/1 % BSA avoiding any air bubbles. The flow was adjusted to dribbling speed by turning the stopcock, and up to 40 ml of a *P. falciparum* culture at 5 % hematocrit was applied. The column was washed at least 5 times with PBS/1 % BSA and the enriched parasite IE eluted by

flushing with PBS/1 % BSA after closing the valve and detaching the column from the magnet. The yield was determined by counting the cells in a Neubauer chamber.

2.3.8 Enrichment of gametocytes with Accudenz

Cushions containing 11 % and 16 % accudenz were prepared in incomplete RPMI-1640 medium supplemented with 25 mM HEPES, pH 7.2. A discontinuous gradient was prepared by resuspending the gametocyte culture at 10 % hematocrit in RPMI-1640 complete medium in a 50 ml centrifugation tube and carefully layering first the 11 %, then the 16 % accudenz cushion underneath the parasite culture at the bottom of the tube. The samples were centrifuged at 2800 x g for 15 min at 4 °C and the parasites collected at the gradient interfaces. Gametocytes were enriched at the interface between the 11 % and the 16 % cushion, while uninfected erythrocytes were found in the sediment. The parasites were washed three times with RPMI incomplete medium before proceeding with following applications.

2.3.9 Enrichment of rosetting parasites on Ficoll-Isopaque

Rosetting parasites can be enriched by density gradient centrifugation using Ficoll-Isopaque (Quakyi et al. 1989). Ice-cold, sterile Ficoll-Paque was added to 15 ml centrifuge tubes in 2 ml aliquots and 2 ml of a rosetting parasite culture were carefully layered on top of it. The tubes were centrifuged at 800 x g for 12 s at room temperature. The rosetting parasites that had passed through the Ficoll-Isopaque layer were collected using a Pasteur pipette, washed three times in RPMI-1640 complete medium and cultivated by addition of fresh erythrocytes and complete medium.

2.3.10 Selection of CSA binding parasites

Petri dishes (∅ 5 cm) were coated overnight at 4 °C with 10 µg/ml chondroitin sulfate A (CSA) in PBS. The CSA solution was aspirated and the dishes blocked with filter sterilized PBS/2 % BSA for 1 h at room temperature. After removal of the blocking solution, 3 ml of parasite culture at 10 % parasitemia and 5 % hematocrit in binding medium was added and incubated at 37 °C for 1 h. The plates were gently swayed every 15 min to resuspend the IE settling to the bottom of the dish. The culture was then removed and the dishes washed carefully 3 – 5 x with binding medium. Finally, 3 ml of RPMI-1640 complete medium substituted with fresh erythrocytes at 5 % hematocrit was added and the cultures placed in the incubator at 37 °C.

2.3.11 Fluorescence activated cell sorting (FACS)

FACS analysis was performed on MACS enriched, trophozoite IE. In each sample, 5x 10^6 IE were analyzed. After blocking for 30 min with PBS/2 % FCS, the cells were incubated with primary antibodies at a dilution of 1:20 (human immune serum) or 1:50 (anti-RIFIN and pre-immune sera) for 1 h at 4 °C. The IEs were washed three times with PBS/2 % FCS and stained with anti-rat or anti-human secondary antibodies (1:400) for 1 h at 4 °C. The cells were washed 3 x before addition of FITC labelled tertiary antibodies (1:250) and EtBr (10 µg/ml). After 1 h at 4 °C and extensive washing, the samples were analyzed in a *FACS scan* (Becton Dickinson, CA) flow cytometer. For data acquisition and evaluation the *CellQuest software* (Becton Dickinson, CA) was applied.

2.3.12 Fractionation of infected erythrocytes

A series of different cell lysis methods and differential fractionation techniques have been applied in this study to answer questions regarding the subcellular localization and solubility of RIFIN proteins. Fractions were either extracted directly in 2x protein loading buffer for examination by western blotting, or the permeabilized cells were morphologically analyzed by immunofluorescence analysis or immunoelectron microscopy. Alternatively, the pellet fractions were subjected to trypsinization in protease protection assays. An overview of the fractionation techniques used here is given in Fig. 5.

(i) Saponin permeabilization:

Saponin selectively permeabilizes the erythrocyte plasma membrane and the parasitophorous vacuole membrane, while leaving the parasite membrane intact. Thus, all soluble components from the IE cytosol and the PV are released into the supernatant, while proteins located inside the parasite segregate with the pellet (Beaumelle et al. 1987).

MACS enriched IE were washed twice with PBS and permeabilized with 0.075-0.15 % saponin in PBS at a concentration of 1x 10^6 IE/µl for 15 min on ice. Protease inhibitor cocktail was added or omitted, depending on the downstream application. The samples were briefly mixed from time to time. The cells were centrifuged at 800 x g for 10 min at 4 °C and the supernatant was transferred into a new vial. The pellet was washed 3 x with PBS and used for subsequent applications.

(ii) Streptolysin O (SLO) permeabilization:

SLO is a bacterial exotoxin that permeabilizes lipid bilayers of erythrocytes by forming stable proteinaceaous pores of > 3 nm in diameter (Bhakdi et al. 1985). Treatment of IE with SLO leads to the release of soluble components of the erythrocyte cytosol, while PVM resident proteins and parasite proteins are retained within the parasite, demonstrating the selectiveness of the permeabilization procedure (Ansorge et al. 1996).

MACS enriched IE were washed twice with PBS and permeabilized with activated SLO. Activated SLO was prepared by adding 10 mM DTT to 4 haemolytic units of SLO (Sigma) in PBS. Protease inhibitor cocktail was added or omitted depending on the downstream application. Incubation was done for 30 min at 37 °C at a concentration of 1x 10^6 IE/µl. Subsequently the cells were centrifuged at 800 x g for 10 min at 4 °C and the supernatant was recovered and transferred to a new vial. The pellet was washed 3 x with PBS and then further processed for downstream applications.

(iii) Hypotonic lysis:

Membrane ghosts of IE can be prepared by hypotonic or mechanical lysis. Here, MACS enriched parasites were resuspended in 10 mM HEPES pH 7.2 at a concentration of 1x 10^6 IE/µl in the presence or absence of protease inhibitors. The cells were lysed by repeated freezing and thawing in liquid nitrogen and supernatant and pellet were separated by centrifugation at 20.000 x g for 10 min at 4 °C. The supernatant was transferred to a new vial and the pellet containing the membrane fraction as well as the crystalline contents of the food vacuole was washed thrice with PBS.

2.3.13 Extraction of membrane fractions of infected erythrocytes

In order to analyze the quality of the membrane association of RIFINs, different extraction techniques were employed. IE membranes were prepared by hypotonic lysis and sequentially treated with different buffers.

(i) Salt extraction

Membranes were treated with salt extraction buffer including protease inhibitors for 30 min on ice at a concentration of 1x 10^6 IE equivalents/µl. The membranes were pelleted by centrifugation at 20.000 x g for 1 h at 4 °C. The supernatant was rescued and transferred to a new vial.

(ii) Carbonate extraction

The membrane pellet depleted of salt soluble proteins was further extracted with carbonate extraction buffer for 30 min on ice and the carbonate soluble fraction separated from the membrane pellet by centrifugation as above. To analyze insoluble membrane proteins, the remaining pellet was extracted with 2x protein loading buffer and boiled for 5 min at 95 °C.

(iii) Urea extraction

Membranes were treated with 8 M urea in 10 mM Tris pH 8 and 1 mM EDTA for 1 h at room temperature at a concentration of 1x 10^6 IE equivalents/µl. Dialysis was performed overnight at room temperature against 0.1 M urea in 10 mM Tris pH 8 and 1 mM EDTA. Urea soluble and insoluble protein fractions were separated by centrifugation at 20.000 x g for 30 min at 4 °C.

(iv) Triton X-100 extraction

Separation of Triton X-100 soluble and insoluble proteins was achieved by incubating MACS enriched IE at a concentration of 1x 10^6 IE/µl with 1 % Triton X-100 in PBS in the presence of protease inhibitors. The samples were left on ice for 30 min with occasional mixing and subsequently centrifuged at 20.000 x g for 1 h at 4 °C to separate soluble and insoluble components.

(v) SDS extraction

Total cell lysates and solubilization of insoluble components after extraction with other methods were prepared by resuspending pellets in 2x protein loading buffer at a concentration of 1x 10^6 IE and boiling the samples for 5 min at 95°C. Insoluble and soluble components were separated by centrifugation at 20.000 x g for 10 min at 4°C.

2.3.14 Protease protection assay

In order to analyze the surface exposure of RIFIN proteins as well as to gain insight into their membrane topology, IE preparations were differentially permeabilized according to the methods described above and treated with trypsin to remove proteins at the exposed sites. Trypsin (Sigma) at a concentration of 1 mg/ml in PBS was added to the permeabilized cells to yield a dilution of 1x 10^6 IE equivalents/µl. As a control, mock treated cells without trypsin were used and treated with PBS only. The samples were incubated for 15 min at 37 °C and the reaction was stopped by the addition of 2 mg/ml soybean-trypsin inhibitor (Sigma) and

incubation for 5 min on ice. After centrifugation at the appropriate conditions indicated above for each of the permeabilization methods, the supernatants were discarded and the pellet fraction extracted in 2x protein loading buffer and analyzed by SDS-PAGE and western blotting.

2.3.15 Immunofluorescence Analysis (IFA)

Smears of parasite cultures were prepared from parasite cultures from which medium was aspirated until the hematocrit was approximately 20 %, air dried and fixed for 5 min in 100 % methanol at -20 °C, or in acetone at RT. Various small fields were marked with a silicon pen (DakoCytomation). After rehydration for 10 min in PBS, the slides were incubated with antisera diluted in PBS/1 % BSA (2 h at RT), washed 3 x with PBS, and incubated with conjugated secondary antibodies and DAPI (1 μg/ml). After repeated washing in PBS, the slides were embedded with MOWIOL, covered with a coverslip and analyzed with a 100 x oil immersion lens in a UV equipped Leica DM RB microscope after drying.

2.3.16 Estimation of fluorescence rates

Smears of different gametocyte stages were double stained with anti-RIFIN antibodies and mouse anti-Pfs16 antibodies or rabbit anti-Pfg27 antiserum to facilitate unequivocal assignment of the gametocytes. Smears of trophozoite IE were stained with anti-RIFIN antisera only. In both cases, primary antibodies were detected with fluorescence labeled secondary antibodies and IE were identified by DAPI staining (1 μg/ml). Fluorescence rates were determined by counting at least 100 individual IE. A minimum of two experiments on individual parasite preparations was performed.

2.3.17 Live and permeabilized IFA

IE were enriched by MACS and either permeabilized with 0.1% saponin as described above or incubated with PBS. Both permeabilized and live cell samples were incubated with primary antibodies diluted in PBS/1% BSA for 1 h at 4°C on a rotating mixing wheel, and then washed three times with PBS. Secondary antibodies and DAPI (1 μg/ml) in PBS/1% BSA were added to the cell pellet and incubated for 1 h at 4°C. Before microscopic analysis, cells were again washed three times with PBS. Centrifugation steps were performed at 800 g for 5 min at room temperature. For preservation of the samples, an aliquot of the suspension was left to settle on poly-L-lysine coated slides for 30 min. Unbound cells were carefully rinsed

off with PBS and the preparations left to air dry. The slides were mounted with MOWIOL, covered with a coverslip and left to dry before examination by microscopy.

2.3.18 Immunoelectron Microscopy (IEM)

In this study, a pre-embedding staining protocol was optimized for the IEM analysis of RIFINs in IE. MACS enriched IE were permeabilized with 0.075 % saponin and sequentially incubated with primary anti-RIFIN antibodies or pre-immune sera, secondary rabbit-anti-rat antibodies at a dilution of 1:500, and protein A-conjugated gold (diameter 10 nm, University of Utrecht) at a dilution of 1:60 in PBS/1 % BSA. Incubation was done for 1 h at 4 °C on a mixing wheel, and the cells were washed 3 x with PBS between each staining step. Subsequently, the cells were fixed in 2 % glutaraldehyde in 0.1 M sodium-cacodylate buffer pH 7.2 for at least 1 h at 4 °C. The cells were dehydrated by stepwise incubation with rising ethanol concentrations between 70 % and 100 %. Afterwards, the cell pellet was embedded in Epon. Ultrathin sections of 70 nm were prepared with the Ultracut-E microtome (Reichert), and contrastation was attained by fixation with uranyl acetate in 70 % methanol and staining with lead citrate according to the protocol established by Reynolds (Reynolds 1963). The sections were analyzed with a CM-10 transmission electron microscope (Philips).
The IEM analysis was performed by the courtesy of Christel Schmetz, BNI, Hamburg.

2.4 In Silico Biology Methods

2.4.1 Databases and Weblinks for sequence retrieval

P. falciparum genomic DNA, cDNA and protein sequences of the 3D7 strain were retrieved from the PlasmoDB database at http://www.plasmodb.org/plasmo/home.jsp.
BLAST similarity searches of the HB3 and Dd2 *P. falciparum* genomes, which are available at *The Broad Institute,* were performed and the sequences downloaded at http://www.broad.mit.edu/annotation/genome/plasmodium_falciparum_spp/Blast.html.
The Wellcome Trust Sanger Institute hosts a BLAST server for analysis of the genome sequences of the IT strain and a Ghanaian isolate and allows sequence retrieval at http://www.sanger.ac.uk/cgi-bin/blast/submitblast/p_falciparum.

2.4.2 In silico Analysis for degenerate primer evaluation

To evaluate the suitability of the subtype-specific degenerate primer pairs, in silico PCR experiments were performed on the 3D7 genome sequence at http://insilico.ehu.es/eukaryota/.

2.4.3 Generation of Sequence Logos

Sequence Logos based on multiple protein or DNA sequence alignments were generated with the web based *WebLogo application* provided at http://weblogo.berkeley.edu/logo.cgiBerkley.

2.4.4 Sequence Analysis

The identity of RT-PCR products which were cloned into the pCR2.1 vector was determined by standard nucleotide BLAST searches at http://130.14.29.110/BLAST/. Multiple protein or DNA sequence alignments were performed using the *ClustalW software* provided as an online application at http://align.genome.jp/. Parameters were used at default settings. Manual corrections of multiple sequence alignments were done with the *BioEdit sequence alignment editor* available as a free application at www.mbio.ncsu.edu/BioEdit/bioedit.html. Graphic illustrations of alignments were also generated with the *BioEdit* software. Comparative analyses for the prediction of transmembrane domains and protein topology were performed with the combined transmembrane topology and signal peptide predictor program *Phobius* at http://phobius.binf.ku.dk/ and with the *TMHMM v2* server available at http://www.cbs.dtu.dk/services/TMHMM/.

2.4.5 Phylogenetic Reconstruction

Phylogenetic reconstructions were performed with the p-distance/Neighbor-Joining (NJ) method using the *MEGA 3.1* software package (Kumar et al. 2004). This method is frequently used to analyze the relationship among members of multigene families based on their distances. For the consideration of gaps in the alignment both pairwise deletion and complete deletion settings were tested and compared. Complete deletion excludes any positions from the analysis at which in one or more sequences an amino acid or nucleotide is missing in the alignment. Pairwise deletion calculates the distance matrix based on comparisons between two sequences at a time. The reliability of the tree topology was assessed by 500 bootstrap replications. Moreover, maximum parsimony (MP) analysis was performed and the resulting optimal tree was compared to the NJ results to assure confidence in the reconstruction.

3 RESULTS

3.1 Membrane association and topology of variant RIFIN proteins

The RIFIN proteins of the human malaria parasite *Plasmodium falciparum* have been predicted to be anchored in the plasma membrane by at least two transmembrane domains (Cheng et al. 1998). After synthesis in the endoplasmic reticulum, RIFIN proteins, as well as other proteins, have to take a complicated route passing several different membrane systems to reach their final destination in the host erythrocyte. Not much is known about the mechanisms guiding these processes or the interactions that are involved. In order to determine how RIFIN proteins are anchored and to gain insight into their topology and subcellular localization, anti-RIFIN antibodies that had been generated against two recombinant RIFIN proteins cloned from the Gabonese isolate Gb21 were used. These proteins, termed RIF40 and RIF50, include the semiconserved as well as parts of the variable domain (Abdel-Latif et al. 2002).

3.1.1 Timing of RIFIN protein expression during asexual development

It has been shown before that RIFIN transcription peaks at around 18 to 24 hours post invasion (Kyes et al. 2000; Kyes et al. 1999). However, although these data suggest that RIFIN protein expression predominates in the second half of the 48 hour asexual *Plasmodium* life cycle, experimental evidence documenting the timing of RIFIN protein expression was lacking so far. In order to analyze the synthesis of RIFIN proteins during asexual development and to find out when expression is maximal, highly synchronized cultures of the FCR3S1.2 parasite clone were harvested in 8 hour intervals starting at 4 hours post invasion. The FCR3S1.2 clone was originally derived by micromanipulation from the parent FCR3 parasite line and is characterized by its capacity to form large rosettes with uninfected erythrocytes (Fernandez et al. 1999). Shown by these authors to express RIFIN proteins at high levels, the clone was selected for the experiments performed here.

In western blot analyses, anti-RIF40 and anti-RIF50 antisera first detected proteins of sizes corresponding to the molecular weight of 30-45 kDa, as predicted for RIFINs, in lysates prepared 12 hours post invasion (Fig. 4). Anti-RIF40 reacted with several proteins between 30 and 40 kDa, whereas the antiserum directed against RIF50 recognized a double band at 40 kDa. The level of RIFIN expression further increased during development and reached peak levels around 36 hours post invasion, as detected with both antisera. At this time point, the culture consisted mainly of mature pigmented trophozoites and young schizonts. Based on these results, the subsequent experiments were chosen to be performed on parasites at these developmental stages.

Apart from showing the kinetics of RIFIN synthesis during the course of asexual development, the experiment moreover demonstrated that anti-RIFIN antisera which were generated against certain RIFIN variants from a Gabonese parasite isolate were capable of reacting with paralogous RIFIN variants expressed in a different parasite strain. This is probably due to the presence of conserved linear epitopes especially in the semiconserved domain of RIFIN molecules. Moreover, both antisera reacted with proteins of disparate sizes, implying that different subsets of the RIFIN pool were being detected. Taken together, the reagents were considered suitable for analysis of RIFIN proteins across strains, particularly since the original parasite clone Gb21 was not available.

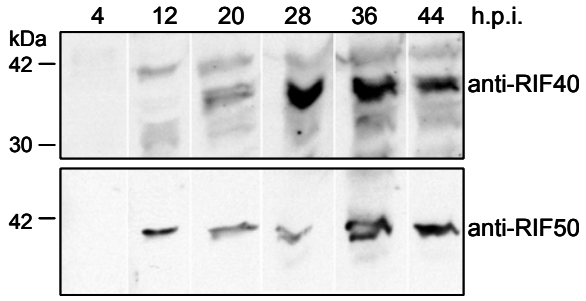

Fig. 4 RIFIN protein expression during the asexual life cycle
Parasite cultures were harvested in 8 hour intervals during the asexual life cycle and analyzed by western blotting for the expression of RIFIN proteins detected with anti-RIF40 and anti-RIF50 antisera. In each lane, lysate corresponding to 1x 10^7 infected erythrocytes was loaded. H.p.i: hours post invasion.

3.1.2 RIFINs are Triton X-100 insoluble membrane associated proteins

In order to determine the subcellular compartments containing the RIFIN proteins as well as their solubility profile, fractionation studies by applying different permeabilization protocols to IE were performed. Trophozoite infected cells were enriched by MACS and selectively permeabilized with saponin or streptolysin O (SLO), disrupted by hypotonic lysis or extracted with Triton X-100. Each of these methods releases the contents of different subcellular compartments into the supernatant, which can be separated from insoluble

components by centrifugation. Both fractions were subsequently analyzed by SDS-PAGE and western blotting. An overview of the selective permeabilization methods is shown in Fig. 5.

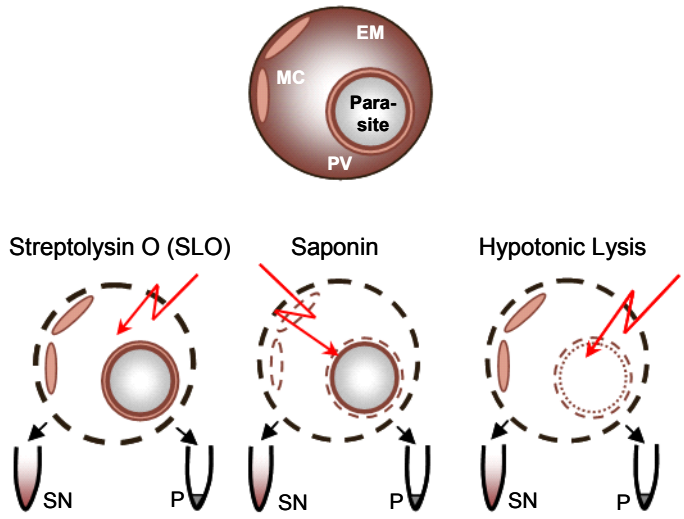

Fig. 5 Overview over selective permeabilization methods
Streptolysin O (SLO), saponin, and hypotonic lysis differentially permebilize the various membrane systems in the infected erytrocyte allowing fractionation of distinct subcellular compartments in the supernatant (SN) and the pellet (P). With SLO, soluble proteins in the erythrocyte cytoplasm are found in the SN, while the contents of the parasite, the parasitophorous vacuole (PV) and the Maurer's clefts (MC) are collected in the pellet. After saponin treatment, contents of the MC and the PV are also released into the SN. Hypotonic lysis, in contrast, protects contents of the MC, while all other soluble proteins are released into the SN.

Treatment with 0.15 % saponin disrupts the host cell membrane as well as the PVM and the MC membrane, while leaving the parasite membrane intact (Beaumelle et al. 1987). SLO, in contrast, permeabilizes only the erythrocyte membrane (Ansorge et al. 1997). The integrity of these permeabilization methods is demonstrated by the presence of the soluble parasite resident protein PP5 (*P. falciparum* protein phosphatase 5) (Lindenthal and Klinkert 2002) solely in the pellet fraction after SLO treatment. After saponin permeabilization it was partially released into the supernatant, probably representing a pool of protein present in the PV (Fig. 6). With both methods, all RIFIN proteins detected with the anti-RIF40 and anti-RIF50 antisera were found in the pellet fraction. The same was observed for the integral membrane protein SBP1, which is known to be associated with the MC (Blisnick et al. 2000).

While SLO and saponin differentially permeabilize membranes of different origin in the IE, hypotonic lysis in combination with repeated freezing and thawing in liquid nitrogen results in mechanical disruption of all membranes including parasite and host derived membranes. This leads to the release of all soluble proteins into the supernatant, while membranous structures segregate with the pellet fraction. In concordance with this, PP5 was located in the supernatant fraction, while SBP1 was found in the pellet fraction. Similar to the latter, RIFIN proteins were detected only in the membrane pellet fraction with both, anti-RIF40 and anti-RIF50 antisera (Fig. 6).

In contrast to the previous methods, Triton X-100 is a non-ionic detergent which is widely used to extract membranes and to solubilize membrane proteins. It has been shown, though, that extraction of cells with Triton X-100 at cold temperatures leads to the enrichment of lipid rafts and their associated proteins in the detergent insoluble fraction (Chamberlain 2004). In the analysis performed here, RIFIN proteins as well as the transmembrane protein SBP1 were found in the Triton X-100 insoluble fraction, while PP5 was present in the supernatant (Fig. 6).

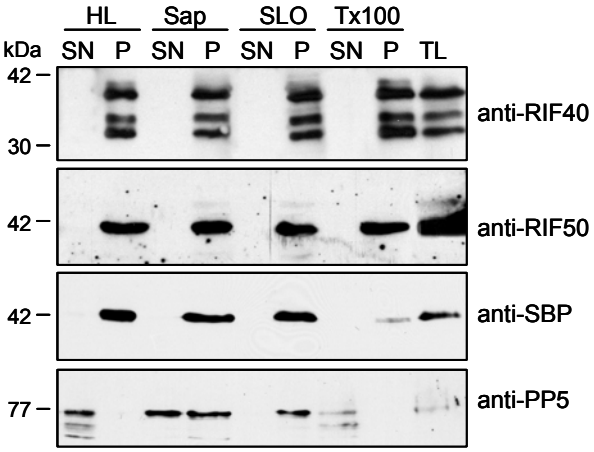

Fig. 6 Western blot analysis of infected erythrocyte fractions
Trophozoite IE of the FCR3S1.2 parasite strain were enriched by MACS and either lysed by hypotonic lysis (HL), permeabilized with saponin (Sap) or streptolysin O (SLO), or extracted with Triton X-100 (Tx100). The pellet (P) and the supernatant (SN) fraction were separated by centrifugation and analyzed by 12% SDS-PAGE and western blotting. Total lysate (TL) was used as a reference. Equivalents of $1x10^7$ cells were loaded in each lane. Blots were probed for the presence of RIFIN proteins with anti-RIF40 and anti-RIF50 as well as the control antigens SBP1 (anti-SBP), and protein phosphatase 5 (anti-PP5).

3.1.3 RIFINs are membrane spanning proteins that are soluble in urea

A recent study analyzed the membrane association of PfEMP1 in great detail (Papakrivos et al. 2005). It was shown that the intracellular pool of PfEMP1 associated with MC behaves differently from the surface exposed population concerning their solubility profiles, thus taken as an indication for distinct mechanisms mediating the membrane association of each of these populations. In contrast to the proteins transported to the surface, the intracellular pool exhibits a solubility profile which is atypical for transmembrane proteins and rather resembles that of peripheral membrane proteins (Papakrivos et al. 2005).

In order to analyze the nature of the membrane association of RIFIN proteins, the membrane fractions of *P. falciparum* IE yielded by hypotonic lysis were sequentially extracted first with a buffer containing a high salt content, which should eliminate soluble proteins, and second with a sodium carbonate buffer at high pH, which dissolves peripheral membrane proteins. The proteins present in the remaining membrane pellet were solubilized

with SDS. In a parallel experiment, extraction with 8 M urea was performed followed by dialysis against 0.1 M urea to yield a urea-soluble and a urea-insoluble fraction. All fractions, including the supernatant and pellet fraction after hypotonic lysis as controls, were analyzed by SDS-PAGE and western blotting (Fig. 7).

As already shown above in Fig. 6, RIFINs detected with anti-RIF40 and anti-RIF50 antibodies as well as SBP1 were present only in the membrane pellet fraction and not in the supernatant upon hypotonic lysis. Neither extraction with high salt buffer nor with carbonate buffer at high pH was efficient at releasing RIFIN proteins or SBP1 from the membrane and all proteins were recovered in the final pellet extracted with SDS (Fig. 7). This behavior is typical for integral membrane proteins which span the lipid bilayer, and is consistent with surface exposed PfEMP1, while it differs from the profile described for the internal PfEMP1 population (Papakrivos et al. 2005). In contrast, upon urea extraction both RIFINs and SBP1 were recovered completely in the urea soluble fraction, which was not expected for integral membrane proteins (Fig. 7) and was reminiscent of PfEMP1 behavior (Papakrivos et al. 2005). Thus, taken together these results may imply that RIFINs and SBP1 do in fact span the membrane, as shown by the failure to be extracted with high pH carbonate buffer, but that this conformation is maintained by protein-protein interactions rather than by direct interaction with the membrane lipids.

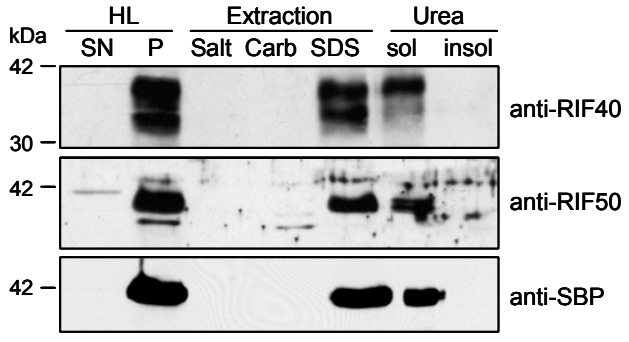

Fig. 7 Solubility of RIFIN proteins
Trophozoite infected erythrocytes of the FCR3S1.2 strain were lysed by hypotonic lysis (HL) and separated by centrifugation into a supernatant (SN) and a pellet (P) fraction. Membrane pellet fractions were either sequentially extracted with salt (Salt) and carbonate (Carb) buffers and the remaining pellet solubilized in SDS buffer (SDS), or extracted with 8M urea and separated into a soluble (sol) and an insoluble (insol) fraction by centrifugation after dialysis. Equivalents of $1x10^7$ cells were loaded in each lane. Samples were analyzed by 12% SDS-PAGE and western blotting. Anitbodies tested were anti-RIF40, anti-RIF50 and anti-SBP.

3.1.4 RIFIN topology diverges from the predicted model

Both the predicted domain structure as well as the assumption that RIFINs are variant antigens at the surface of the IE endorse a model for the membrane topology of RIFINs according to which the variable domain would be exposed at the surface of the IE, while the semiconserved domains point inwards (Cheng et al. 1998). However, evidence for an association of RIFINs with the erythrocyte membrane thus far only comes from surface iodination experiments of IE (Fernandez et al. 1999), and the surface topology has not yet been studied. It was therefore aimed to examine surface exposure and topology of RIFINs in more detail.

3.1.4.1 FACS analysis of infected erythrocytes

First, flow-cytometry experiments were performed on MACS enriched parasites using anti-RIF40 and anti-RIF50 antisera as well as a pool of human immune sera from African adults living in endemic areas (Fig. 8B). As negative controls, parasite IE were in parallel incubated with secondary and tertiary antibodies only, or rat pre-immune sera were used as an isotype control. The human immune sera readily reacted with the majority of the IE in comparison with the secondary/tertiary antibody negative control. In contrast, no positive cell population was detected with either of the two anti-RIFIN antisera, as evidenced by the comparison of the fluorescence intensity with both isotype and secondary/tertiary antibody controls (only shown for the pre-immune serum isotype control) (Fig. 8B).

The lack of RIFIN-specific surface reactivity was surprising given that the recombinant proteins RIF40 and RIF50 used in this study stretch over both the semiconserved domain and parts of the variable domain (Fig. 8A). As a consequence, it was actually expected that the polyclonal animal antisera contain antibodies directed against semiconserved as well as against variable epitopes. However, sequence alignments suggest that short conserved stretches potentially serving as epitopes for immune recognition of paralogous variants are rarely found in the variable domain of RIFINs, and such epitopes are more frequent in the semiconserved domains (as for example evident in the alignment in Fig. 12). From this, it follows that reactivity of the anti-RIFIN antisera against variable domains of RIFIN variants in FCR3 parasites would be limited, and most likely restricted to epitopes in the semiconserved regions of the proteins. Therefore, the lack of surface reactivity of the anti-RIFIN antisera is in support of the aforementioned model for exposure of variable domains on the IE surface.

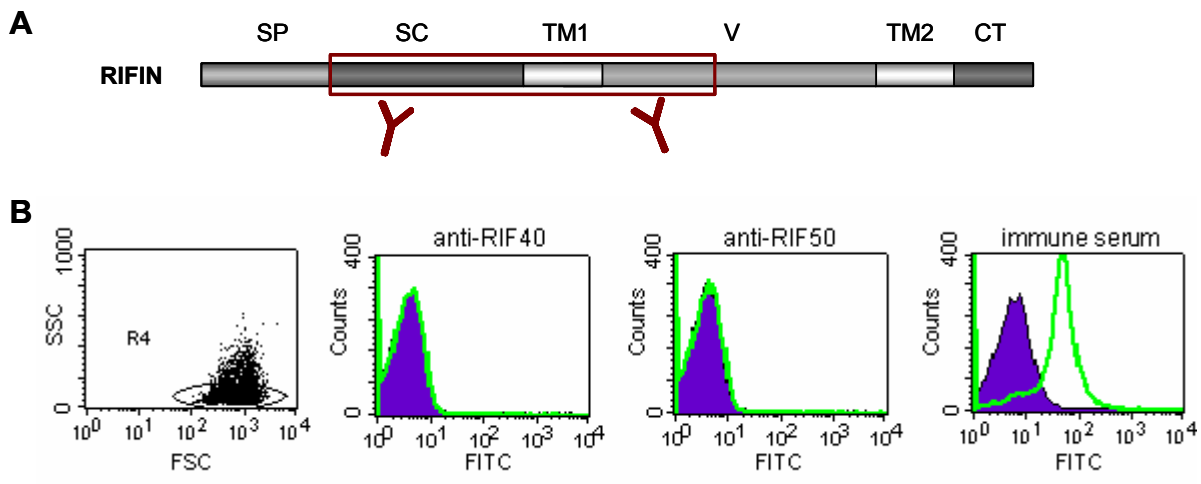

Fig. 8 FACS-analysis of RIFIN surface exposure
A: Graph depicting the region comprising the recombinant RIFIN proteins used for the generation of anti-RIF40 and anti-RIF50 antisera (red frame). Both, parts of the semi-conserved (SC) as well as of the variable region (V) are included. SP: signal peptide, TM: transmembrane domain, CT: conserved C-terminal domain. **B**: The surface recognition of anti-RIF40 and anti-RIF50 antisera on trophozoite infected erythrocytes was tested by FACS analysis. MACS enriched trophozoite infected erythrocytes were incubated with anti-RIF40, anti-RIF50 or human immune serum. Primary antibodies were detected by staining with FITC labelled secondary goat anti-mouse or goat anti-human antibodies. Panel 1: Forward/Side scatter plot. The gate R4 contains the infected erythrocyte population. FSC: forward scatter, SSC: side scatter. Panels 2-4: Proportion of FITC positive infected erythrocytes in comparison to negative controls. Green peak: anti-RIF40, anti-RIF50 and human immune serum, respectively; purple peak: negative controls.

3.1.4.2 Surface trypsinization experiments

According to the model, the semiconserved N-terminal domain of the protein would project into the lumen of the IE. To test this, MACS enriched IE were treated with trypsin at a concentration of 1 mg/ml to remove all protein domains which are exposed at the surface. As a control, an aliquot of the cells was left untreated. After inactivation of the protease, both samples were lysed and extracted with SDS and the lysates were analyzed by western blotting (Fig. 9A). Under these conditions, antibodies directed against the C-terminal ATS segment of PfEMP1 detect a characteristic 80 kDa tryptic fragment corresponding to the intracellular PfEMP1 domain in the trypsin treated IE lysate, which differentiates the surface exposed population of molecules from an internal pool (Papakrivos et al. 2005; Waterkeyn et al. 2000). In this analysis, a tryptic fragment of the corresponding size was indeed evident in the treated sample (Fig. 9A, blue asterisk), and the intensity of the full length PfEMP1 proteins of approximately 250 kDa was markedly reduced in comparison with the untreated cells. In contrast, surprisingly neither of the two anti-RIFIN antisera reacted with a smaller fragment of the estimated size of roughly 18 kDa for the semiconserved domain, and the intensity of the main RIFIN bands did not decrease significantly. Interestingly, however, a weaker protein

band detectable with anti-RIF40 at ~35 kDa in untreated cells disappeared completely after trypsinization, possibly representing a surface exposed pool of RIFINs (Fig. 9A, red asterisk). Human spectrin, which is a cytoskeletal protein that lines the inner face of the erythrocyte plasma membrane, as well as the MC protein SBP1 were both resistant to trypsinization, indicating that the integrity of the IE was not disrupted after surface trypsinization and that internal proteins were indeed protected from digestion by the protease (Fig. 9A). However, the results concerning RIFINs lacking a protected peptide representing the semiconserved N-terminal domain contradicted the proposed topology model.

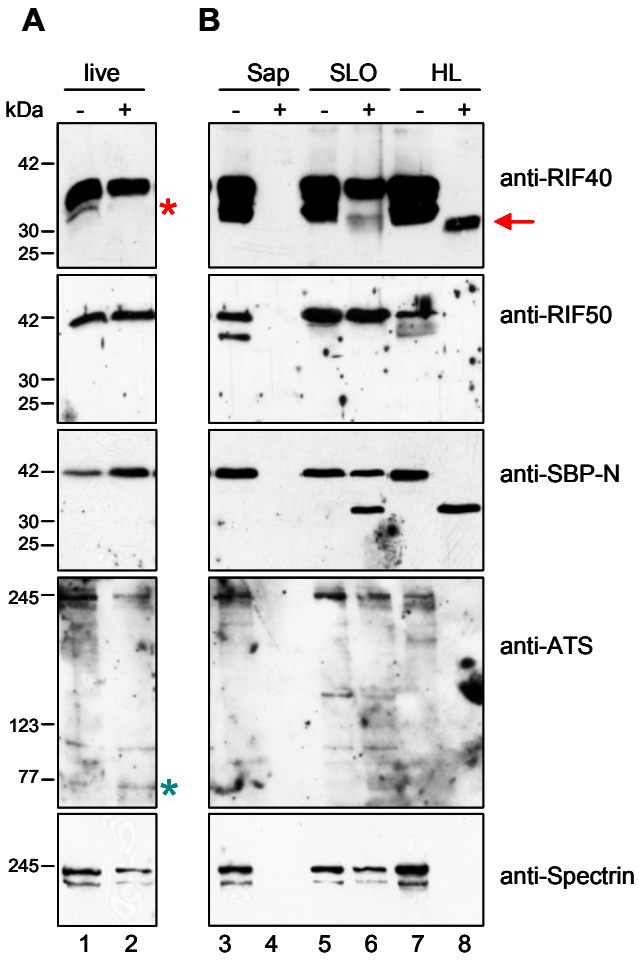

Fig. 9 Protease protection assay
MACS enriched trophozoite infected erythrocytes of the FCR3S1.2 strain were **A:** left intact (live) and **B:** permeabilized with saponin (Sap), streptolysin O (SLO), or subjected to hypotonic lysis (HL). The cells were separated into a pellet and a supernatant fraction by centrifugation. The pellet fractions were subsequently either treated with trypsin (+; lanes 2, 4, 6 and 8) or left untreated (-; lanes 1, 3, 5 and 7). The samples were solubilized in SDS sample buffer, separated by 15% SDS-PAGE and analyzed by western blotting. Equivalents of $1x10^7$ cells were loaded in each lane. The blots were probed with anti-RIF40 and anti-RIF50 antisera. As controls, anti-SBP-N antibodies directed against the N-terminal domain of the skeleton binding protein SBP1, anti-ATS antibodies against the acidic terminal sequence of PfEMP1 proteins, and anti-Spectrin antiserum directed against human spectrin were used. Red asterisk: RIFIN band dissapearing upon trypsinization, green asterisk: tryptic PfEMP1 fragment protected in live cells, red arrow: tryptic RIFIN fragment protected after SLO and HL.

3.1.4.3 Trypsinization of permeabilized IE

To further decipher this puzzle it was next aimed to analyze the topology of RIFINs in permeabilized IE, which allows access to the internal protein pools. Since RIFINs have been described to be transported towards the erythrocyte surface via MC (Haeggstrom et al. 2004),

protease treatment in conjunction with differential permeabilization should allow assessment of the transmembrane topology at these structures.

MACS enriched IE were treated with saponin or SLO, or disrupted by hypotonic lysis according to the methods described before, incubated with or without trypsin, and analyzed by western blotting (Fig. 9B). Upon saponin permeabilization, trypsin treated IE were negative for RIFINs and PfEMP1 as well as the two marker proteins used in this study, in contrast to the untreated control samples. This indicated that at the developmental stage chosen for the analysis, the complete pool of these parasite-derived proteins had been exported from the parasite into the erythrocyte cytoplasm (Fig. 9B, lanes 3 and 4).

After SLO permeabilization or hypotonic lysis (lanes 5-8), antibodies directed against the N-terminal domain of the transmembrane protein SBP1 reacted with a 32 kDa tryptic fragment that was protected from cleavage. This is in concordance with the experimentally determined topology for this protein at the MC membrane (Blisnick et al. 2000). Neither anti-Spectrin nor anti-ATS antibodies reacted with truncated proteins, as predicted for the topology of their respective target proteins. However, anti-RIF40 antibodies detected a fragment of approximately 30 kDa protected from the protease in the trypsinized preparation, which was absent in the untreated controls (Fig. 9B, red arrow). In contrast, no such fragment was detected by anti-RIF50 antibodies, indicating different topologies for the RIFIN variants labelled by the two antisera at the MC membrane.

The observation that a large amount of full length SBP1, spectrin and PfEMP1 proteins was still present after SLO treatment demonstrated that permeabilization had been inefficient and that a great proportion of the cells had resisted the perforation. Nonetheless, the results showing the protection of the N-terminal domain of the MC spanning transmembrane protein SBP1 after hypotonic lysis indicate that the quality of the membrane association and the topology of proteins at the MC membrane are equally well represented using this technique.

Notably, the 35 kDa band detected with anti-RIF40, which was observed to disappear upon surface trypsinization and thus interpreted to represent a surface exposed pool of RIFINs (lane 2, red asterisk), was more strongly visible in the permeabilized fraction than in the non-permeabilized fraction, when both were untreated. It is speculated that this might be the result of degradation of the protein, since this set of experiments was performed in the absence of inhibitors in order to facilitate trypsin cleavage.

The interpretation of the results presented here would be much simplified by the knowledge of the identity of the recognized proteins and the tryptic fragment. Several attempts to isolate the RIFIN molecules by immunoprecipitation using the anti-RIF40 and

anti-RIF50 antisera were made, with the aim to analyze the immunoprecipitated proteins individually by mass spectrometry. Until now, however, all efforts to purify RIFINs and the tryptic fragment in large enough quantities necessary for mass spectrometry have failed.

3.1.5 Immunoelectron microscopy demonstrates RIFIN association with knobs and Maurer's Clefts

Since the results from the FACS analysis and the protease protection assays shed doubts about the surface association of RIFINs, the next step was to examine these molecules using microscopic techniques in conjunction with immunolabeling. Initial attempts to localize RIFINs in IE by immunoelectron microscopy (IEM) failed repeatedly using various protocols, possibly due to rarity of expressed antigens or fixation-induced modifications of the epitopes. In view of this, a pre-embedding staining protocol was established on saponin permeabilized parasitized RBC. Under these conditions, all proteins that are exported into the erythrocyte are accessible to the antibodies, while those within the parasite are covered (Fig. 5).

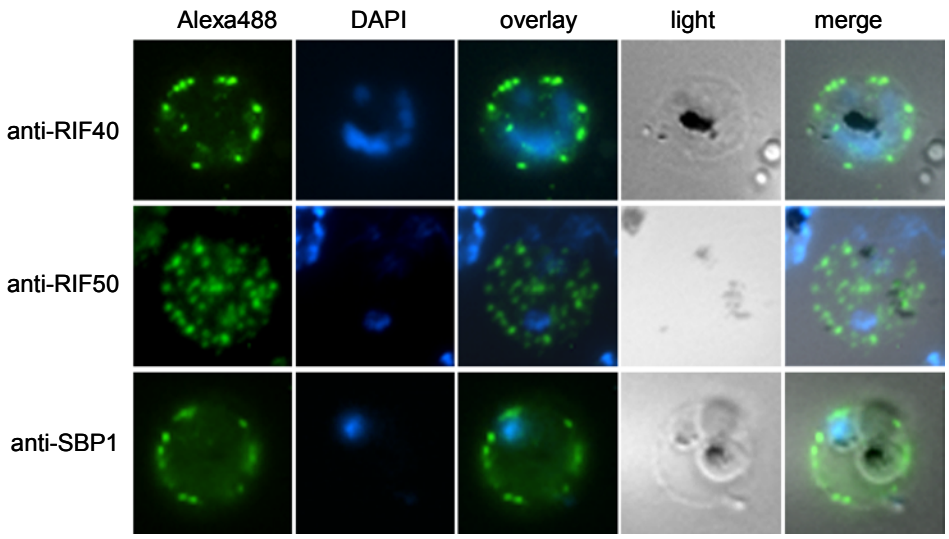

Fig. 10 Immunofluorescence anlaysis of saponin permeabilized infected erythrocytes
MACS enriched trophozoite infected erythrocytes were permeabilized with saponin and incubated with anti-RIF40, anti-RIF50 or anti-SBP1 antibodies. For detection of the primary antibodies, Alexa488 coupled secondary antibodies were used (green). Nuclei were stained with DAPI (blue).

In order to check out optimal conditions for IEM, MACS enriched permeabilized IE were first analyzed by immunofluorescence microscopy. Both anti-RIF40 and anti-RIF50 antisera created a strong punctate pattern reminiscent of the one obtained for the MC protein SBP1 (Fig. 10). Discrimination between potentially surface associated proteins and MC restricted

proteins is, however, not possible with this method. No staining was seen with pre-immune antisera tested in parallel.

Electronmicrographs depicting the intracellular localization of RIFIN molecules in the permeabilized IE are presented in Fig. 11. RIFINs were detected with anti-RIF40 antibodies and visualized by immunogold labeling. A most striking observation is the presence of gold particles decorating electron-dense knobs at the membrane of the parasitized cell (Fig. 11A). This provides clear evidence for the surface association of RIFINs and in addition characterizes for the first time the knobs as the sites of RIFIN anchorage in the membrane. Moreover, the MC, visible as slender membrane bordered tubes, were covered with gold particles (Fig. 11A and B). In some sections it was observed that spherical electron-lucent structures extended from the MC and the inner face of the host cell membrane and were labeled with the anti-RIF40 antibodies (Fig. 11B, arrow heads). Similar sites have previously been reported to be associated with PfEMP1 molecules and have been discussed as regions at which PfEMP1 carrying structures are released from the MC (Kriek et al. 2003).

Currently, only data for anti-RIF40 are available. Experiments using anti-RIF50 antiserum for comparison have been performed but the analysis is not yet completed.

3.1.6 Conclusion

The results presented in this section demonstrate that RIFIN protein expression starts 12 hours post invasion and is at its maximum 36 hours post invasion. RIFINs are insoluble under conditions in which the soluble protein PP5 is released from the cells, indicating that they are associated with membranes. With respect to the extractability in detergent, high pH carbonate buffer and urea, RIFINs behave in a similar fashion to the integral MC resident membrane protein SBP1, thus pointing to them as membrane-spanning proteins that are anchored by protein-protein interactions, probably in cholesterol-rich raft-like microdomains. In FACS analysis, surface exposure of RIFINs was not detected with the reagents under investigation. Nevertheless, IEM demonstrated a clear association of RIFINs with knobs at the IE membrane. Protease protection assays in permeabilized or non-permeabilized IE suggest that different RIFIN populations distinguished by anti-RIF40 and anti-RIF50 antisera exhibit different properties concerning their topologies at the MC and the IE membrane.

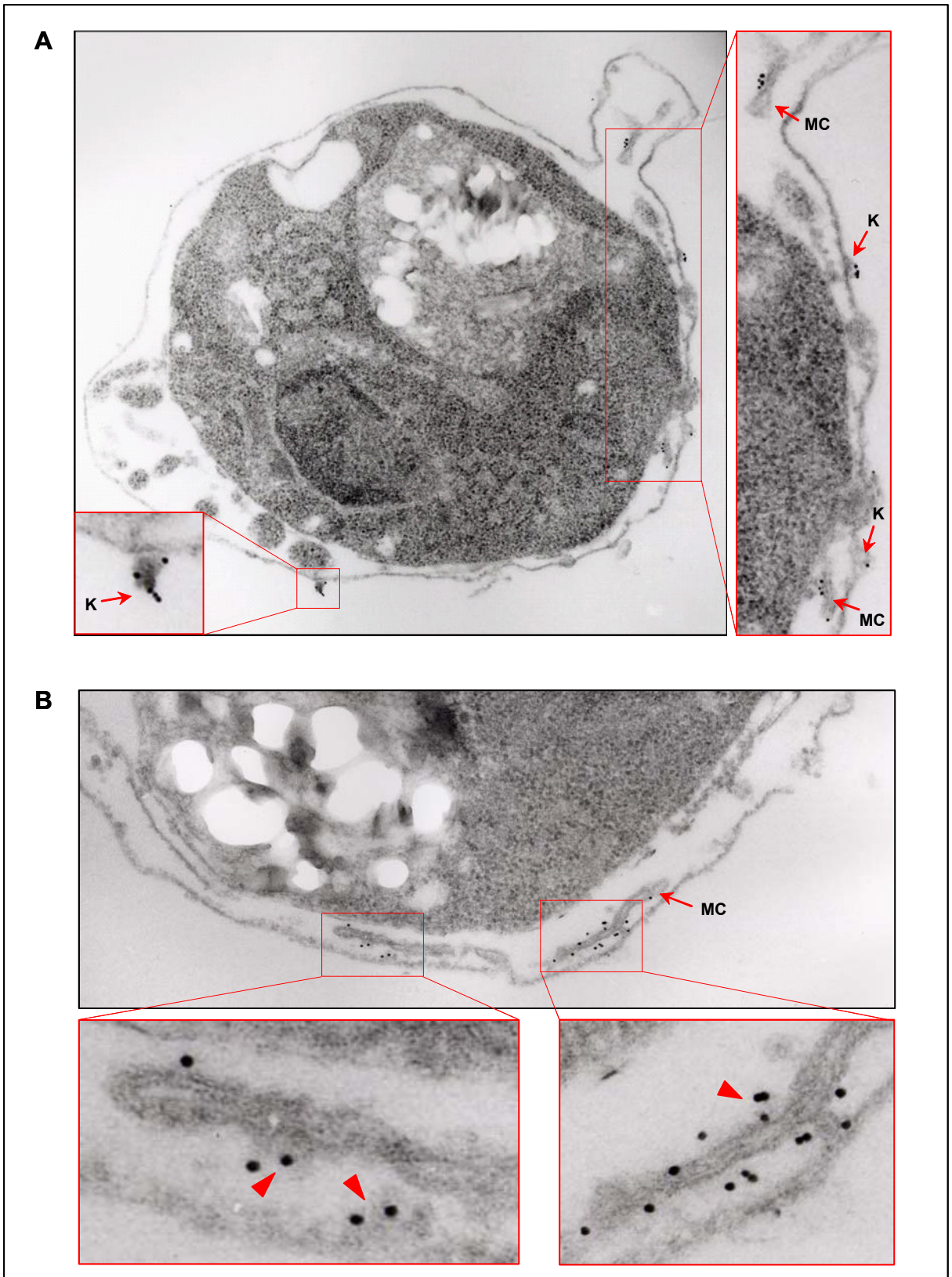

Fig. 11 Immunoelectron microscopy (IEM) of saponin permeabilized infected erythrocytes
A pre-embedding staining protocol was applied to analyze RIFIN membrane association by IEM. Trophozoite infected erythrocytes were permeabilized with saponin and sequentially incubated with rat anti-RIF40 or rat pre-immune antiserum, secondary rabbit anti-rat antibodies, and protein A coated gold particles. **A** and **B**: Different sections are shown depicting RIFIN association with knobs (K) and with Maurer's clefts (MC). Enlargements are framed in red. Arrowheads: translucent bulges eminating from the MC.

3.2 Characterization of two RIFIN subgroups in the asexual life cycle

The above experiments demonstrated the existence of RIFIN variants which differ from each other with respect to their topological association with the plasma membrane. This heterogeneity motivated us to take a closer look at the available sequence data, with the aim to possibly identify and characterize structurally distinct subgroups in the multigene family of RIFINs.

3.2.1 Subgrouping into A- and B-type RIFINs

Alignments of multiple RIFIN sequences showed first indications for the existence of two subgroups which differ from each other by the presence or absence of a 25 amino acid consensus peptide, located approximately 66 residues downstream of the PEXEL/HT motif (Fig. 12). A search of the literature revealed that such a distinction had previously been noted after completion of the genome sequencing project on the 3D7 parasite (Gardner et al. 2002).

To determine whether these groups were also present in other parasite strains and patient isolates, BLAST searches were performed on the sequence data of the IT strain and a Ghanaian isolate, which are both available at The Wellcome Trust Sanger Institute (http://www.sanger. ac.uk/cgi-bin/blast/submitblast/p_falciparum), as well as on the sequence data of the strains HB3 and Dd2 accessible at the Broad Institute (http://www.broad.mit.edu/annotation/genome/plasmodium_falciparum_spp/Blast.html). Published RIFIN sequences from field isolates originating from Gabon (Abdel-Latif et al. 2002) and Brazil (Albrecht et al. 2006) were also included in the study. The analyses confirmed that all of these parasite genomes carried genes encoding variants of the two RIFIN subtypes.

In order to discriminate the two groups, RIFIN variants containing the consensus peptide were termed A-type RIFINs, and those variants lacking it B-type RIFINs (Joannin et al. submitted manuscript). In the 3D7 genome, 73 % of all RIFINs belong to the A-type and 23 % to the B-type. An alignment of representative variants of each subgroup from 3D7 and isolates originating from different geographic regions is shown in Fig. 12.

To identify other subtype specific features, the consensus sequences derived by alignment of all 3D7 A- and B-type RIFINs were represented as sequence logos, in which the frequency of an amino acid at a certain position is symbolized by letter size (Schneider and Stephens 1990). Sequence logos for all RIFINs as well as separately for A- and B-type RIFINs are shown in the supplementary material (Fig. S1, S2). Several distinctive features discriminating

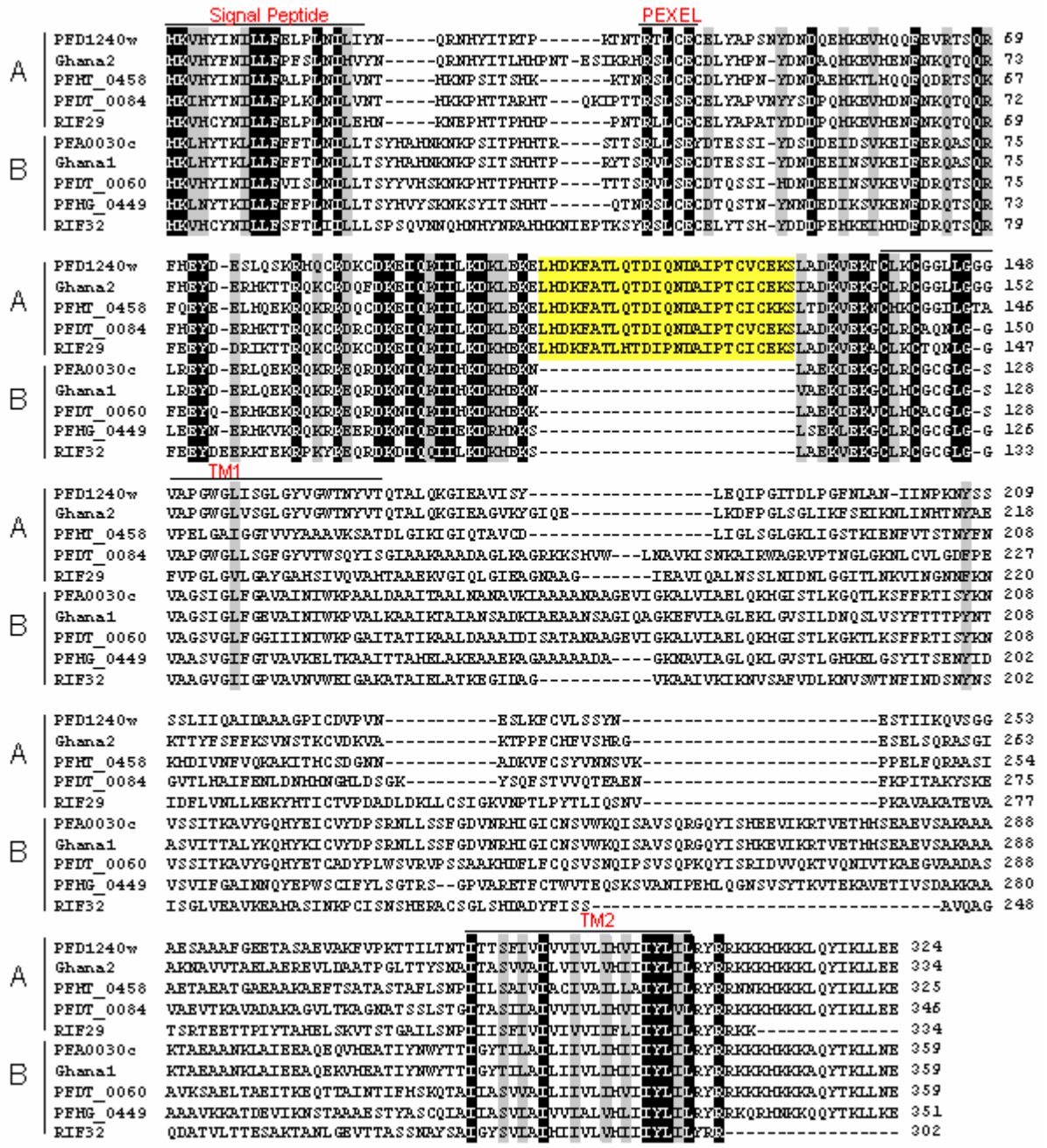

Fig. 12 Alignment of RIFIN amino acid sequences from laboratory adapted strains and isolates originating from different geographic regions

3D7 sequences PFD1240 and PFA0030c were retrieved from PlasmoDB. RIFIN amino acid sequences from the parasite clones HB3 (PFHT_04587 and PFHG_04496), originating from Honduras, and Dd2 (PFDT_00841 and PFDT_00601), originating from Indochina, were retrieved from The Broad Institute. The sequence of the Ghanaian isolate is available at The Wellcome Trust Sanger Institute, and RIFIN sequences Ghana 1 and Ghana 2 were identified by BLAST searches. Accession numbers for the RIFIN sequences RIF29 and RIF32, originating from Gabon, are AF483817 and AF483818. Identical residues are highlighted in black, while similar residues are shaded in grey. The 25 amino acid peptide which distinguishes the A- and the B-type RIFINs is highlighted in yellow. TM: transmembrane domain.

the two groups apart from the 25 amino acid peptide were thus revealed, and some of these differences are depicted in the graphical illustration given in Fig. 13 and summarized in Table 1. For example, although several conserved cysteine residues are common to all RIFINs (Fig. 13, grey arrows) five cysteines are found exclusively in the semiconserved domain of A-type RIFINs (Fig. 13, blue arrows), and another one only in the putative first transmembrane domain of B-type RIFINs (Fig. 13, red arrows). Other highly conserved subtype-specific residues are found in the small C-terminal domain (Table 1). Moreover, several conserved amino acids are present in the A-type specific 25 amino acid motif, as depicted by the representation as a sequence logo in Fig. 13.

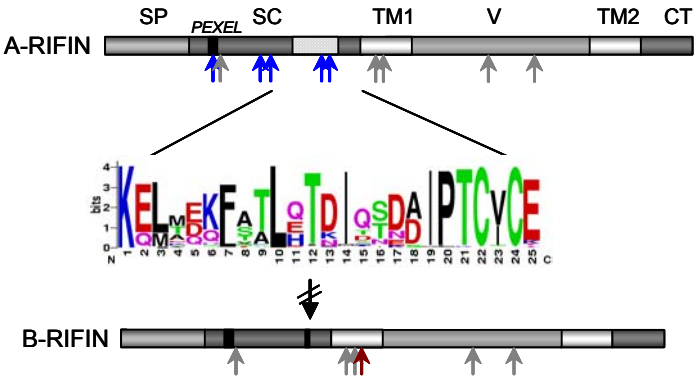

Fig. 13 Definition of two RIFIN subgroups
A-type and B-type RIFINs share the same predicted structure but differ by the presence or absence of the 25 amino acid motif depicted as a sequence logo. Conserved cysteine residues are represented by arrows. Grey: conserved in both groups, blue: conserved in A-types, red: conserved in B-types. SP: signal peptide, SC: semiconserved domain, TM: transmebrane domain, V: variable domain, CT: conserved C-terminal domain. (compiled in collaboration with Nicolas Joannin, Karolinska Institutet, Stockholm).

Table 1: Summary of RIFIN subgroup specific features

	A-Type	B-Type
Proportion of RIFIN variants	73 %	27 %
Protein size	310-390 AA	280-365 AA
PEXEL/HT	+	+
25 AA motif	+	-
No. of subtype specific conserved cysteines	5	1
Distinct conserved residues in certain positions in the C-ter domain	Isoleucine Glutamate/Lysine Glutamate	Threonine Asparagine Glutamate/Glutamine

To further evaluate the definition of the two groups by phylogenetic methods, distance trees were inferred from the RIFIN amino acid sequences using the p-distance/Neighbor-Joining method. Gaps were treated as complete deletions in this analysis, thus the resulting tree is constructed only on information from sites that are present in all sequences. The 25 amino acid insertion thus has no impact on the tree topology. Despite the exclusion of this

discriminative feature, A- and B-type sequences clearly separated into two clades (Fig. 14). Although bootstrap values at the A- and B-type branches were not significant, a second analysis was performed using the Maximum Parsimony method and found to confirm the tree topology. Only few sequences were seen to group under the other RIFIN subtype.

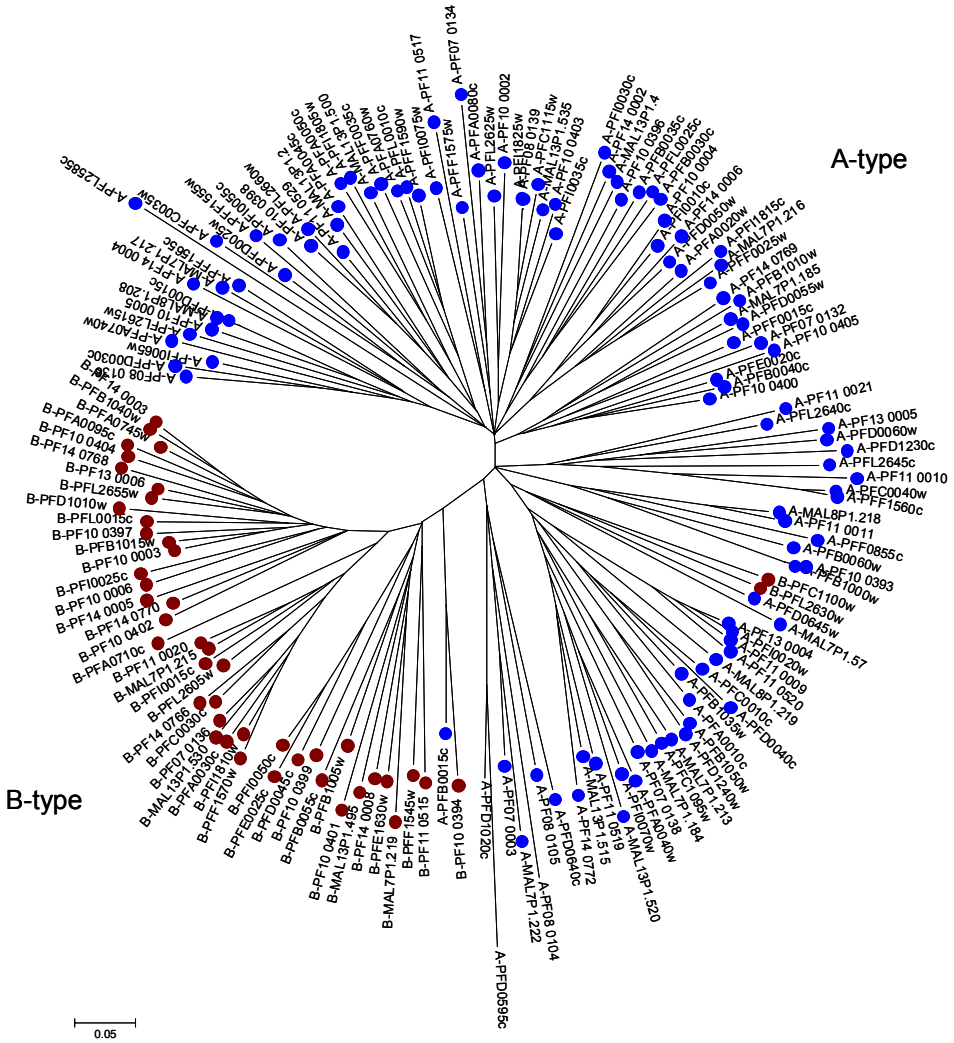

Fig. 14 Distance tree of protein coding RIFIN sequences
Distance trees were constructed using the p-distance/Neighbor-Joining method. Sites exhibiting gaps in the alignment were treated as complete deletions. A-type RIFINs are labelled with a blue dot, B-type RIFINs with a red dot. Bootstrap values discriminating the two groups were not significant and are thus not shown, but Maximum Parsimony analysis confirmed the tree topology.

3.2.2 RT-PCR analysis of RIFIN expression

To analyze the expression of variants of both subtypes in asexual parasites, reverse transcriptase PCR (RT-PCR) experiments were performed. Subgroup specific degenerate primer pairs were designed on sequences in the semiconserved region of both RIFIN-types incorporating the region coding for the 25 amino acid peptide (Fig. 15A). The primer pairs

were first evaluated by performing virtual PCR experiments on the 3D7 genome sequence at http://insilico.ehu.es/eukaryota/. Of the 102 A-type RIFINs, the degenerate primer sequences RIF-A For and RIF-A Rev were capable of "amplifying" 45 variants with the calculated size of 134 bp when no mismatch was allowed, but the coverage increased up to 99 variants when 1 mismatch was admitted. Similarly, B-type specific primer pairs RIF-B For and RIF-B Rev could according to this model detect 21 sequences of the predicted length of 178 bp without mismatch, and 37 sequences with 1 mismatch allowed (Table 2). The oligonucleotide primers thus appeared theoretically to be highly specific for each subtype (as indicated by the conserved size of the amplicons) and widely reactive with various sequences belonging to the corresponding group, covering almost the entire repertoire.

Table 2: Evaluation of degenerate primer pairs by virtual PCR

	No. of RIFINs	0 mismatches	1 mismatch
RIF-A For and Rev	102	45 sequences 134 bp	99 sequences 134 bp
RIF-B For and Rev	41	21 sequences 178 bp	37 sequences 178 bp

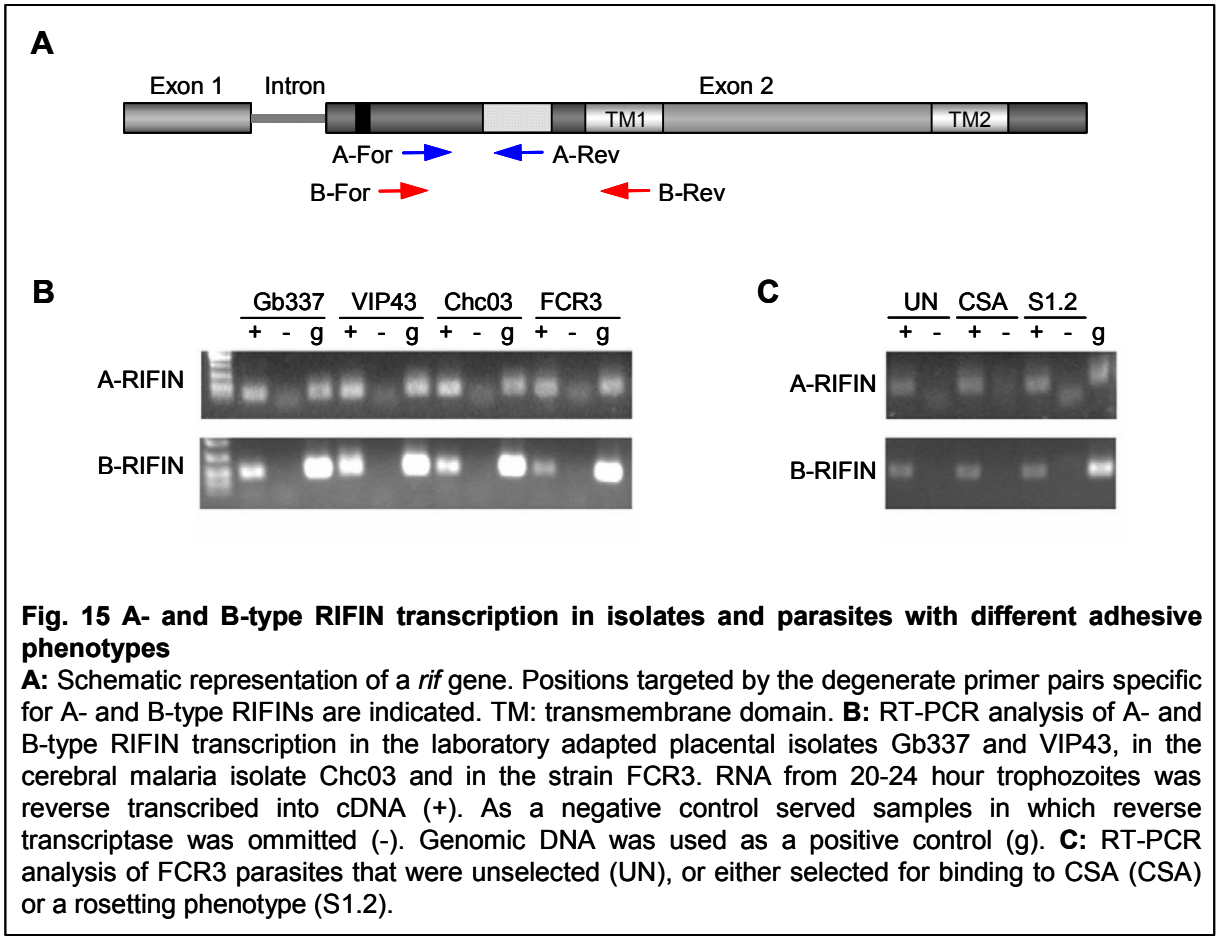

Fig. 15 A- and B-type RIFIN transcription in isolates and parasites with different adhesive phenotypes
A: Schematic representation of a *rif* gene. Positions targeted by the degenerate primer pairs specific for A- and B-type RIFINs are indicated. TM: transmembrane domain. **B:** RT-PCR analysis of A- and B-type RIFIN transcription in the laboratory adapted placental isolates Gb337 and VIP43, in the cerebral malaria isolate Chc03 and in the strain FCR3. RNA from 20-24 hour trophozoites was reverse transcribed into cDNA (+). As a negative control served samples in which reverse transcriptase was ommitted (-). Genomic DNA was used as a positive control (g). **C:** RT-PCR analysis of FCR3 parasites that were unselected (UN), or either selected for binding to CSA (CSA) or a rosetting phenotype (S1.2).

Based on the above findings, transcriptional analysis was carried out using RNA purified from 20 to 24 hour trophozoite IE from different *Plasmodium* field isolates (Gb337, VIP43, Chc03) and the laboratory adapted strain FCR3. Equal amounts of RNA were reverse transcribed into cDNA and one sample each in which reverse transcriptase was omitted served as control to test for DNA contamination. The A- and B-type RIFIN transcripts were amplified by PCR with the degenerate primer pairs from the template cDNA. Genomic DNA was amplified in parallel as a positive control. In all parasite strains, both A-type and B-type RIFIN transcripts were detectable (Fig. 15B).

In order to assess whether certain binding phenotypes might be linked to subtype specific *rif* transcription, RNA from unselected and CSA selected FCR3 parasites as well as the rosetting FCR3 subclone FCR3S1.2 was analyzed. Both the 134 bp A-type product as well as the 178 bp B-type product were detected after RT-PCR amplification, indicating that RIFIN subtype expression was not restricted to any of the binding phenotypes analyzed (Fig. 15C).

3.2.3 Characterization of the subgroup-specificity of anti-RIFIN antisera

To carry out a more extensive analysis of the two RIFIN subfamilies on the protein level, a panel of anti-RIFIN antisera was evaluated for their specificities to react with A- and B-type RIFINs. Two antisera each against A-type RIFINs (rabbit anti-A_{565} and rat anti-A_{RIF29}) and B-types (rabbit anti-B_{562} and mouse anti-$B_{RIF\Delta NC}$) were available for study (Abdel-Latif et al. 2002; Fernandez et al. 1999; Khattab and Klinkert 2006). The RIFIN sequences included in the recombinant proteins and peptides used for antibody production are outlined in Fig. 16A and described in Table 3.

Table 3: Description of antisera

Antiserum	Gene ID	Covered sequence
anti-A_{565}	PFB1035w	LVLRYLRKKKMKKKLEYIKLLKE
anti-B_{562}	PFB1040w	LVLRYRRKKKMKKKAEYTKLLNQ
anti-A_{RIF29}	AF483817	Leu38 - Ile201
anti-$B_{RIF\Delta NC}$	PFI0050c	Pro34 - Gly261

Since all four antisera were elicited against peptides or proteins of semiconserved or conserved nature, it was important to address the extent to which they crossreact with different RIFIN variants. In previous experiments, both the anti-A_{565} and anti-B_{562} sera were capable of immunoprecipitating several RIFIN variants from wild isolates, demonstrating their specific reactivity with RIFIN sequences (Fernandez et al. 1999). Both antisera are

directed against peptides in the highly conserved C-terminus of RIFINs. In comparison to the use of recombinant proteins containing only partially conserved parts of the proteins, these sera have the advantage of covering a much wider range of different variants. Despite the high conservation in this area, A- and B-type variants differ in their consensus motifs by two or three conserved amino acids, as highlighted in red in Table 3. Regarding the high selectivity of antibodies, these differences could well be sufficient to mediate subtype specificity of the peptide antisera, although the possibility of cross-reactivity between the two subtypes can not entirely be ruled out.

To evaluate anti-A_{RIF29} and anti-$B_{RIF\Delta NC}$ antisera for reactivity with their respective subtype, their capacity to recognize recombinant RIFIN variants of both types in western blots was tested. Three A-type RIFINs (RIF29, RIF44 and RIF50) (Abdel-Latif et al. 2002) as well as one B-type RIFIN (RIFΔNC) (Khattab and Klinkert 2006) were available as 6x histidine tagged recombinant proteins. Of each, 150 ng were analyzed and equal loading was verified by reactivity with anti-His_6 antiserum (Fig. 16B, 1st panel). Prior to the analysis, both anti-RIFIN antisera were cross-adsorbed with 1 μM of unrelated recombinant proteins, the genes of which were cloned into the same vector backbone, in order to eliminate antibodies reactive with vector-derived epitopes (such as the 6x histidine tag). Consequently, anti-A_{RIF29} was found to react exclusively with itself and the other two recombinant A-type RIFIN proteins RIF44 and RIF50, but not with recombinant B-type RIFIN RIFΔNC. Vice versa, anti-$B_{RIF\Delta NC}$ specifically recognized the corresponding B-type variant only, but none of the A-type variants (Fig. 16B, 2nd and 3rd panels). These results confirmed subtype specificity by showing that crossreactivity of the antisera with variants of the other subgroup was minimal. Moreover, crossreactivity of anti-A_{RIF29} with other A-type RIFINs demonstrated the capacity of the polyclonal serum to recognize paralogous RIFIN variants of the same subtype. The availability of only one B-type recombinant protein did not allow a similar evaluation for the reactivity of anti-$B_{RIF\Delta NC}$ antiserum with other B-type variants. Nonetheless, the findings suggested that in combination the four antiserum samples should be sufficiently reactive with a large array of RIFIN variants in the parasite to allow rather general conclusions to be drawn for each subfamily.

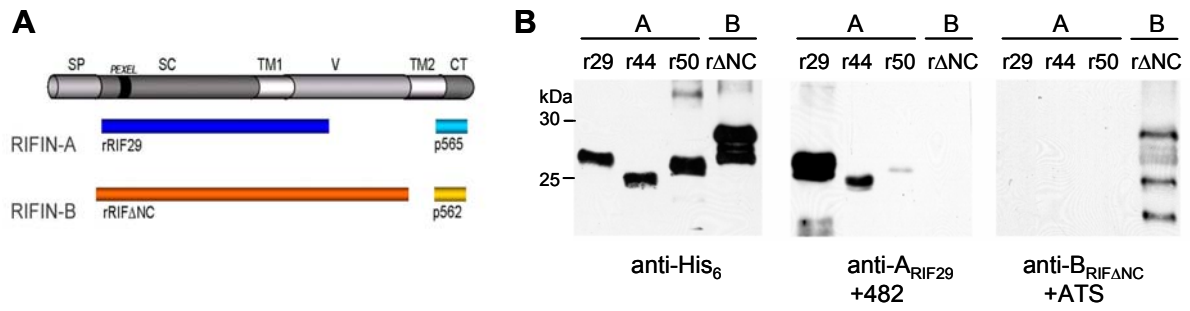

Fig. 16 Characterization of subtype specific antisera
A: Schematic representation of a RIFIN protein. The bars depict the RIFIN regions included in the recombinant proteins rRIF29 and rRIFΔNC as well as the peptides p565 and p562, which are representative A- or B-type RIFIN sequences. The recombinant proteins span both, regions of the semiconserved (SC) and of the variable (V) domain and contain the first putative trans-membrane domain (TM). The peptide sequences are derived from the conserved C-terminal domain (CT) which differs silghtly between A- and B-type RIFINs. SP: Signal peptid. **B:** Analysis of the subtype specific RIFIN recognition of anti-A_{RIF29} and anti-$B_{RIFΔNC}$ antisera. Equal amounts of recombinant A-type (RIF29, RIF44, RIF50) and B-type (RIFΔNC) RIFINs were seperated by SDS-PAGE and analyzed by western blotting. Probing with anti-His_6 antibodies verified equal loading. In order to eliminate antibodies reactive with vector derived epitopes such as the 6x His-tag, the anti-RIFIN antisera were pre-adsorbed with irrelevant recombinant proteins (482 and ATS) expressed from the same cloning vector background. Both, anti-A_{RIF29} and anti-$B_{RIFΔNC}$ react specifically with proteins of their respective subtype. Reactivity of anti-A_{RIF29} with other A-type RIFINs moreover demonstrates crossreactivity with other variants of the same subtype.

3.2.4 A- and B-type RIFINs exhibit differential subcellular localizations in infected erythrocytes

In order to examine the two RIFIN subgroups at the cellular level, their expression patterns were characterized by immunofluorescence analysis (IFA). Time course studies were performed on IE at the ring stage (8-12 hours post invasion), mid trophozoite stage (24-30 hours post invasion) and schizont stage (40-48 hours post invasion) (Fig. 17A). Smears of synchronized cultures of the FCR3S1.2 parasite line were prepared and fixed with methanol before incubation with the antisera.

Using anti-A_{565} and anti-A_{RIF29} antisera, staining of dotted structures in the cytosol of ring-, trophozoite- and schizont-IE was observed (Fig. 17A). During the development of the parasites from ring to schizont stages, the proportion of positive cells was found to increase steadily up to over 90 % for both antisera. Colocalization with SBP1 confirmed association of anti-A_{RIF29} with the MC (Fig. 17B, upper panel), as previously described for anti-A_{565} (Haeggstrom et al. 2004) and reported here for the anti-RIF40 antiserum (see 3.1.5 and Fig. 10). Using anti-A_{565} antiserum, a strong parasite-associated immunofluorescence, in addition to MC labeling was also observed.

In contrast, no signals related to vesicular structures were detected with the anti-$B_{RIF\Delta NC}$ and anti-B_{562} antisera throughout the different life cycle stages of the parasite. Instead, the bulk of the fluorescence was restricted to the inside of the PV and only a faint diffuse staining of the IE cytosol was observed (Fig. 17A). Double staining with anti-$B_{RIF\Delta NC}$ and antibodies directed against the PVM protein Exp1 (Simmons et al. 1987) showed that the B-type RIFIN-related fluorescence did not overlap with the PVM; instead the fluorescence signal seemed to be confined to the parasite (Fig. 17B, lower panel).

The data presented in this section were obtained with parasites of the FCR3S1.2 clone, however, comparable results were seen when the experiments were repeated on the strains 3D7 and Gb337, indicating conservation of these patterns across *P. falciparum* isolates (data not shown). The results were identical, when air-dried instead of methanol-fixed parasite preparation were used (data not shown).

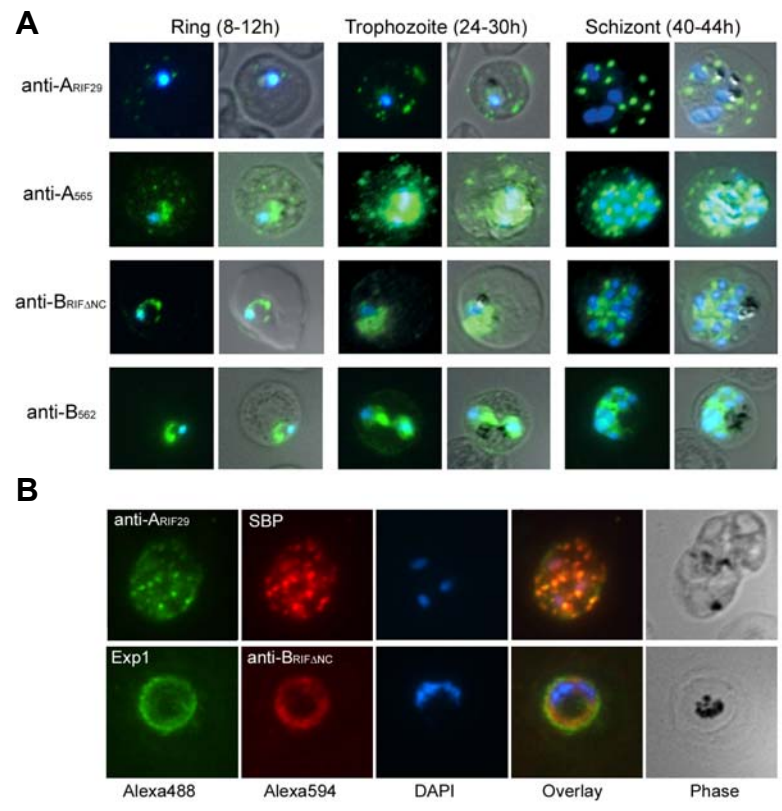

Fig. 17 Immunofluorescence analysis of A- and B-type RIFIN expression in asexual parasites
A: Infected erythrocytes of the FCR3S1.2 parasite clone at ring, trophozoite, and schizont stages were fixed with methanol and RIFIN localization was visualized using anti-A_{RIF29}, anti-A_{565}, anti-$B_{RIF\Delta NC}$ and anti-B_{562} antibodies (green). Nuclei were stained with DAPI (blue). **B:** Analysis of the subcellular localization of RIFINs by double staining with marker proteins. Upper row: anti-A_{RIF29} (green, panel 1) and anti-SBP (red, panel 2); lower row: anti-$B_{RIF\Delta NC}$ (red, panel 2) and anti-Exp-1 (green, panel 1).

3.2.5 Different RIFIN variants exhibit differential developmental regulation

When examining the expression patterns of RIFIN subtypes in fixed preparations of 40-44 hour schizonts, a striking association of the fluorescence with the developing merozoites was observed. A punctate fluorescence was still evident in the erythrocyte cytosol with both anti-

A_{565} and anti-A_{RIF29} antibodies. However, while the anti-A_{RIF29} antiserum exclusively stained the MC in the IE, anti-A_{565}, anti-$B_{RIF\Delta NC}$ and anti-B_{562} additionally showed a strong parasite-associated signal (Fig. 17A).

3.2.5.1 Immunofluorescence analysis of RIFINs in merozoites

Taking this further, the fluorescence pattern of RIFINs in merozoites was investigated by performing IFA on highly synchronized parasite preparations containing mostly mature and rupturing schizonts as well as free merozoites. Here, three different patterns associated with individual merozoites were observed (Fig. 18A). First, with the anti-A_{RIF29} antiserum, no obvious staining was seen to be associated with individual merozoites. Second however, using the anti-A_{565} antiserum, merozoites exhibited a discrete staining at the apical end. Third, with both anti-B-type antibodies anti-$B_{RIF\Delta NC}$ and anti-B_{562}, fluorescence was distributed in a diffuse fashion inside the merozoite cytosol (Fig. 18A). It thus appears that A- and B-type RIFIN variants are not only localized in different subcellular compartments in IE, but are also present in different locations in merozoites. Moreover, the finding that anti-A_{565} is capable of detecting RIFIN variants in merozoites while anti-A_{RIF29} is not, suggests that A-type variants are subject to differential regulation resulting in the divergent developmental expression patterns observed during the maturation of the parasite.

3.2.5.2 Western blot analysis of RIFIN expression in schizonts and merozoites

To confirm the unequal expression of RIFIN polypeptides in merozoites that was detected with the antisera, protein extracts of late schizonts and free naturally released merozoites were analyzed in immunoblots (Fig. 18B). Schizonts were harvested by MACS, while merozoites were purified by repeated centrifugation followed by passage through the MACS column to deplete any contaminating IE. To allow precise comparisons of the proteins that were detected, the blots were stripped and reprobed with the individual antisera. As a control, antibodies against the merozoite-specific protein $MSP1_{42}$ were used (Blackman et al. 1990). As expected, this protein was only observed in the merozoite fraction, thereby ruling out the presence of contaminating proteins from free merozoites in the schizont fraction (Fig. 18C).

In schizont preparations from 3D7, FCR3S1.2 and Gb337 parasite IE, anti-A_{RIF29} antibodies recognized RIFIN variants of around 38, 44 and 43 kDa, respectively (Fig. 18B, blot 1). Only in Gb337 merozoites a faint protein band was seen, whereas no protein from 3D7 and FCR3S1.2 merozoites was recognized by this antiserum. This is concordant with

IFA observations that a minority of merozoites show anti-A_{RIF29} specific labeling on the outside of the merozoite, interpreted here as membrane remnants from ruptured schizonts.

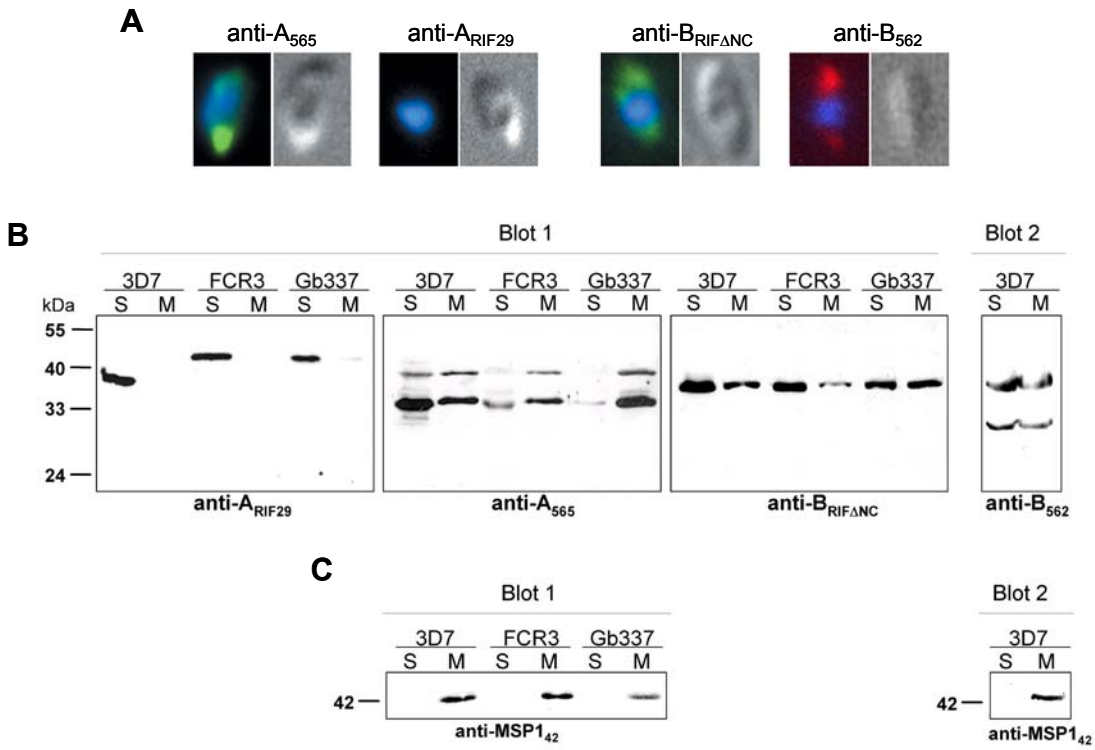

Fig. 18 Expression of A- and B-type RIFINs in merozoites
A: Different patterns of fluorescence were detected with anti-A_{565}, anti-A_{RIF29} and anti-$B_{RIFΔNC}$ (green) or anti-B_{562} (red) in free merozoites. Nuclei were stained with DAPI (blue). **B:** Western blot analysis of parasite extracts from schizonts and merozoites. Schizont (S) and merozoite (M) extracts from 3D7, FCR3S1.2 (FCR3) and Gb337 parasites were separated by 12% SDS-PAGE and analyzed for RIFIN expression by probing sequentially with anti-A_{RIF29}, anti-A_{565} and anti-$B_{RIFΔNC}$ antisera (Blot 1). In an independent experiment, schizont and merozoite extracts from 3D7 parasites were probed with anti-B_{562} antiserum (Blot 2). **C:** Both blots were also probed with mAb 1E1 which detects the 42 kDa proteolytic product $MSP1_{42}$.

With the anti-A_{565} antiserum, several RIFIN variants were recognized in each parasite strain (Fig. 18B, blot 1). Interestingly, none of these proteins correlated in size with the variants recognized by anti-A_{RIF29}. One major band around 39 kDa was consistently recognized in merozoites and to a lesser extent in schizonts of all strains. Another major band of around 35 kDa was evident in schizont extracts of 3D7 and FCR3S1.2 parasites, whereas in the merozoite fractions of all strains and in the Gb337 schizont extract, a slightly larger protein band was observed (36 kDa, Fig. 18B, blot 1). In summary it appears that the set of A-type RIFINs detected in schizonts is partially different from the set in merozoites. Possible explanations for this observation might be the occurrence of a switch in the A-type RIFIN

expression to a different variant, or the involvement of post-translational modifications of the proteins during maturation. Moreover, the results demonstrate that the pool of A-type RIFIN variants recognized by the two anti-A-type antisera does not overlap, but that instead different variants are recognized.

The anti-$B_{RIF\Delta NC}$ antiserum was only reactive with a single protein band around 37 kDa in all strains at both stages (Fig. 18B, blot 1). Because after repeated stripping the blots failed to detect any more proteins, an independent experiment was performed with the anti-B_{562} antiserum on 3D7 parasites. Anti-B_{562} also recognized proteins of the same sizes around 37 and 32 kDa in schizonts and in merozoites (Fig. 18B, blot 2). Stripping and reprobing with anti-$B_{RIF\Delta NC}$ showed that the 37 kDa band exactly corresponded to the protein band detected with anti-$B_{RIF\Delta NC}$, indicating an overlap in the RIFIN repertoires recognized by the two antisera. Taken together, the results obtained with the anti-B-type antisera suggest that the B-type repertoire does not switch during the development from schizonts to merozoites, although the similar size characteristic for different B-type RIFINs does not guarantee for it.
As controls for unspecific background, pre-immune sera for all antibodies were tested in parallel, but were found to show no reactivity.

3.2.5.3 RT-PCR analysis of RIFIN expression in trophozoites and schizonts

To shed light on the switching of variants during development, an analysis of the events occurring on the RNA level was performed. RIFIN transcripts were amplified with the degenerate primer pair *Rif*-For and *Rif*-Rev targeting conserved regions at the 5'- and 3'-termini of the *rif*-genes (Fig. 19A). This positioning of these primers has the advantage of covering the intron sequence, thereby allowing an unequivocal distinction of spliced variants from genomic contaminants. RNA was harvested from highly synchronized 20-24 hour trophozoites and 44-48 hour schizonts, assuming that *rif*-transcripts relevant in merozoites would be present in these late stage parasites. To simplify the analysis, 3D7 parasites were used, based on the fact that the genome sequence of this strain is known. Thus, cDNA was synthesized and amplified using the RIFIN primers; in parallel primers specific for actin were used as a control (Fig. 19B). As shown, samples in which reverse transcriptase was omitted were negative and the PCR products amplified from cDNA were markedly smaller then the ones from genomic DNA, thereby ruling out any DNA contamination. The cDNA products were subsequently cloned into a TOPO-TA cloning vector and single colonies were analyzed by sequencing. The results are depicted in Fig. 19C.

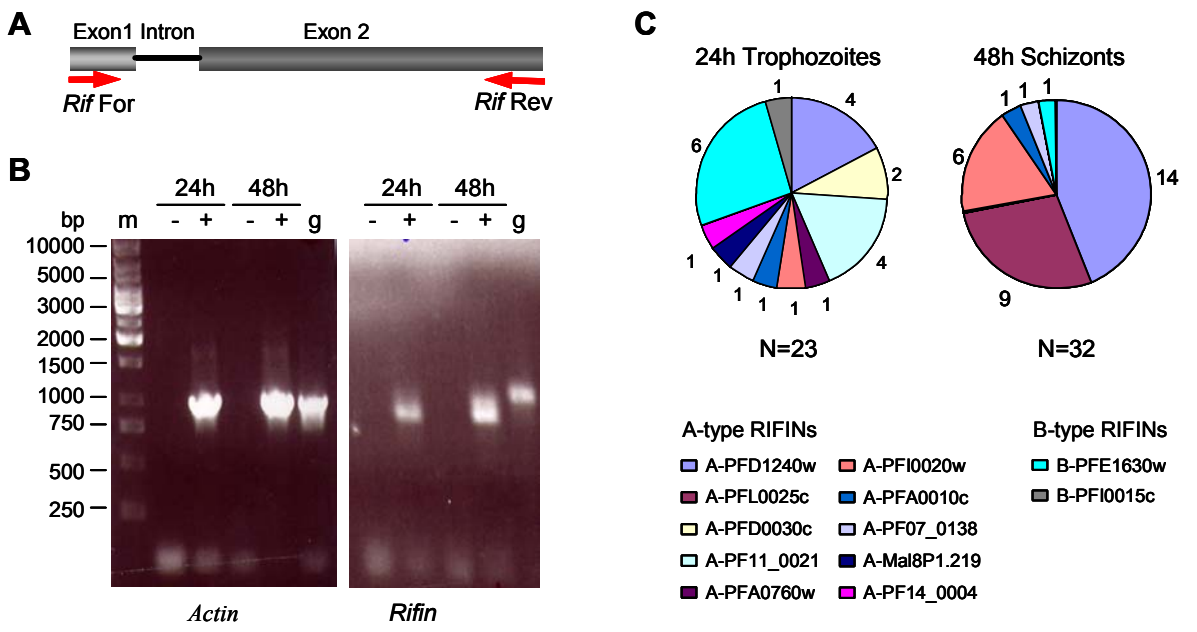

Fig. 19 Comparison of RIFIN transcription in trophozoites and schizonts
A: The graph illustrates the regions in *rif*-genes targeted by the degenerate oligonucleotide primers *Rif*-For and R*if*-Rev. These primers are complementary to sequence at the very 5‘ and 3‘ ends of the *rif* sequence and therefore span the intron sequence. **B:** RT-PCR analysis of RIFIN transcripts from 24 hour trophozoites and 48 hour schizonts. Total RNA was reverse transcribed into cDNA (+) and amplified with an actin specific primer pair or with the degenerate *Rif*-For and *Rif-Rev* primers. As negative controls, samples in which reverse transcriptase was omitted were used (-). Genomic DNA was amplified as a positive control (g). The smaller size of the *rif-RT*-PCR products in comparison to PCR products from genomic DNA results from the absence of the intron in the spliced transcripts. **C:** Relative abundance of different RIFIN variants in trophozoites and schizonts. The *rif*-RT-PCR products were cloned and single colonies analyzed by sequencing. The graph shows the proportion of each variant in trophozoites and schizonts. The total number (N) of analyzed clones is indicated below.

In trophozoites, one dominant B-type transcript (PFE1630w) and two dominant A-type transcripts (PFD1240w and PF11_0021) were detected as well as various sporadic sequences. In schizonts, three dominant A-type transcripts were found (PFD1240w, PFL0025c and PFI0020w). No dominant B-type transcript was present here, although the same B-type variant that was mostly found in trophozoites (PFE1630w) was identified in one of the clones, most likely demonstrating the persistent expression of this RIFIN. Despite the limited number of clones analyzed (for cost and time reasons), the data reflect well what has been observed before on the protein level. While some of the A-type variants (PFD1240w) were present in both early and late stages, others were downregulated during development from trophozoites to schizonts (PF11_0021). Interestingly, yet other variants were in turn switched on during parasite maturation (for example those encoded by genes PFL0025c and PFI0020w). This confirmed that differential developmental regulation of A-type variants occurs, although similar conclusions concerning B-type RIFINs are to date not possible.

3.2.6 Intracellular localization of A- and B-type RIFINs in merozoites

In the merozoite, proteins performing different functions during processes such as erythrocyte invasion or the subsequent establishment of the PV are located in distinct organelles (Preiser et al. 2000). To examine more precisely the location of A- and B-type RIFINs in merozoites and thus gain indications of their possible functional relevance in the invasive stages, colocalization studies using known merozoite proteins were performed. Double staining with anti-A_{565} or anti-B_{562} antiserum and a monoclonal antibody directed against the merozoite surface protein $MSP1_{42}$ (Blackman et al. 1990) confirmed the intracellular distribution of both RIFIN subtypes (Fig. 20A and B, 1st panel). A comparison with proteins known to be located in apical organelles, such as the micronemal protein AMA1 and the rhoptry-associated protein RAP1 indicated that the anti-A_{565} detectable RIFINs were located at the apex of the merozoite (Fig. 20A, 2nd and 3rd panel) (Kocken et al. 1998; Schofield et al. 1986). However, there was no clear colocalization with either of the two markers.

When testing anti-$B_{RIF\Delta NC}$, the fluorescent signal overlapped only partially with the microneme protein EBA181 and the rhoptry protein RhopH2 (Gilberger et al. 2003; Holder et al. 1985). The B-type RIFIN specific fluorescence extended beyond the confines of these organelles to the cytoplasm of the merozoite (Fig. 20B, 2nd and 3rd panel).

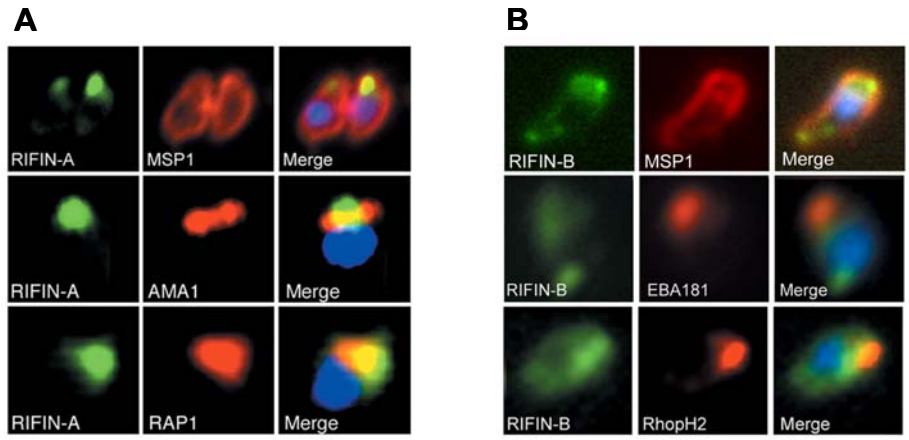

Fig. 20 Subcellular localization of A- and B-type RIFINs in merozoites
Colocalization studies with merozoite markers in free merozoites. **A:** A-type RIFINs were labelled with anti-A_{565} antibody (green), and double-stained with anti-MSP1, anti-AMA1 or anti-RAP1 antibodies (red). **B:** B-type RIFINs were detected with anti-B_{562} antibody (green) and double stained with anti-MSP1 (red); or with anti-$B_{RIF\Delta NC}$ antibody (green) and double stained with anti-EBA181 or anti-RhopH2 antisera (red). Nuclei were stained with DAPI (blue). (A, panel 2 and 3 courtesy of Malin Haeggström, Karolinska Institutet, Stockholm, published in (Petter et al. 2007))

3.2.7 A- and B-type RIFINs can be coexpressed by a single parasite

Recent studies analyzing the expression of *var* genes in IE have shown that despite the detection of several different *var* transcripts in individual ring-infected erythrocytes, only one single PfEMP1 variant is translated and transported to the erythrocyte membrane (Chen et al. 1998; Dzikowski et al. 2006a; Scherf et al. 1998). To date, corresponding data are lacking for RIFINs, although the detection of several RIFIN proteins in a cloned parasite line and in patient isolates was previously interpreted to show that RIFINs are not expressed in a clonal fashion (Fernandez et al. 1999). To investigate whether mutually exclusive expression indeed does or does not prevail between RIFIN variants, double staining with A- and B-type specific antisera was performed on IE. The results show that individual cells were characteristically labeled with both anti-A_{RIF29} and anti-B_{562}, demonstrating that RIFIN variants of both subtypes can be synthesized by a single parasite. The same results were obtained with the combination of anti-A_{RIF29} and anti-$B_{RIF\Delta NC}$ and the combination of anti-A_{565} and anti-$B_{RIF\Delta NC}$, with the latter compilation demonstrating a certain degree of colocalization within the parasite (Fig. 21A). Thus, unlike PfEMP1 proteins, simultaneous expression rather than mutual exclusion seems to be a feature of RIFIN variant proteins in IE.

Similarly, double staining with anti-A_{565} and anti-$B_{RIF\Delta NC}$ antiserum indicated coexpression of both variants in free merozoites (Fig. 21B). Besides demonstrating polyallelic expression of RIFIN variants in the invasive stages, this experiment also points out the differential subcellular localization of A- and B-type RIFINs with A-type RIFINs displaying an apical focus and B-type RIFINs showing a cytoplasmic distribution.

To address whether polyallelic expression in a single cell was restricted to the synthesis of one A- and one B-type variant, or whether several different variants of the same subgroup can be coexpressed, double staining experiments with the two anti-A-type antisera were performed. These two antisera recognize different A-type variants as shown by the labeling of bands with differing sizes in western blots (Fig. 18C), and thus appeared suited for this experiment. Both antisera showed colocalizing signals in the MC (Fig. 21C), demonstrating that polyallelic expression of several A-type variants within an individual cell is possible. The same was observed for both B-type sera (data not shown), although for these antisera recognition of the same B-type variant could not be ruled out according to the western blot results.

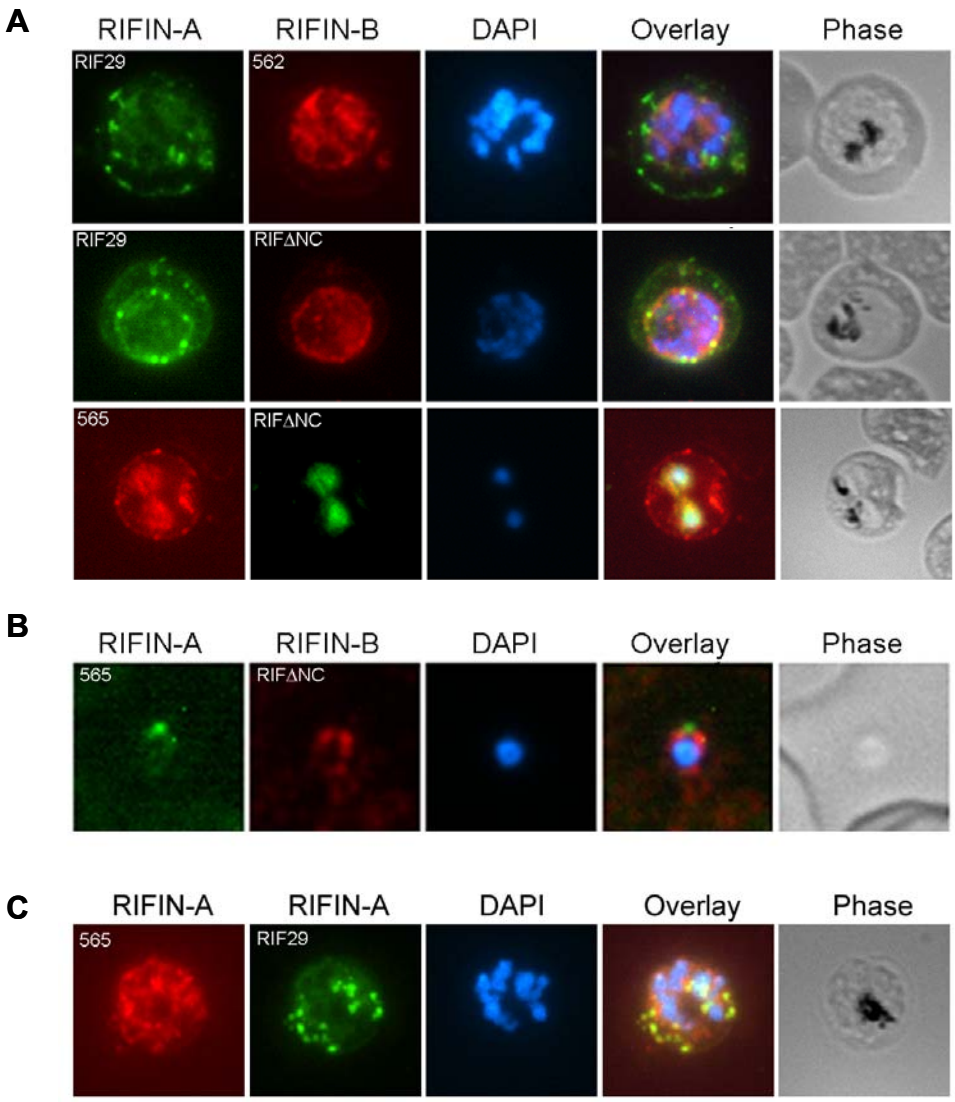

Fig. 18 Analysis of A- and B-type RIFIN coexpression in individual cells
Colocalization experiments for A- and B-type RIFINs were performed on methanol fixed preparations of trophozoites and merozoites. **A:** A- and B-type RIFINs are both expressed in the same trophozoite infected erythrocyte as detected by the combinations of anti-A_{RIF29} (green) and anti-B_{562} (red), anti-A_{RIF29} (green) and anti-$B_{RIF\Delta NC}$ (red), or anti-A_{565} (red) and anti-$B_{RIF\Delta NC}$ (green). **B:** Similarly, A- and B-type RIFINs were both present in individual merozoites as shown by double staining using anti-A_{565} (red) and anti-$B_{RIF\Delta NC}$ (green) antisera. In both, trophozoites and merozoites, the different staining patterns verified the subtype-specific recognition of the antisera. **C:** Double staining with anti-A_{565} (red) and anti-A_{RIF29} (green) shows colocalization of different A-type RIFINs. Nuclei were stained with DAPI (blue).

3.2.8 Conclusion

The careful inspection of an alignment of all RIFIN amino acid sequences revealed the existence of two RIFIN subgroups in the *P. falciparum* genome. They differ mainly by a 25 amino acid peptide that is present in the first group termed A-type RIFINs and absent in the

second group termed B-type RIFINs. Examination of the two groups with bioinformatic tools showed several more subtype-specific features, suggesting that these paralogous clades might have evolved to fulfill different functions. Localization studies using antisera specific for each subtype indeed demonstrated that A- and B-type RIFINs are present in different subcellular compartments: A-types are being exported into the MC, while B-types stay within the parasite compartment. Moreover, both A- and B-type RIFINs were found to be expressed in merozoites. In this context, A-type RIFINs exhibited differences concerning their expression during development from trophozoite to merozoite, which was substantiated on the RNA as well as on the protein level. Unequivocal conclusions concerning the localization of RIFINs in merozoites could not be drawn from double staining studies. Finally, double staining using both A- and B-type specific antisera showed that unlike *var* gene expression, *rif* gene expression is not limited to one variant per cell. Moreover, the differential distribution of A- and B-type RIFINs in merozoites and trophozoites could be confirmed in these experiments.

3.3 Analysis of RIFIN expression during sexual development

A notable observation in transcriptome- and proteome-wide expression analyses was a particularly high rate of RNA and protein expression from variant antigen families in gametocytes and sporozoites (Florens et al. 2002; Le Roch et al. 2003). The heterogeneity in RIFIN expression which was observed in these high-throughput studies, as well as the observation of different variants with divergent expression profiles made here, inspired a closer look at the sexual stages during intraerythrocytic development of *P. falciparum*. In the following paragraph, biochemical, genetic and phylogenetic tools were applied to investigate the regulation of RIFIN expression during gametocytogenesis and to compare the expression patterns with those from asexual parasites.

3.3.1 Cultivation of *P. falciparum* gametocytes

In culture, sexual development can be induced by stressing a fast growing ring stage culture with a sudden increase of the hematocrit in the presence of partially spent medium (Fivelman et al. 2007). Afterwards, the expansion of asexual stages can be inhibited by adding 50 mM N-acetyl-D-glucosamine to the culture (Ponnudurai et al. 1982), the result of which are highly enriched gametocyte preparations. Here, the NF54 parasite strain was used because it is characterized by a high sexual conversion rate. To assess gametocyte development, smears of the cultures were surveyed regularly and the stages were classified according to the system suggested by Carter and Miller (Carter and Miller 1979). An example for the monitoring of parasite differentiation is shown in Table 4. On day two after addition of N-acetyl-D-glucosamine, residual ring and trophozoite stage parasites were present, whereas the majority of the parasites was committed to sexual development evident as stage I and stage II gametocytes. On day four, the culture consisted mainly of stage III gametocytes. On day eight, the parasites had matured to stage IV or V gametocytes.

Table 4: Distribution of developmental stages during gametocytogenesis

Day		Asexual		Gametocytes (Carter and Miller 1979)					Gamete	Total
		R	T	I	II	III	IV	V		
2	N[1]	7	12	70	112	21	7	3	0	233
	%	3.0	5.1	**30.0**	**48.0**	9.0	3.0	1.5	0	100
4	N[1]	0	1	3	5	159	43	2	0	213
	%	0	0.5	1.4	2.3	**74.6**	20.2	0.9	0	100
8	N[1]	0	0	7	5	16	101	95	10	234
	%	0	0	3.0	2.1	6.8	**43.16**	**40.5**	4.2	100

[1] N: number of parasites of the corresponding stage determined by Giemsa staining

3.3.2 Examination of RIFIN protein expression during sexual development

To examine RIFIN expression in gametocytes, IFA was performed on methanol fixed smears of pigmented trophozoite IE as well as on gametocyte preparations harvested at day 6 after induction, when the majority of the cells consisted of immature sexual stages III and IV. The anti-RIF40 and anti-$B_{RIF\Delta NC}$ antisera which have been described above were used to visualize representatives of A- and B-type RIFINs. As was shown before (section 3.2.4), A-type RIFINs were exported to the host cell in asexual parasites and were associated with the MC, while B-type RIFINs were located mainly intra-parasitically (Fig. 22A, 1st panel). The subcellular localization of RIFINs in gametocytes resembled the one found in trophozoites, in that A-type RIFINs detected with anti-RIF40 accumulated in dotted structures associated with the host cell, whereas B-type RIFINs labeled with anti-$B_{RIF\Delta NC}$ were distributed inside the parasite (Fig. 22A, 2nd panel). An estimation of the fluoresecence rates revealed that both subtypes were expressed in over 90 % of the trophozoite IE population. In contrast, the proportion of A- and B-type RIFIN expressing cells was around 89 % or 53 %, respectively, among immature stage III to IV gametocytes harvested at day 6. The levels of RIFIN labeled gametocytes decreased during maturation to stage V gametocytes at day 10 to 63 % for A-type RIFINs and 16 % for B-type RIFINs (Fig. 22B).

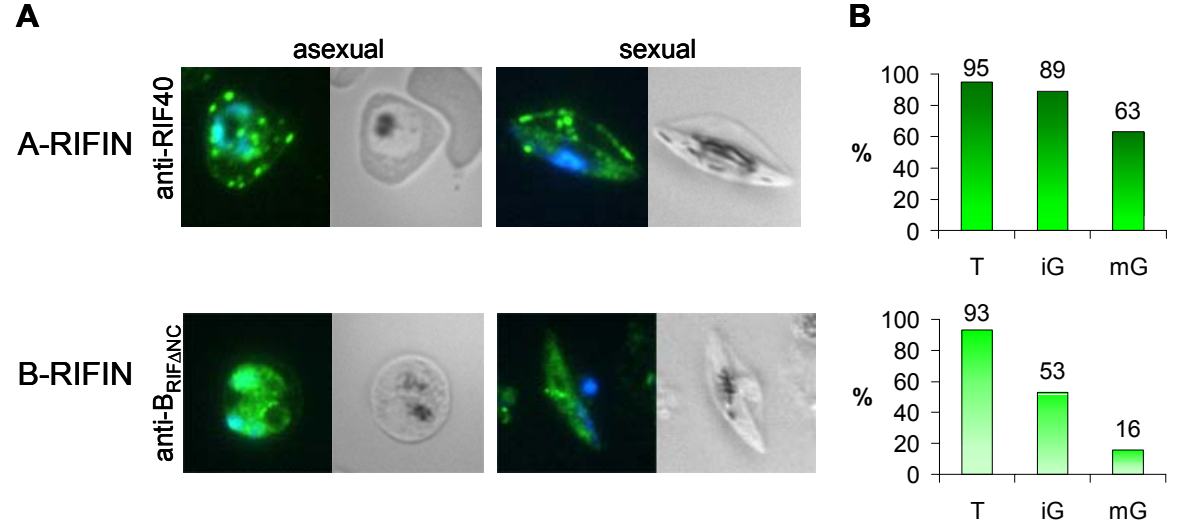

Fig. 22 Immunofluorescence analysis of RIFIN expression in asexual and sexual parasites
A: Smears of trophozoite and gametocyte infected erythrocytes were fixed with methanol and analyzed for RIFIN localization by staining with rat anti-RIF40 and mouse anti-$B_{RIF\Delta NC}$ antisera (green). Nuclei were stained with DAPI (blue). A-type RIFINs visualized with anti-RIF40 show a punctate pattern in cytoplasm of the infected erythrocyte reminiscent of Maurer's Cleft staining, while B-type RIFINs detected with anti-$B_{RIF\Delta NC}$ display a parasite restricted pattern in both, sexual and asexual stages. **B:** Quantification of the proportion of RIFIN positive cells in trophozoites (T), immature gametocytes at day 6 (iG) and mature gametocytes at day 10 (mG) after induction of gametocygenesis.

To substantiate the presence of RIFINs in gametocytes, lysates of MACS enriched trophozoites, stages I and II (day 2), stages III and IV (day 6) or mainly mature stage V (day 10) gametocytes were prepared and analyzed by western blotting (Fig. 23). Indeed, with anti-RIF40 and anti-$B_{RIF\Delta NC}$ bands of 38 and 32 kDa, respectively, were detected in all fractions. The intensity of both protein bands in early stages I and II as well as in mature stage IV/V gametocytes was markedly reduced, demonstrating that peak expression of RIFIN variants detected with anti-RIF40 and anti-$B_{RIF\Delta NC}$ occurred in stage III and IV gametocytes, and well reflecting the results obtained by IFA. The gametocyte specific antigen Pfg27 (Alano et al. 1991) was used as a stage control and was found to be highly expressed in the gametocyte fractions. The soluble protein PP5 was used as a loading control. Also, the transmembrane protein SBP1 was equally present at all stages. Interestingly, when testing a third anti-RIFIN antiserum directed against a recombinant A-type RIFIN (RIF44), two protein bands of 32 and 37 kDa were apparent (Fig. 23). While the 32 kDa protein was exclusively expressed in asexual parasites, the 37 kDa protein was first observed in early gametocytes and its intensity increased during maturation. Although this result clearly demonstrates that the RIFIN pool in gametocytes differs from the one in asexual parasites, it is unknown whether the two protein bands represent differentially processed or otherwise modified types of the same RIFIN, or whether they derive from distinct variants.

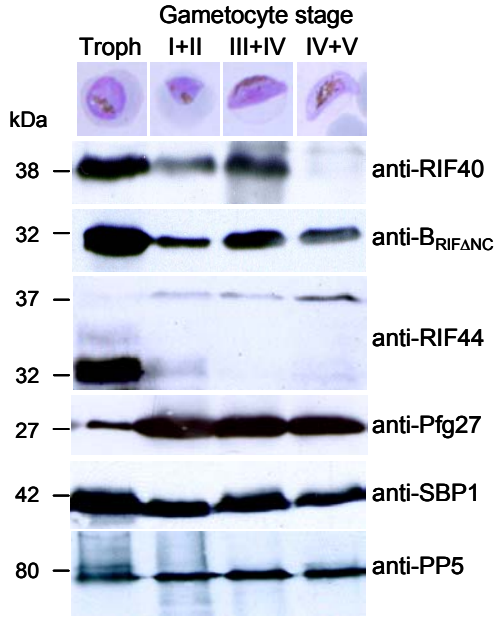

Fig. 23 Western Blot Analysis of RIFIN expression during gametocytogenesis
Trophozoite infected erythrocytes and gametocyte infected erythrocytes at different time points during sexual development were enriched and harvested by MACS. Total parasite lysates were analyzed by SDS-PAGE and Western Blotting. Antisera against RIFIN proteins RIF40, RIFΔNC and RIF44 were tested. As a stage specific control served the antiserum against the gametocyte specific protein Pfg27. As loading controls served antibodies against the Maurer's clefts marker protein SBP1 and the soluble parasite protein phosphatase PP5.

3.3.3 A-type RIFINs localize to the erythrocyte membrane in gametocytes

Elucidation of the subcellular compartments harboring RIFINs in gametocytes might help to uncover the functional relevance of these variant antigens during sexual development. Therefore, colocalization studies were performed to visualize the RIFIN distribution in relation to subcellular marker proteins of known locations. Since in the previous paragraph it was shown that gametocytes exhibited maximal RIFIN expression at the stages III to IV present around day 6 during gametocyte maturation, methanol fixed smears of cultures at this time point were chosen for analysis.

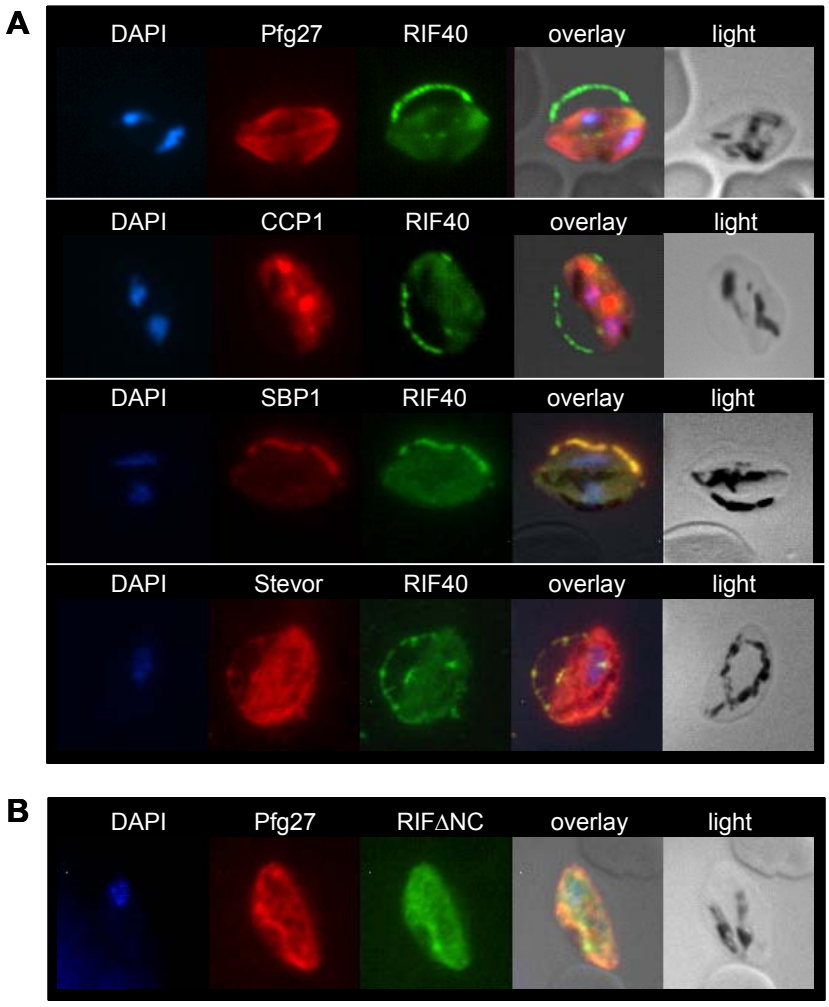

Fig. 24 Immunofluorescence colocalization study in stage III gametocytes
Methanol fixed smears of stage III gametocytes were incubated with antibodies against RIFIN and marker proteins. **A:** rat anti-RIF40 antibodies (green) and rabbit anti-Pfg27, mouse anti-CCP1, mouse anti-SBP1 or mouse anti-Stevor (red). **B:** mouse anti-$B_{RIF\Delta NC}$ (green) and rabbit anti-Pfg27 (red). Nuclei were stained with DAPI (blue).

Double staining using an antiserum directed against the cytoplasmic parasite protein Pfg27 (Alano et al. 1991; Carter et al. 1989) largely revealed colocalization with B-type RIFINs

(Fig. 24B). In contrast, A-type RIFINs and Pfg27 only showed a faint overlap within the parasite (Fig. 24A, 1st row). Instead, the A-type RIFIN related fluorescence was concentrated in a "string of pearls" pattern at the erythrocyte membrane. According to the IFA study it seems that A-type RIFINs accumulate in the tubular space defining the fringe of the hemoglobin depleted erythrocyte apron referred to as Laveran's bib.

Whether the punctuate fluorescence detected with the A-type specific antiserum anti-RIF40 overlapped with the recently discovered LCCL domain-containing family protein PfCCP1 was studied. PfCCP1 has been described to display a discretely dotted appearance in IFA and was shown to be exported to the PV in gametocytes (Pradel et al. 2004; Pradel et al. 2006). However, the fluorescence patterns of A-type RIFINs and PfCCP1 did not coincide thereby ruling out a PV restricted localization of A-type RIFINs (Fig. 24A, 2nd row).

Finally, the staining of A-type RIFINs in gametocytes was examined in relation to the MC protein SBP1 and variant antigens of the STEVOR family, which are present at the host cell membrane in gametocytes. Anti-RIF40 fluorescence nicely overlapped with both marker proteins (Fig 24A, 3rd and 4th row). This result indicated that all three proteins appear to be located in the same subcellular compartment, although it has previously been suggested that STEVORs reach the erythrocyte surface in gametocyte IE via a MC-independent pathway (McRobert et al. 2004).

3.3.4 Examination of RIFIN RNA expression during sexual development

3.3.4.1 RNA expression of A- and B-type RIFINs

The analysis of RIFIN expression on the protein level using crossreactive antisera has its limitations in assigning the exact identity to the detected proteins. To overcome this problem, *rif* gene expression was investigated on the RNA level.

The expression of *rif*-transcripts during gametocytogenesis was first analyzed in RT-PCR experiments. RNA was isolated from trophozoites 20 – 24 hours post invasion as well as from gametocyte cultures prepared at days 2, 4, 6, 8 and 10 after induction, and reverse transcribed into cDNA. The A- and B-type RIFIN subgroup specific primer pairs RIF-A For/Rev and RIF-B For/Rev characterized in section 3.2.2 were used to amplify RIFIN encoding cDNA molecules. In parallel, gDNA was included as a positive control, and samples in which reverse transcriptase was omitted during cDNA synthesis served as negative controls. Products of the predicted sizes of 134 bp and 178 bp for A- and B-type RIFINs, respectively, were amplified from gDNA as well as from all cDNA samples of asexual and sexual stage

parasites, but not from the negative controls (Fig. 25A). This result indicated that both A- and B-type RIFIN expression proceeded throughout sexual development.

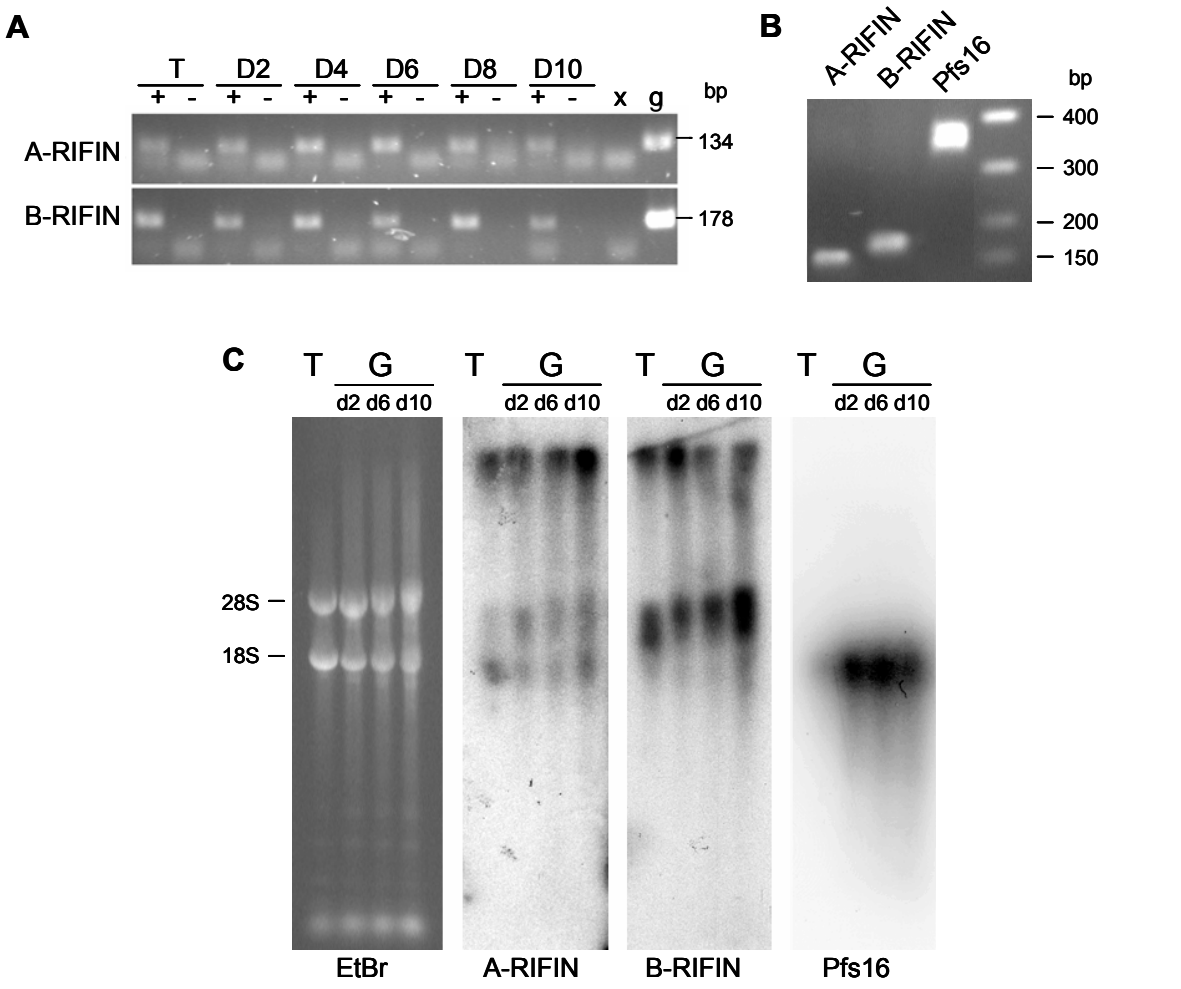

Fig. 25 RIFIN RNA expression during sexual development
A: RT-PCR analysis of A- and B-type RIFINs in asexual and sexual stage of the NF54 parasite strain. RNA was harvested from 20-24 hour trophozoites (T) and at days 2, 4, 6, 8 and 10 of gametocytogenesis (D2-D10). RNA was reverse transcribed into cDNA (+) and PCR was performed with primers specific for A- or B-type RIFINs (A-RIFINs and B-RIFINs). RNA samples in which reverse transcriptase was omitted served as negative controls (-). Positive controls were performed on genomic DNA (g). **B:** Generation of probes for northern analysis. PCR was performed on genomic DNA with degenerate oligonucleotide primers specific for A- or B-type RIFINs and with specific primers targeting the gametocyte specific Pfs16 gene. **C:** Northern analysis of trophozoite (T) and gametocyte (G) RNA at days 2, 6 and 10 during gametocytogenesis. RNA was separated on 1% agarose gels and equal loading was documented by ethidiumbromide (EtBr) staining. The RNA was transferred to nylon membranes and the membranes sequentially probed with the A-RIFIN, B-RIFIN and Pfs16 specific DNA probes. The position of the 18S and the 28S rRNA is indicated.

To verify that *rif* transcripts were full length and not the result of promiscuous or aborted transcription, northern blot analysis of RNA samples from young trophozoites and

gametocytes at days 2, 6 and 10 after induction of sexual development was performed. A- and B-type RIFIN specific probes and a probe targeting the gametocyte specific gene Pfs16 (Baker et al. 1994; Bruce et al. 1994) were generated by PCR using gDNA as a template (Fig 25B).

In each lane, 5 μg of total RNA were loaded and separated electrophoretically. Equal loading was verified by EtBr staining (Fig. 25C, 1st panel). Transcripts of Pfs16 were present at high levels only in gametocyte preparations and not in trophozoite RNA, controlling the stage specificity of the preparations (Fig 25C, 4th panel). Hybridization with the A-type RIFIN specific probe resulted in detection of RNA products of about 1.8 – 2.2 kb corresponding to the transcript size previously shown for RIFINs (Kyes et al. 1999). Interestingly, a second band was apparent at around 3 kb. While the lower band was present in both asexual and sexual stages, the upper RNA species appeared to be slightly less abundant in the trophozoite fraction (Fig. 25C, 2nd panel). Upon hybridization with the B-type specific probe, a signal was detected between 2.5 and 3 kb (Fig 25C, 3rd panel).

For both A- and B-type RIFINs additional signals corresponding to high molecular weight nucleic acid species were detected. Given the high copy number of RIFINs in the *P. falciparum* genome, these signals are interpreted to derive from hybridization with residual contaminating gDNA molecules.

3.3.4.2 RT-PCR of single variants

To gain insight into the regulation of single *rif* genes during gametocytogenesis, RT-PCR experiments with specific primer pairs were performed. Variants whose peptides had been detected in gametocyte preparations during proteomic analysis (Florens et al. 2002) were chosen (A-PFA0740w, A-PFD1230c, B-PFA0710c) as well as several other A- and B-type representatives (A-PFI0020w, A-PFD1240w, A-PFA0760w, A-PFL0025c, B-PFE1630w, B-PFA0745w).

Different transcription patterns for the variants under investigation were observed (Fig. 26). The A-type variants A-PFI0020w, A-PFD1240c and A-PFA0740w as well as the B-type variant B-PFE1630w were detected in both trophozoites and in gametocytes. Interestingly, while A-PFA0740w was constitutively expressed, the level of transcription of the other variants seemed to fluctuate during gametocyte development, exhibiting a predominance in the middle stages present at days 4 to 8. The variant A-PFD1230c, on the other hand, was downregulated during progression of sexual differentiation and was only detected in trophozoites and in early day 2 gametocytes. In contrast, B-PFA0710c was only observed in

sexual but not in asexual parasites. Some of the variants were transcribed in neither population (A-PFA0760w, A-PFL0025c, B-PFA0745w).

In parallel, transcription levels of the gametocyte specific protein Pfs16 and the ring-infected erythrocyte surface antigen (RESA) were monitored. Rather surprisingly, both were detected throughout all stages. However, given the high sexual conversion rate observed for the NF54 strain even under optimal culture conditions in combination with the high sensitivity of RT-PCR assays, the presence of Pfs16 in the trophozoite preparation might have derived from a fraction of parasites already committed to sexual differentiation. Moreover, RESA, although originally identified as a ring associated antigen, has repeatedly been reported to be expressed in gametocytes (McRobert et al. 2004; Quakyi et al. 1989), thereby supporting the results (Fig. 26).

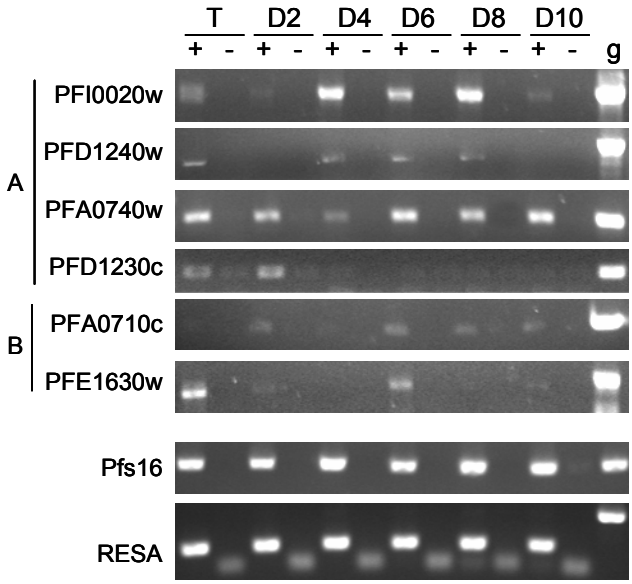

Fig. 26 RT-PCR analysis of single RIFIN variants
RNA was harvested from 20-24 hour trophozoites (T) and at days 2, 4, 6, 8 and 10 of gametocytogenesis (D2-D10) of the NF54 parasite strain. RNA was reverse transcribed into cDNA (+) and PCR was performed with primers specific for single RIFIN variants and the control genes Pfs16 and RESA. RNA samples in which reverse transcriptase was omitted served as negative controls (-). Positive controls were performed on genomic DNA (g). Different developmental regulation patterns can be observed for both A- and B-type RIFINs.

3.3.5 Analysis of untranslated flanking regions allows definition of further RIFIN subgroups

Taken together, the results from the analysis of single variants yielded a rather confused picture of the developmental expression of A- and B-type RIFIN variants, and no clear patterns were discernable. Since it is known that the developmental expression of genes is often regulated by elements which are present in the untranslated regions (UTRs) flanking a protein coding gene (Meijer and Thomas 2002; Wilkie et al. 2003), the next intention was to characterize the different *rif* upstream regions. A recent publication has shown that *var* genes under the control of a 5'-UTR belonging to the upsC type are preferentially expressed in

gametocytes (Sharp et al. 2006). This emphasizes the urge of a similar classification for RIFINs, as a step towards understanding their biology.

3.3.5.1 Phylogenetic analysis of rif 5' UTRs

Taking into account the estimated *rif* gene transcript size of 2 – 3 kb determined by northern blot analysis (Fig. 25C), and based on a similar analysis that has been performed to classify *var* genes (Lavstsen et al. 2003), it was decided to incorporate 1.5 kb of the noncoding 5' upstream regions into the analysis. A distance tree was inferred from an alignment of all *rif* upstream regions using the p-distance/Neighbor-Joining method. Gaps were treated as pairwise deletions. To test the reliability of the classification, 500 bootstrap replications were performed.

The resulting tree revealed the existence of five major *rif* upstream groups, henceforth referred to as "rups" (for *rif* upstream) (Fig. 27). Two large sequence clusters contained exclusively A-type *rif* gene UTRs and were named rupsA1 (22 variants) and rupsA2 (54 variants), the latter further segregating into two smaller groups (18 and 36 variants respectively). One sequence cluster consisted mainly of B-type *rif* gene UTRs and is thus referred to as rupsB (34 variants). Another cluster contained both A- and B-type sequences and was called rupsA/B (19 variants). A very small fifth cluster was evident, which according to the long branches contained rather divergent sequences, and was named rupsC (5 variants). Bootstrapping showed that all definitions except for rupsC were highly reliable. A few single sequences did not group with any of the rups clusters.

3.3.5.2 Classification of RIFINs according to rups group

An analysis of the *rif* genes belonging to the different rups subgroups with regard to their genomic position, orientation, neighboring genes and protein coding region revealed some interesting characteristics typical for each of the new clusters. These are specified in Table 5. In the following, a short résumé will be given to summarize these rups group specific features. All information including the prediction of structural features was retrieved from PlasmoDB.

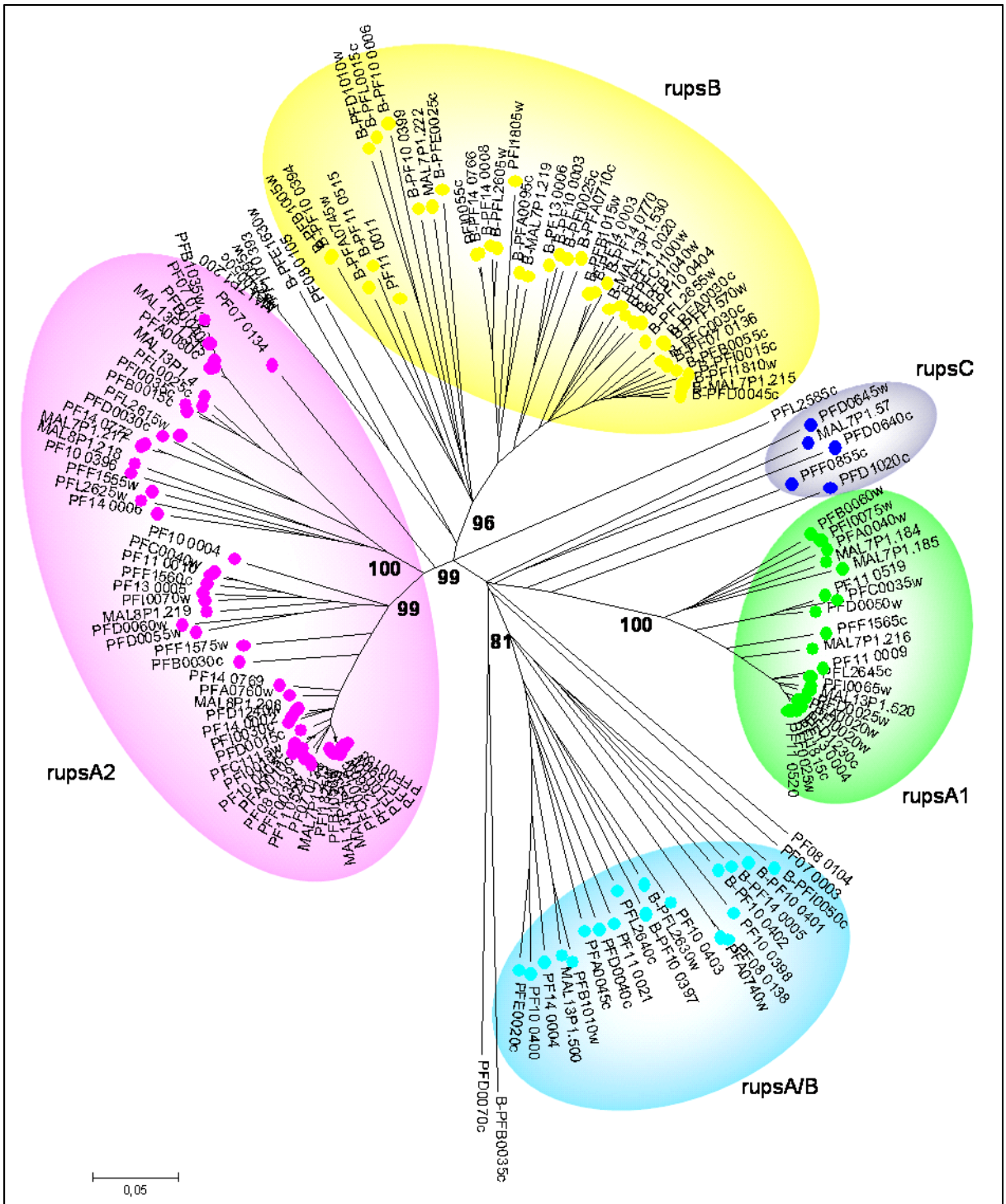

Fig. 27 Distance tree of *rif* gene upstream regions (rups) from 3D7
The 5‘ sequences containing 1500 bp upstream of each *rif* gene were aligned with ClustalW. Distance trees were generated using the p-distance/Neighbor-Joining method with pairwise deletion of gaps. The clusters rupsA1, rupsA2, rupsA/B and rupsB were verified by bootstrapping, and bootstrap values are indicated at the branches. The cluster rupsC could not be verified by bootstrapping.

rupsA1

RupsA1 related variants are encoded on all chromosomes (chr) but chr 5, 8, 10 and 14. All sequences are found in the telomeric ends of the *Plasmodium* chromosomes and display a transcription orientation towards the centromere. The genes adjacent to the 5' end of the rupsA1 region are mainly oriented in a head to head fashion (with two exceptions) and consist of *var* genes, other *rif* genes or hypothetical genes. The orientation of 3' neighboring genes can be either way, same or opposite. Interestingly, a subcluster of closely related sequences contains all *rif* genes which have been previously categorized to share their 5'-UTR with a flanking upsA *var* promoter region (designated rupsA1 *var* in Table 5) (Lavstsen et al. 2003).

Concerning protein features, the majority of A-type variants exhibiting a rupsA1 5'-UTR are predicted to have only one transmembrane domain according to the algorithm implemented at PlasmoDB. Canonical signal sequences are found in 6 out of the 22 sequences.

rupsA2

Genes sharing a rupsA2 5'-UTR are present in the telomeres of all chromosomes except for chr 5. The transcriptional direction of 45 out of the 54 sequences is towards the telomere, however, 9 rupsA2 related sequences exhibit the opposite orientation. All 5' adjacent genes are either *rif*, *var*, or *stevor* genes, of which a considerable number are pseudogenes. They have the same transcription orientation as the rupsA2 related genes, independent of whether these are centromere or telomere oriented variants. In contrast, the orientation of 3' flanking genes is not specified.

Similar to the rupsA1 related sequences, RIFINs expressed under the control of rupsA2 promoter regions are mostly predicted to have only one transmembrane domain and a minority of 10 out of 54 variants enocdes a canonical signal peptide.

rupsB

The *rif* genes falling into the third large group exhibiting a 5'-UTR of the rupsB type are found on all chromosomes near the telomeres, and their transcription orientation is mainly towards the telomeric chromosomal ends. Preceding genes include predominantly other *rif* genes and hypothetical genes, but occasionally also *var* and *stevor* genes. The transcription orientation of 5' and 3' adjacent genes is not fixed but can be either the same or opposite as the *rif* gene. A small number of UTRs groups closely to the rupsB cluster in the inferred

distance tree (Fig. 27), however statistical support was low (65 %). These 5'-UTRs are referred to as rupsB'.

In contrast to the *rif* genes belonging to the rupsA1 and rupsA2 groups, the majority of the rupsB related variants (except for 5) encode a canonical signal peptide. Also, predictions for two transmembrane domains were found more frequently among variants grouping with this cluster (12 out of 45 sequences) than with the others.

rupsA/B

The fourth cluster containing 5'-UTRs of both A- and B-type sequences is present on all chromosomes excluding chr 3, 6 and 7. Transcription orientation of the *rif* genes controlled by these upstream regions is mainly towards the telomere with only one exception. Upstream adjacent genes share the same orientation. Only two upstream encoded genes are still hypothetical, whereas all others code for RIFINs.

With respect to the protein features inherent in these *rif* genes, about half are predicted to express a signal peptide, and the majority to possess only one transmembrane domain.

rupsC

Finally, a small number of not very closely related sequences which are embraced in the subgroup rupsC exist in the central region of chr 4, 6 and 7 and are oriented either towards the centromere or the telomere. Preceding genes have opposite transcriptional directions, while following open reading frames (ORFs) are directed likewise. The structural predictions argue for a signal peptide in 4 out of 5 sequences and 1 transmembrane domain in all but 1 variant, in which such a prediction is lacking completely.

In summary, a striking correlation between the 5'-UTR and structural features related to the genomic organization was observed. This encourages the new classification of *rif* genes. However, examination of the records from transcriptomic and proteomic studies for each *rif* gene, as well as the results regarding single *rif* gene expression (Fig. 27) did not allow any conclusions concerning stage-specific expression related to any of the rups groups to be drawn (Table 5).

Table 5: Overview over *rif* gene rups groups and features

PlasmoDB ID	orientation[1]	chrom. postition	rups NJ[2]	A / B	SP[3]	TM[4]	upstream gene[5]	downstream gene[5]	Transcription[6]	Mass Spec[6]
>PF10_0397	tel	right tel 10	rups A/B	B	yes	1	*rif*	*rif*	S,M,Sp	
>PF10_0401	tel	right tel 10	rups A/B	B	yes	1	*rif*	*rif*	Sp	Sp
>PF10_0402	tel	right tel 10	rups A/B	B	yes	1	*rif*	*rif*		
>PF14_0005	tel	left tel 14	rups A/B	B	yes	1	*rif*	*rif*	Sp	
>PFI0050c	tel	left tel 9	rups A/B	B	yes	2	*rif*	*stevor*		G
>PFL2630w	tel	right tel 12	rups A/B	B	no	1	*rif*	*stevor*		
>PFL2640c	cen	right tel 12	rups A/B	A	no	1	*rif*	*stevor* <->		
>MAL13P1.500	tel	right tel 13	rups A/B	A	no	1	*rif*	*stevor*		
>PF08_0138	tel	left tel 8	rups A/B	A	yes	1	*hyp*	*rif*	Sp	
>PF10_0398	tel	right tel 10	rups A/B	A	no	1	*rif*	*rif*	Sp	
>PF10_0400	tel	right tel 10	rups A/B	A	no	1	*rif*	*rif*	Sp	
>PF10_0403	tel	right tel 10	rups A/B	A	yes	1	*rif*	*rif*	Sp	
>PF11_0021	tel	left tel 11	rups A/B	A	yes	2	*rif psi*	*rif*	Sp	
>PF14_0004	tel	left tel 14	rups A/B	A	yes	2	*rif*	*rif*	Sp	Sp
>PFA0045c	tel	left tel 1	rups A/B	A	yes	1	*rif*	*rif* <->		
>PFA0740w	tel	right tel 1	rups A/B	A	no	1	*hyp*	*rif*		Sp,G
>PFB1010w	tel	right tel 2	rups A/B	A	no	1	*rif*	*rif*		
>PFD0040c	tel	left tel 4	rups A/B	A	no	1	*rif*	*stevor*	T,Sp	
>PFE0020c	tel	right tel 5	rups A/B	A	no	1	*rif*	*rif psi*	Sp	
>MAL13P1.520	cen	right tel 13	rups A1 *var*	A	no	1	*hyp* <->	*rif* <->		
>MAL7P1.216	cen	left tel 7	rups A1 *var*	A	yes	1	*rif* <->	*rif* <->		
>PF11_0009	cen	left tel 11	rups A1 *var*	A	no	1	*var* <->	*rif*		
>PF11_0520	cen	right tel 11	rups A1 *var*	A	no	1	*var* <->	*rif*		
>PF13_0004	cen	left tel 13	rups A1 *var*	A	no	1	*var* <->	*rif*		
>PFA0020w	cen	left tel 1	rups A1 *var*	A	no	1	*var like* <->	*var psi* <->	T,G	
>PFD0025w	cen	left tel 4	rups A1 *var*	A	no	1	*var* <->	*rif* <->		
>PFD1230c	cen	right tel 4	rups A1 *var*	A	no	1	*var* <->	*rif psi* <->		G
>PFF0025w	cen	left tel 6	rups A1 *var*	A	yes	1	*var* <->	*var psi* <->		
>PFF1565c	cen	right tel 6	rups A1 *var*	A	no	2	*rif* <->	*rif*		
>PFI0065w	cen	left tel 9	rups A1 *var*	A	no	1	*hyp* <->	*rif*	Sp	
>PFL2645c	cen	right tel 12	rups A1 *var*	A	no	1	*hyp* <->	*rif*		
>MAL7P1.184	cen	right tel 7	rups A1	A	no	1	*rif*	*rif* <->		
>MAL7P1.185	cen	right tel 7	rups A1	A	yes	1	*hyp* <->	*rif*		
>PF11_0519	cen	right tel 11	rups A1	A	no	1	*rif*	*rif psi* <->		
>PFA0040w	cen	left tel 1	rups A1	A	no	1	*hyp* <->	*rif* <->		
>PFB0060w	cen	left tel 2	rups A1	A	yes	1	*hyp* <->	*stevor*		
>PFC0035w	cen	left tel 3	rups A1	A	yes	1	*rif* <->	*rif*		Sp
>PFD0050w	cen	left tel 4	rups A1	A	no	1	*rif* <->	*rif*		Sp
>PFI0075w	cen	left tel 9	rups A1	A	yes	1	*rif*	*stevor*	Sp	
>PFD0640c	tel left	central 4	rups C	A	yes	1	*rif* <->	*var*		
>PFF0855c	tel left	central 6	rups C	A	no	1	*hyp* <->	*stevor*		Sp
>PFD0645w	tel right	central 4	rups C	A	yes	1	*rif* <->	*hyp*		
>PFD1020c	cen	central 4	rups C	A	yes	0	*var* <->		Sp	
>MAL7P1.57	cen	central 7	rups C	A	yes	1	*var* <->	*hyp*		
>MAL13P1.515	tel	right tel 13	rups A2	A	no	1	*var psi*	*rif* <->		
>PF07_0132	tel	right tel 7	rups A2	A	yes	2	*var psi*	*rif* <->		

PlasmoDB ID	orientation[1]	chrom. postition	rups NJ[2]	A / B	SP[3]	TM[4]	upstream gene[5]	downstream gene[5]	Transcription[6]	Mass Spec[6]
>PFA0760w	tel	right tel 1	rups A2	A	no	1	*var psi*	*var* <->	R,T,Sp	
>PF14_0769	tel	right tel 14	rups A2	A	no	1	*rif*	*rif*		
>PFB0030c	tel	left tel 2	rups A2	A	no	1	*rif*	*stevor*	Sp	
>PFB0040c	tel	left tel 2	rups A2	A	no	1	*var psi*	*rif*	Sp	Sp
>PFB1035w	tel	right tel 2	rups A2	A	no	1	*hyp*	*var*		
>MAL13P1.2	tel	left tel 13	rups A2	A	no	1	*var*	*var* <->		
>MAL13P1.535	tel	right tel 13	rups A2	A	no	1	*rif*	*var* <->		
>MAL7P1.213	tel	left tel 7	rups A2	A	no	1	*var psi*	*var* <->		
>MAL8P1.208	tel	right tel 8	rups A2	A	no	1	*var*	*var psi* <->		
>PF07_0138	tel	right tel 7	rups A2	A	no	1	*var psi*	*var* <->		
>PF11_0529	tel	left tel 11	rups A2	A	no	1	*rif*	*var psi* <->	T	
>PFA0010c	tel	left tel 1	rups A2	A	no	1	*var like*	*var* <->	T,Sp	
>PFB1050w	tel	right tel 2	rups A2	A	no	1	*var psi*	*var* <->	T,Sp	Sp
>PFC0010c	tel	left tel 3	rups A2	A	no	1	*var psi*	*var* <->		
>PFD0015c	tel	left tel 4	rups A2	A	no	1	*var*	*var* <->		Sp
>PFD0030c	tel	left tel 4	rups A2	A	no	1	*stevor*	*rif* <->	Sp	
>PFD1240w	tel	right tel 4	rups A2	A	no	1	*var*	*var* <->	T,S	
>PFF0015c	tel	left tel 6	rups A2	A	no	1	*var*	*var* <->		
>PFF0035c	tel	left tel 6	rups A2	A	no	1	*rif psi*	*var psi* <->		
>PFF1590w	tel	right tel 6	rups A2	A	no	1	*rif psi*	*var* <->		
>PFI0010c	tel	left tel 9	rups A2	A	no	1	*rif*	*var* <->		Sp
>PFI0030c	tel	left tel 9	rups A2	A	no	1	*rif*	*rif*		
>PFI1825w	tel	right tel 9	rups A2	A	no	1	*var*	*var* <->		
>PFL0010c	tel	left tel 12	rups A2	A	no	1	*rif*	*var* <->	Sp	
>PFL2615w	tel	right tel 12	rups A2	A	no	1	*stevor*	*stevor*	Sp	Sp
>PFL2660w	tel	right tel 12	rups A2	A	no	1	*rif*	*var* <->	Sp	
>MAL8P1.219	cen	right tel 8	rups A2	A	no	1	*var*	*rif* <->		
>PF11_0010	cen	left tel 11	rups A2	A	no	1	*rif*	*rif* <->		Sp
>PF13_0005	cen	left tel 13	rups A2	A	no	1	*rif*	*rif* <->		
>PFC0040w	cen	left tel 3	rups A2	A	no	1	*rif*	*rif like*	Sp	
>PFD0055w	cen	left tel 4	rups A2	A	no	1	*rif*	*rif*		Sp
>PFD0060w	cen	left tel 4	rups A2	A	yes	1	*rif*	*stevor psi*	Sp	
>PFF1560c	cen	right tel 6	rups A2	A	no	1	*rif*	*rif* <->		
>PFI0070w	cen	left tel 9	rups A2	A	yes	1	*rif*	*rif*		
>MAL13P1.4	tel	left tel 13	rups A2	A	no	1	*var psi*	*rif*		
>MAL7P1.217	tel	left tel 7	rups A2	A	no	1	*stevor*	*rif* <->		
>MAL8P1.218	tel	right tel 8	rups A2	A	yes	2	*stevor*	*rif* <->		
>PF10_0396	tel	right tel 10	rups A2	A	yes	1	*stevor*	*rif*		
>PF14_0006	tel	left tel 14	rups A2	A	no	1	*stevor*	*rif*	T	
>PF14_0772	tel	right tel 14	rups A2	A	no	1	*stevor*	*var*		
>PFF1575w	tel	right tel 6	rups A2	A	no	1	*rif*	*var* <->		
>PFI0035c	tel	left tel 9	rups A2	A	yes	1	*var psi*	*rif*	T,S,G,Sp	
>PFL0025c	tel	left tel 12	rups A2	A	no	1	*var*	*var* <->		
>PFL2625w	tel	right tel 12	rups A2	A	yes	1	*stevor*	*rif*	T,S,Sp	
>PF10_0004	tel	left tel 10	rups A2	A	no	1	*rif*	*rif*		
>PF14_0002	tel	left tel 14	rupsA2	A	no	1	*rif*	*var psi*	T,Sp	Sp
>PF07_0134	cen	right tel 7	rupsA2	A	yes	2	*rif*	*rif*	T,Sp	
>MAL13P1.530	tel	right tel 13	rups B	B	yes	1	*hyp*	*rif*		
>MAL7P1.215	tel	left tel 7	rups B	B	yes	1	*rif* <->	*var psi*		
>MAL7P1.219	tel	left tel 7	rups B	B	no	1	*hyp*	*stevor*		

PlasmoDB ID	orientation[1]	chrom. postition	rups NJ[2]	A / B	SP[3]	TM[4]	upstream gene[5]	downstream gene[5]	Transcription[6]	Mass Spec[6]
>PF10_0006	tel	left tel 10	rups B	B	yes	2	*hyp*	*rif psi?*	T	
>PF07_0136	tel	right tel 7	rups B	B	yes	2	*hyp*	*var*		Sp
>PF10_0394	tel	right tel 10	rups B	B	yes	1	*rif*	*stevor*		
>PF10_0399	tel	right tel 10	rups B	B	yes	1	*rif*	*rif*	R,T,S,Sp	
>PF10_0404	tel	right tel 10	rups B	B	no	1	*rif*	*rif*	Sp	
>PF11_0020	tel	left tel 11	rups B	B	yes	1	*rif*	*rif*	Sp	
>PF11_0515	tel	right tel 11	rups B	B	yes	1	*hyp*	*stevor*	Sp	
>PF13_0006	tel	left tel 13	rups B	B	yes	1	*rif* <->	*rif*	G,Sp	Sp
>PF14_0003	tel	left tel 14	rups B	B	yes	2	*rif*	*rif*	T,Sp	Sp
>PF14_0008	tel	left tel 14	rups B	B	yes	2	*stevor*	*hyp*		
>PF14_0766	tel	right tel 14	rups B	B	yes	2	*hyp*	*stevor*	Sp	
>PF14_0770	tel	right tel 14	rups B	B	yes	1	*rif*	*stevor*	Sp	
>PFA0030c	tel	left tel 1	rups B	B	yes	1	*hyp*	*var psi*		
>PFA0095c	tel	left tel 1	rups B	B	yes	1	*hyp*	*stevor*		
>PFA0710c	cen	right tel 1	rups B	B	yes	1	*hyp*	*stevor*		G,M
>PFA0745w	tel	right tel 1	rups B	B	yes	1	*rif*	*stevor*	Sp	
>PFB0055c	tel	left tel 2	rups B	B	yes	2	*hyp*	*stevor*		
>PFB1005w	tel	right tel 2	rups B	B	yes	1	*rif*	*rif*		
>PFC0030c	tel	left tel 3	rups B	B	yes	1	*rif* <->	*stevor*		
>PFC1100w	tel	right tel 3	rups B	B	yes	2	*rif*	*stevor*		
>PFD0045c	tel	left tel 4	rups B	B	yes	1	*rif* <->	*rif*	M,Sp	
>PFD1010w	tel	right tel 4	rups B	B	yes	1	*var* <->	*var* <->	Sp	
>PFE0025c	tel	left tel 5	rups B	B	no	2	*stevor psi*	*rif*		
>PFF1570w	tel	right tel 6	rups B	B	yes	1	*rif* <->	*rif*		G
>PFI0015c	tel	left tel 9	rups B	B	yes	1	*rif* <->	*rif*	Sp	Sp,G,M
>PFI0025c	tel	left tel 9	rups B	B	yes	1	*RIF*	*rif* <->	S,M.Sp	~
>PFI1810w	tel	right tel 9	rups B	B	yes	1	*RIF*	*rif* <->		Sp
>PFL0015c	tel	left tel 12	rups B	B	yes	1	*var* <->	*rif*	S,Sp	Sp
>PFL2605w	tel	right tel 12	rups B	B	yes	1	*hyp*	*stevor*	Sp	
>PFL2655w	tel	right tel 12	rups B	B	yes	2	*hyp*	*rif*	S,M,G,Sp	
>PFF1545w	tel	right tel 6	rups B	B	yes	1	*rif psi*	*stevor*		
>PF11_0011	tel	left tel 11	rups B	A	yes	2	*hyp*	*rif* <->		
>PFI0055c	tel	left tel 9	rups B	A	no	1	*hyp*	*rif*		M
>PFI1805w	tel	right tel 9	rups B	A	no	2	*hyp*	*rif*	Sp	
>MAL7P1.222	cen	left tel 7	rups B	A	yes	1	*stevor psi*	*stevor*		
>PF10_0393	tel	right tel 10	rups B'	A	yes	1	*hyp*	*rif*		
>PFA0050c	tel	left tel 1	rups B'	A	yes	1	*hyp*	*rif*		
>PF08_0105	cen	left central 8	rups B'	A	yes	1	*var*	*rif*		
>PFE1630w	tel	right tel 5	rups B'	B	yes	2	*var psi* <->	*rif psi*		
>PFL2585c	cen	right tel 12	x	A	yes	1	*hyp* <->	*rif psi* <->		
>PF08_0104	cen	left central 8	x	A	no	2	*rif*	*var*	T,S,Sp	
>PF07_0003	tel	left tel 7	x	A	no	1	*hyp*	*hyp*		
>PFD0070c	tel	left tel 4	x	A	yes	2	-	*stevor psi* <->	R,T,S,M	
>PFB0035c	tel	left tel 2	x	B	no	1	*rif*	*rif*	Sp	

[1] transcription orientation (tel/cen: towards telomere/centromere); [2] rups NJ determined by Neighbor-Joining distance tree; [3] SP: signal peptide predicted by SignalP; [4] TM: transmembrane domain predicted by TMHMM 2.0; [5] adjacent genes with orientation in the same or opposite (<->) direction, psi: pseudogene; [6] Expression in developmental stages based on transcriptional and mass spectrometry evidence (R: ring, T: trophozoite, S: schizonts, M: merozoite, Sp: sporozoite, G: gametocyte) (Florens et al. 2002; Le Roch et al. 2003)

3.3.6 RNA expression patterns related to rups classification

To analyze *rif* mRNA expression during gametocytogenesis with respect to the newly assigned subgroups, the *rif* cDNA products amplified with A- and B-type specific primer pairs as described in section 3.3.4.1 (Fig. 25A) were cloned into the pCR2.1 TOPO vector. PCR products amplified from gDNA were also included to allow an assessment of the coverage among *rif* sequences picked up by the primers. In a preliminary analysis performed to evaluate this approach, the inserts of single clones originating either from gDNA or from cDNA of trophozoites, immature day 4 or mature day 10 gametocytes were sequenced. Between 20 and 32 colonies from each stage were examined.

3.3.6.1 Analysis of A- type rif gene transcription in asexual and sexual parasites

Sequencing of the A-type *rif* clones which originated from genomic DNA amplification revealed that among 20 clones 15 different variants were present, all of them A-type (Fig. 28A, 1st graph). None of the sequences was detected more than twice, and the distribution of variants belonging to the groups exhibiting rupsA1, rupsA2 or rupsA/B 5'-UTRs resembled that found in the genome (Fig. 29, 1st graph). This result indicated that the primers were not biased towards amplification of specific variants, thereby emphasizing their value for our analysis.

In 20-24 hour trophozoites, two major A-type transcripts were prevalent, namely PFL0025c and PFF1590w constituting 25 and 21 % of all clones, respectively (Fig. 28A, 2nd graph). In contrast, at day 4 during gametocytogenesis the PFD1240w variant was dominant representing 52 % of all sequenced colonies (Fig. 28A, 3rd graph). Interestingly, abundance of this latter variant decreased during gametocyte maturation in relation to other variants, resulting in a miscellaneous distribution of *rif* sequences in day 10 gametocytes (Fig. 28A, 4th graph). Corresponding to our finding here, the same developmental regulation of PFD1240w during maturation of sexual parasites has above been demonstrated by RT-PCR with specific primers at the absolute expression level (Fig. 26). Generally, the transcription profile of A-type *rif* genes significantly differed between asexual and sexual stage parasites.

Hypothetically, the subsets expressed in trophozoites and gametocytes might be subject to differential regulation mechanisms. To examine the contribution of variants with specific 5'-UTRs, we next sorted the A-type sequences according to their allocated rups groups and compared the abundance of each type in the different parasite stages (Fig. 29). Strikingly, in day 4 gametocytes 95 % of the clones belonged to the rupsA2 type, whereas only 5 % were rupsA1 RIFINs. No variants with a rupsA/B 5'-UTR were detected (Fig. 29, 2nd graph). In

trophozoites, a less pronounced shift towards rupsA2 expression was observed. Here, 82 % of the sequences were of the rupsA2-type, and 9 % each belonged to rupsA1 and rupsA/B. Thus, in both asexual and immature sexual stages expression of RIFIN variants with a rupsA2-type 5'-UTR prevailed (Fig. 29, 4th graph). In day 10 gametocytes, however, the proportion of variants belonging to each rups-type resembled approximately the distribution in the genome (Fig. 29, 3rd graph).

The shift towards the rupsA2 type resulted from the overrepresentation of single A2-type variants in trophozoites and immature gametocytes. Within the rupsA2 group, sequences expressed in asexual and sexual parasites were distributed equally between the two subclusters evident in Fig. 27.

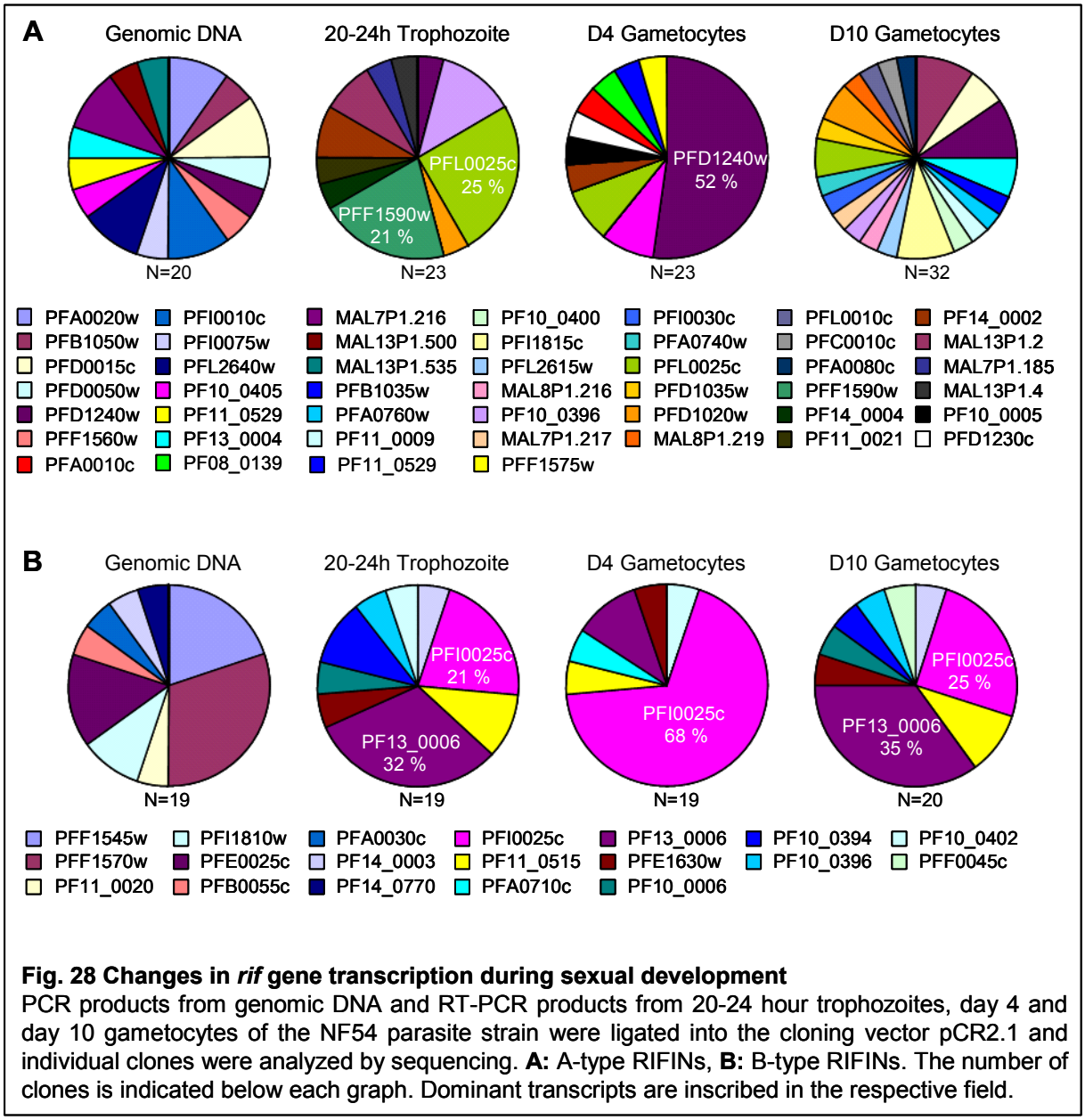

Fig. 28 Changes in *rif* gene transcription during sexual development
PCR products from genomic DNA and RT-PCR products from 20-24 hour trophozoites, day 4 and day 10 gametocytes of the NF54 parasite strain were ligated into the cloning vector pCR2.1 and individual clones were analyzed by sequencing. **A:** A-type RIFINs, **B:** B-type RIFINs. The number of clones is indicated below each graph. Dominant transcripts are inscribed in the respective field.

3.3.6.2 Analysis of B- type rif gene transcription in asexual and sexual parasites

Sequencing of the gDNA-derived B-type *rif* clones uncovered a bias towards the amplification of specific variants with the RIF-B For/Rev primer pair, although the high similarity of the variants in the amplified region sometimes complicates a correct assignment (Fig. 28B, 1st graph). In spite of this, *rif* transcripts different from the gDNA clones were predominantly amplified from cDNA samples, allowing us nevertheless to draw conclusions on B-type RIFIN expression. Both trophozoites and day 10 gametocytes exhibited an almost identical pattern with two dominating variants, PF13_0006 and PFI0025c constituting about 30 or 20 % of the clones, respectively. In day 4 gametocytes, the same dominant transcripts were detected, although PFI0025c contributed 68 % of the clones (Fig. 28B, 2nd – 4th graph). In contrast to the findings observed for A-type RIFINs, it appears that the B-type profiles in asexual and sexual stages are similar to each other.

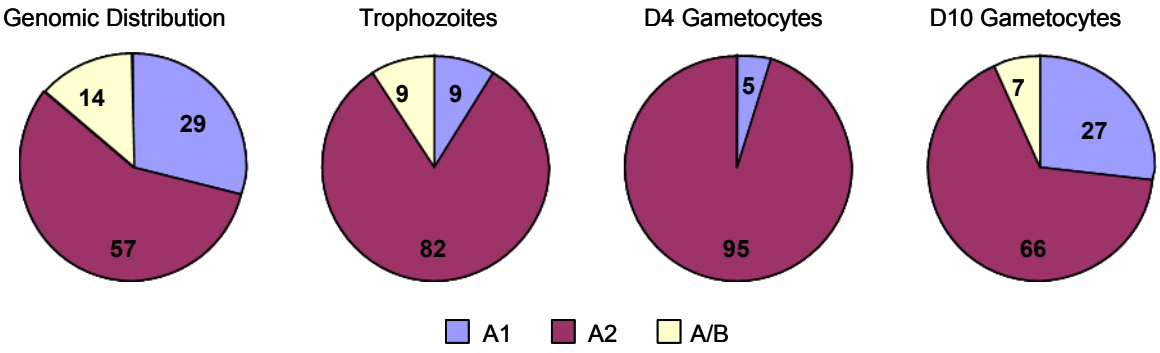

Fig. 29 Relative abundance of the A-type RIFIN subfamilies in different parasite stages
A-type RIFIN transcripts were grouped according to the A1, A2 and A/B subfamilies that were defined based on the 5‘ flanking regions and geomic organization of RIFINs. The percentage of clones belonging to each subgroup is indicated.

3.3.7 Conclusion

For the first time our results demonstrate RIFIN expression in sexual stages of *P. falciparum*. The localization pattern of A-type RIFINs in gametocytes resembles a crescent-shaped “string of pearls” at the erythrocyte membrane and coincides with STEVOR and SBP1 location. B-type RIFINs, in contrast, were not exported and remained parasite restricted. Western blots and IFA showed that A- and B-type RIFIN protein expression peaks in stage III-IV gametocytes. Some variants, though, were only present in asexual parasites while yet others were upregulated during gametocytogenesis. Similar patterns were revealed by RT-PCR analysis of single variants, showing that asexual and sexual RIFIN repertoires differ

from each other. These results highlighted the existence of complex developmental regulation mechanisms among members of the *rif* multigene family.

To elucidate these obscure mechanisms, the 5'-UTRs of all *rif* genes were analyzed using tree-building methods. This led to the definition of five clusters, which were termed rupsA1, rupsA2, rupsA/B, rupsB and rupsC (standing for *rif*-upstream). The variants of each rups group mainly shared the same transcription orientation as well as several other features. An examination of the RNA expression of RIFINs classified into these newly defined groups supplied evidence for a predominant expression of *rif* genes with rupsA2 5'-UTRs in both trophozoites and immature gametocytes, though the repertoires were different, while mature gametocytes showed no preference for either group. In contrast, B-type RIFIN profiles were largely identical in the different stages. However, the analysis of a larger number of clones will be necessary to draw more concrete conclusions.

4 DISCUSSION

4.1 RIFIN membrane association and topology

In the first part of this work, the membrane association and topology of RIFINs were analyzed in comparison to other *Plasmodium* proteins using two polyclonal anti-RIFIN antisera, anti-RIF40 and anti-RIF50. Both proteins belong to the A-type of RIFINs after the nomenclature developed in the course of this thesis. According to predictions, RIFINs are thought to be anchored in the erythrocyte membrane by two transmembrane domains exposing the hypervariable region to the periphery, while the semiconserved N- and C-terminal domains protrude into the erythrocyte cytoplasm (Cheng et al. 1998). Our data challenge this model, as will be discussed in the following paragraphs.

4.1.1 Membrane anchorage of RIFINs

Differential permeabilization was applied to determine the intracellular compartments containing RIFINs. After SLO and saponin permeabilization, RIFINs were associated with the pellet fraction allowing the conclusion that antigens detected with the two antisera are not exported to the erythrocyte cytoplasm or the PV as soluble proteins, which is consistent with the prediction of RIFINs as membrane proteins. The results from both hypotonic lysis and Triton X-100 extraction verified the membrane association of RIFINs. Similar profiles had previously been obtained for PfEMP1 molecules, highlighting related properties for both variant antigens (Kriek et al. 2003). Triton X-100 extraction at cold temperatures results in an enrichment of lipid rafts and their associated proteins in the detergent insoluble fraction (Chamberlain 2004). Thus, the insolubility of RIFINs suggests that they might be associated with cholesterol-rich microdomains exhibiting characteristics of lipid rafts, as has recently been shown for PfEMP1 (Frankland et al. 2006; Papakrivos et al. 2005).

Papakrivos and colleagues recently proposed PfEMP1 to be first synthesized as a carbonate extractable peripheral membrane protein, only assuming its transmembrane topology when it reaches its final destination at the erythrocyte surface (Papakrivos et al. 2005). However, at the surface PfEMP1 exhibits urea solubility characteristics, which are incompatible with

anchorage by hydrophobic interactions. Applying similar conditions, we found that RIFINs are insoluble in carbonate buffer (which characterizes them as membrane spanning proteins), but completely soluble in urea. Urea is a chaotropic agent which allows proteins to unfold and can thus disrupt protein complexes. However, because of their hydrophobic cores transmembrane proteins are usually not readily released from the association with the lipid bilayer in the presence of urea, except when detergents are added (Rabilloud 1996). Thus, our results strongly suggest that the integral transmembrane topology of RIFINs is also maintained by protein-protein rather than protein-lipid interactions, as suggested for PfEMP1 (Papakrivos et al. 2005). Surprisingly, SBP1, which was introduced as an experimentally characterized transmembrane protein (Blisnick et al. 2000), was also extractable with urea, and other studies have confirmed a partial solubility in urea for STEVOR (Przyborski et al. 2005). In summary, these results might thus point out a *Plasmodium*-specific mechanism of protein anchorage in the membrane, which strongly relies on protein-mediated rather than hydrophobic interactions. However, more control experiments are needed to establish such a model, for example by comparing the membrane associated parasite proteins with erythrocyte-derived membrane proteins such as glycophorins.

4.1.2 Facing up or staying down?

FACS analysis using anti-RIF40 and anti-RIF50 failed to detect RIFINs at the IE surface. Moreover, in contrast to PfEMP1, surface trypsinization of IE did not result in the recognition of the (according to the proposed topology) expected truncated peptide representing the intracellular domain of a surface exposed pool of RIFINs. Although the lacking FACS signal might simply imply low sensitivity, the incapacity of our antisera to detect RIFINs at the IE membrane from both sides challenges their surface exposure. However, with anti-RIF40, a band of approximately 35 kDa completely disappeared upon trypsinization, likely representing a processed portion of surface exposed RIFIN proteins. Moreover, IEM experiments using anti-RIF40 demonstrated labeling at the knobs, indicating IE membrane association of RIFIN molecules recognized by this antiserum. For anti-RIF50, though, no such evidence could be presented.

In a previous study, surface iodination was successfully used to label RIFINs at the IE membrane (Fernandez et al. 1999). Since radioactive labeling is more sensitive than Western blotting, it cannot be ruled out that a surface-associated tryptic fragment present in limited amounts might have slipped detection, given the finding that the majority of the proteins remain associated with the MC as shown by their accessibility after selective

permeabilization. Two studies have shown that RIFINs are resistant to trypsin at concentrations at which PfEMP1 is removed from the RBC surface, indicating that RIFINs are less prone to protease action than PfEMP1 (Fernandez et al. 1999; Kyes et al. 1999). It is thus conceivable that surface-exposed RIFINs are folded and arranged in such a way that antibodies do not gain access to the relevant epitopes in the native setting, but only after treatment with saponin. This would explain the discrepancies between FACS and IEM results for anti-RIF40 under consideration of the surface trypsinization assay.

In the preceding experiments, it was shown that RIFINs were likely to be associated with a Triton X-100 insoluble fraction possibly representing cholesterol-rich microdomains which are also important for transport of the major virulence factor, PfEMP1 to the host cell surface (Frankland et al. 2006). Saponin is known to intercalate with lipids like cholesterol and may therefore affect some forms of protein-membrane association (Ansorge et al. 1997). Saponin has properties of a detergent. Thus, a direct impact on the protein structure of RIFINs leading to the exposure of buried epitopes might provide an additional possible explanation for the detection of anti-RIF40 associated RIFINs at the IE surface after saponin permeabilization, as visualized by IEM, despite the failure to label them in FACS analysis. Still, no proof for surface association of RIFINs recognized by anti-RIF50 could be presented, although they were clearly associated with internal membranes. Together, the data argue for different properties inherent in the distinct RIFIN subpopulations detected by the two antisera.

4.1.3 Modeling the topology of RIFINs at the surface and the MC

To gain an understanding of the physiological role of RIFINs, it is important to uncover the topology of these proteins. Because so far no system is known to select for homogeneous expression of single RIFIN variants in a parasite culture, as done for PfEMP1 via panning on certain receptor proteins (Salanti et al. 2003; Smith et al. 1998), selection of suitable target variants for study is not trivial. Here, antibodies recognizing semiconserved parts of RIFINs were used to analyze an array of RIFINs. As a result, clear-cut interpretation of the results is inevitably complicated by the fact that the exact target protein and recognized epitopes are not known.

Interestingly, while no surface associated tryptic fragment was detected, anti-RIF40 revealed a protected protein domain in the MC after hypotonic lysis. With approximately 30 kDa, the molecular weight of this domain does not agree with the predicted size of any of the RIFIN domains flanked by the two putative TM domains. Reassessment of the TM predictions for all 3D7 RIFIN variants using various algorithms such as TMHMM 2.0

(suggested to be one of the most accurate programs for TM predictions in eukaryotes (Ikeda et al. 2002)) and Phobius (able to differentiate signal peptide and TM predictions (Kall et al. 2004)) showed that only the C-terminal hydrophobic segment is in the majority of RIFINs (including RIF40 and RIF50) clearly calculated to span the membrane (also compare to Table 5). This was in contrast to STEVORs and Pfmc2TM proteins, both of which showed strong predictions for two hydrophobic segments, confirmed experimentally for STEVORs (Lavazec et al. 2006; Przyborski et al. 2005; Sam-Yellowe et al. 2004). However, in agreement with its biochemical properties algorithms also failed to predict the putative membrane spanning domain of PfEMP1 (Papakrivos et al. 2005).

While these findings do not rule out the possibility that RIFINs indeed exist as two-transmembrane proteins, they allow a conceivable model explaining the results, which are summarized in Table 6. Thus, according to the trypsinization results, anti-RIF50 specific variants would display a topology in which both the semiconserved as well as the variable domain extend from the MC membrane into the erythrocyte cytoplasm, the first predicted transmembrane domain being non-functional (Fig. 30). It is not clear at present whether anti-RIF50 linked variants are associated with the erythrocyte membrane or not, where they would assume a similar topology. The relevance in antigenic variation for RIFINs with such a topology would however be of doubt, unless mechanisms exist which flip the protein to the other side, for example in the presence of immune pressure. Alternatively, these variants might exert their function at the MC membrane, as has been suggested for STEVORs (Kaviratne et al. 2002).

Anti-RIF40 specific variants in turn seem to have buried the semiconserved domain into the MC lumen, as evidenced by the 30 kDa tryptic fragment. In the presence of only one transmembrane domain, also the variable domain would remain inside, explaining the high molecular weight. The 35 kDa band that completely disappears after trypsin treatment of non-permeabilized cells might in such a scenario resemble a pool of surface exposed proteins that undergo some form of processing (for example delayed cleavage of the signal peptide or removal of other posttranslational modifications) during transit to the erythrocyte membrane, differentiating it in size from the MC associated fraction (Fig. 30). The lack of successful FACS staining might then, as discussed above, be either the result of a protected topography, or due to marginal sensitivity. In summary, RIFIN membrane topology still remains largely speculative and requires different tools for analysis.

Table 6: Summary of results from topology studies

	anti-RIF40	anti-RIF50
FACS	no surface staining	no surface staining
IEM	knob and MC association	not determined
surface trypsinization	38 kDa protected 35 kDa sensitive	40 kDa protected
HL permeabilized trypsinization	30 kDa tryptic fragment	no tryptic fragment

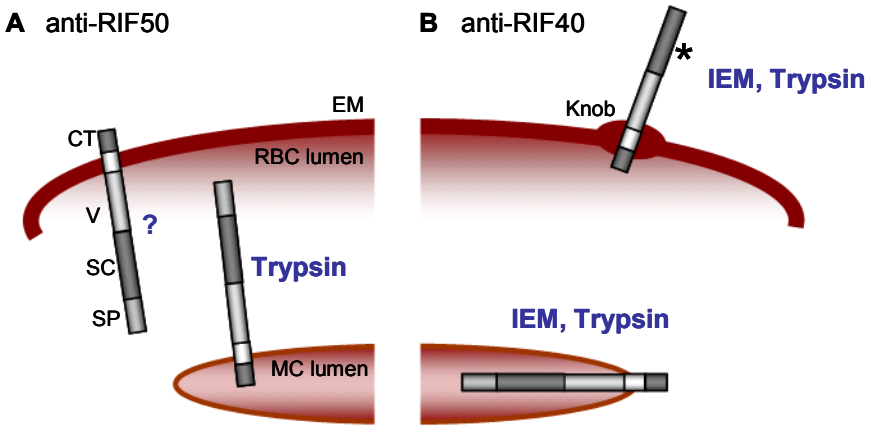

Fig. 30 Models for RIFIN membrane topology and supporting results
A: Anti-RIF50 detected variants proposedly expose both the semiconserved domain (SC) as well as the variable domain (V) and possibly an unprocessed signal peptide (SP) into the lumen of the RBC. The conserved C-terminal domain (CT) is protected inside the Maurer's clefts (MC). Evidence comes from trypsinization of permeabilized cells, although the association with the erythrocyte membrane (EM) could not be shown. **B:** Anti-RIF40 detected variants conceal both SC and V domain in the MC lumen, as demonstrated by detection of a protected 30 kDa fragment after trypsinization of hypotonically lysed cells, and by IEM. At the EM, RIF40 related RIFINs are found in the knobs, as seen in IEM, but in a slightly smaller processed form (asterisk: modified variant) which was shown to dissappear upon surface trypsinization.

An alternative method to analyze RIFIN topology would be to force the parasite to express a selected variant by putting it under control of a selectable marker. However in the absence of the known physiological expression pattern of single RIFIN variants and considering the fact that tagging *Plasmodium* proteins and expression under heterologous promoters has been shown to lead to mistargeted localization in some occasions (Knuepfer et al. 2005; Rug et al. 2004), results of such an approach have to be interpreted with great caution. A recent study for instance applied the transfection technology for the analysis of RIFIN trafficking signals by constructing green fluorescent protein (GFP) fusion proteins (Khattab and Klinkert 2006). Interestingly, the randomly selected variant of choice had two strongly predicted

transmembrane domains, and truncated chimeric proteins expressing only the first one were successfully targeted to the MC, indicating that the required targeting signals for this location were present. Notably, full length variants containing both putative transmembrane domains with GFP C-terminally appended were incapable of trafficking over the parasite membrane (Khattab and Klinkert 2006) despite presence of the PEXEL/HT motif (Hiller et al. 2004; Marti et al. 2004). However, using the aforementioned C-terminally truncated and tagged construct, GFP and the variable RIFIN region were shown to be covered in the MC lumen, while it was impossible to detect the semiconserved domain in the IE cytoplasm. This would be indicative of the complete protein, possibly soluble, being present in the MC, rendering the putative first transmembrane domain non-functional, as similarly proposed in the present work.

In parallel, another fusion protein of the same RIFIN variant carrying GFP in an internal position upstream of the first transmembrane domain showed a rather distinct MC topology, exposing the variable domain to the erythrocyte cytoplasm while enclosing the semiconserved region. Considering the co-translational translocation mechanisms known to determine protein topology in the endoplasmic reticulum (Higy et al. 2004), it is difficult to conceive how the different structures of the two chimeras might arise, given that the N-termini of both were identical. Possibly, the introduced GFP sequence in that case exerted some remodeling signals. The results of that study thus underline the difficulties in working with GFP tagged proteins for characterization of RIFIN membrane association and at the same time point out the delicate dependency of both protein structure and trafficking on functional motifs, supporting the possibility of different topologies identified for anti-RIF40 and anti-RIF50 related variants here.

Currently, we have initiated a transfection study in which smaller tags were introduced into different positions in a newly identified and highly conserved RIFIN variant (Petter et al., in preparation). This strategy may help overcome GFP-induced topology variations and might contribute to elucidation of the correct RIFIN topology, at least of that specific variant. Since the protein was found to be stably expressed in various isolates, it is an ideal study object for analysis using specific reagents targeting different domains of this variant.

4.2 Bioinformatic analysis of the RIFIN family

The different topologies inferred for two pools of RIFIN proteins, together with the notion of structural and functional diversity in subgroups of the *var* gene family (Kraemer and Smith 2003; Kyes et al. 2007), highlighted the importance of a careful examination of the many *rif* genes present in the *Plasmodium* genome. Phylogenetic comparisons performed to date have classified interspersed repeats from several *Plasmodium* species, including the *P. falciparum rif* and *stevor* families as well as multigene families encoded in the genomes of *P. vivax* (*vir*), *P. knowlesi* (*kir*) and three rodent malaria parasites (*bir/cir/yir*) as members of an inter-species super-family designated *pir* (*Plasmodium* interspersed repeats) (Janssen et al. 2004). However, despite this higher order classification of *rif* genes in the context of other multigene families from different species, no functional parallels have thus far been discovered.

4.2.1 Classification of A- and B-type RIFINs

The presence of two RIFIN subgroups in the P*lasmodium* genome differentiated by the presence or absence of a 25 amino acid motif was previously noted (Gardner et al. 2002) and analyzed here in greater detail. Phylogenetic trees inferred from the protein sequences by Neighbor-Joining and Maximum Parsimony methods showed clustering of A-type and B-type variants. Phylogenetic analysis performed in a collaborative project on RIFIN cDNA sequences identified largely the same topology and suggested to further subdivide the B-type *rif* genes into subclusters B1, B2 and B3 (Joannin et al., submitted). Separate examination of the variable and the semiconserved domains revealed that the variants of the B3 cluster were hybrid variants sharing their N-terminal region with B-type RIFINs, while their C-terminal half including the variable domain grouped with the A-type variants. On the protein level, however, such a segregation of the variable domains was not apparent in the work presented here (data not shown), indicating that the differences on the DNA level might reflect evolutionary processes, while preserving functional constraints.

The evolution of protein families adopting different subfunctions is accompanied by the accumulation of mutations at individual sites throughout the protein sequence. Functional changes might imply different selective pressure on certain sites (Golding and Dean 1998). Such sites can either be conserved in each subfamily but use different amino acids, or conserved in one family and variable in the other (Abhiman and Sonnhammer 2005a; Abhiman and Sonnhammer 2005b). Applying a bioinformatic analysis based on the divergence of A- and B-type RIFINs at such important sites, the biological relevance of the

A- and B-type RIFIN subgroups was further substantiated by prediction of a functional shift between the two families (Joannin et al., submitted). Several of the identified shifted sites are concordant with the subgroup specific features noted in this study here, such as the conserved cysteines and the modified residues in the C-terminal domain, summarized in Table 1.

4.2.2 Classification of rups groups

The segregation of A- and B-type RIFINs into two separately evolving groups was further supported by the phylogenetic analysis of the 5'-UTRs performed in the third part of this thesis. Distance tree reconstruction led to the proposal to classify RIFINs into five major subfamilies based on sequence similarities in coding and non-coding regions, as well as on the chromosomal context. Of the B-type variants, 37 fall mainly in one large cluster, called rupsB. A-type variants segregate in two major groups, of which rupsA1 contains 22 and rupsA2 54 variants. An intermediate group characterized by the distinctive 5'-UTR rupsA/B embraces most of the remaining A-type (13) and B-type (6) variants. A small cluster of five centrally located A-type *rif* genes featured by divergent upstream regions is summarized in rupsC. Sporadic sequences did not cluster with any of the rups groups, as for example PFD0070c. This particular gene was found to be strongly conserved across different isolates (data not shown), possibly pointing towards a similar highly specific function related conservation as has been shown for the upsE related var2CSA gene with a role in pregnancy associated malaria (Viebig et al. 2005). Alternatively, it might represent an ancestral conserved variant from which other *rif* genes have evolved by duplication events, as could be similarly true for the *var1csa* gene (Kraemer et al. 2007; Kyes et al. 2003). To attest a correlation of such kind, characterization of this specific *rif* gene is currently under way.

Notably, the rups clusters did not only largely distinguish A- and B-type RIFINs, but also exhibited strongly conserved patterns with respect to the chromosomal organization of the dedicated variants. Thus, rupsA1 variants were exclusively transcribed towards the centromere, while the majority of rupsA2, rupsA/B and rupsB associated variants exhibited the opposite orientation. However, a small number of rupsA2 sequences showed the same transcriptional orientation as rupsA1 variants. Such a preservation of combinations of both non-coding and coding regions with the chromosomal organization is also known to prevail between the *var* gene subfamilies (Kraemer and Smith 2003; Lavstsen et al. 2003). It was suggested that *var* gene clusters might evolve according to recombination hierarchies (Kraemer and Smith 2003; Lavstsen et al. 2003). This idea was strongly supported by a recent comparison of *var* genes from 3D7 and two other newly sequenced isolates stemming from

geographically distinct origins, IT4 (southeast Asia) and HB3 (Central America), showing that the organization of the *var* gene groups was preserved across the three isolates (Kraemer et al. 2007).

The generation of diversity in the *P. falciparum* genome is critical for the evolution of drug resistance and antigenic variation contributing to the success of the malaria parasite (Jeffares et al. 2007; Kidgell et al. 2006; Mu et al. 2007; Volkman et al. 2007). Mechanism implicated in the evolution of the variant gene repertoires apart from meiotic crossover events include ectopic gene recombination (Freitas-Junior et al. 2000; Kraemer et al. 2007; Taylor et al. 2000; Ward et al. 1999) as well as gene conversion (Bonnefoy et al. 1997; Freitas-Junior et al. 2000). These processes were described to involve clustering of the chromosomal ends in so called “bouquets”, that is regions in the nuclei of sexual parasites promoting efficient recombination (Freitas-Junior et al. 2000). Given the spatial proximity in the subtelomeric regions and the common organization in clusters, it is possible that similar mechanisms are responsible for the generation of diversity in the *rif* gene repertoire (Kyes et al. 2007).

Generally, it appears that the *rif* genes related to certain rups groups evolve preferably separately, preserving their respective genetic structures and possibly distinct inherent functions. A hint towards a constraint in recombination events might also be found in the *rif* arrangement with respect to the neighboring genes, that is either in tandem (tail to head) or in opposition (head to head), showing largely conserved patterns in each rups group. However, theoretically recombination between variants sharing the same orientation is possible, and indeed the presence of a few chimeric genes exhibiting an A-type coding sequence in combination with rupsB-type 5’-UTRs was noticed. This finding might point towards rare inter-subtype gene recombination events, contributing to the evolution of new functionally and developmentally distinct subfamilies and further shaping diversity in the *rif* gene family.

Evolution has shuffled variants present in the rupsA/B group to share the same class of 5’-UTR, independently of their protein clade. Interestingly, when inferring a phylogenetic tree from an alignment of *stevor*, *rif* and *var* upstream regions, rupsA/B sequences clustered much closer to *stevor* 5’-UTRs than to other *rif* 5’-UTRs (supplementary Fig. S3). The significance of this remains speculative at the moment, but might point to similar regulatory elements involved in the expression of the two variant antigen groups (Jegga et al. 2002). Notably, this analysis also revealed that the upsE 5’-UTR of the *var*2csa gene clustered together with the rupsB UTRs (supplementary Fig. S3). Though this might suggest involvement in similar biological mechanisms (Jegga et al. 2002), B-type RIFIN expression was not restricted to the CSA binding phenotype, as shown in this thesis by RT-PCR.

4.3 Multistage expression of two RIFIN subfamilies

Comprehensive proteomic and trancriptomic analysis of the many intermediate stages of the *Plasmodium* life cycle have revealed highly complex expression patterns for members of variant antigen families, including RIFINs (Florens et al. 2002; Le Roch et al. 2003). This was rather unexpected, because research had so far mainly focused on the role of variant antigens as mediators of immune evasion and inducers of pathology in asexual blood stage parasites (Dzikowski et al. 2006b; Ferreira et al. 2004; Rasti et al. 2004). Multistage expression of RIFINs was confirmed here and extended by the characterization of stage related localization data and subtype specific patterns.

4.3.1 Intracellular localization

In asexual parasite IE, A-type RIFINs were transported to the MC as shown by colocalization with the marker protein SBP1, and some of them onwards to the erythrocyte surface, as evident in the IEM analysis in the first part of this thesis. B-type RIFINs, in contrast, more prominently resided inside the parasite, as shown by comparative staining with the PVM marker Exp1. Interestingly, the presence of subgroups exhibiting different subcellular localizations has recently also been described for the RIFIN related *P. vivax* VIR family (Merino et al. 2006)

In sexual parasites, the intracellular patterns resembled that of asexual parasites. B-type RIFINs were found in the parasite compartment labeled with Pfg27, while A-type RIFINs localized in a “string of pearls” pattern along the membrane of the hemoglobin depleted erythrocyte, colocalizing with SBP1 and STEVOR. The presence of the MC marker protein SBP1 in gametocytes shown by both IFA and western blot analysis was surprising, as it is generally assumed that such membranous structures are not formed during sexual development. Instead, the existence of a sexual-stage intraerythrocytic tubular compartment (STIC) has recently been described, demonstrated to harbor an experimentally truncated version of the Pfs230 protein (Eksi et al. 2002). Interestingly, in the same study SBP1 was found to be located in a different compartment marked by a punctuate pattern. The nature of these two structures, however, was not further explored. Together, it appears that unequivocal subcellular assignment of RIFINs, STEVORs, and SBP1 is currently not possible due to the lack of characterized markers in gametocytes. Anti-RIF40 labeled IEM preparations of gametocytes to allow straightforward localization of RIFINs are currently underway.

In merozoites, A- and B-type RIFINs were also located in different subcellular compartments, as was demonstrated by double staining using antisera directed against members of each family. Interestingly, the distribution in the invasive stage of the parasite reflected that in IE, in that B-type RIFINs displayed a cytoplasmatic pattern, while A-type RIFINs were concentrated apically, indicating an association with the secretory organelles present in the apical complex. Colocalizing with neither microneme nor rhoptry marker, A-type RIFINs detected with anti-A_{565} may reside in a rhoptry subcompartment different from the marker protein RAP1. Such a distinctive localization as evident by IFA has previously been demonstrated for rhoptry proteins of *Toxoplasma gondii,* differentiating residents of the rhoptry bulb and rhoptry neck from each other (Bradley et al. 2005) However, IEM experiments using anti-A_{565} have so far failed to establish a connection between RIFINs and rhoptries or other merozoite organelles (Haeggstrom et al., unpublished). Dense granules might pose another possible compartment housing RIFINs, but have not been tested here (Torii et al. 1989).

4.3.2 The function of trafficking signals

Although all RIFIN variants bear the PEXEL/HT motif in their sequence (Hiller et al. 2004; Marti et al. 2004), B-type variants as detected by two antisera (anti-$B_{RIF\Delta NC}$ and anti-B_{562}) exhibited a block in export and resided instead in an intra-parasitic fashion in asexual and sexual stages. Thus, additional factors not yet characterized might enhance or interfere with protein export. A- and B-type RIFINs encode several highly conserved but subtype specific cysteine residues which are possibly involved in disulfide bonding and therefore might contribute to different tertiary protein structures. Noteworthy, two highly conserved cysteine residues are specifically found within the PEXEL/HT motif of A-type RIFINs, while in most B-type RIFINs a serine residue replaces the first cysteine (compare to supplementary Fig. S2). Various other subtype specific residues are obvious in the proximity of this targeting signal. These differences might provide an explanation for their distinct export behavior and subcellular localization. Moreover, certain subtype-specific motifs such as the distinctive 25 amino acid stretch displaying high conservation in A-type variants, or the different C-terminal signatures could be important players in protein-protein interactions involved in trafficking. However, transfection of an A-type RIFIN variant in which large parts of the semiconserved domain including the 25 amino acid peptide were replaced by GFP trafficked successfully to the MC (Marti et al. 2004), rendering the direct involvement of this motif in export unlikely.

In support of our data, Khattab et al. showed that the B-type variant encoded by the *rif* gene PFI0050c when expressed as a C-terminal GFP-tagged fusion protein accumulated in the parasite and was not exported to the erythrocyte (Khattab and Klinkert 2006). However, trafficking of the chimeric B-type variant to the MC occurred when the C-terminus was deleted or when GFP was introduced into the semi-conserved region of this variant. Topological studies showed that contrary to the truncated C-terminal GFP chimera, the insertion of the GFP sequence into the coding region drastically changed the conformation of the protein. These data stress the impact of sequence manipulations on RIFIN trafficking behavior and topology, highlighting the importance of certain motifs for correct localization.

4.3.3 Functional implications for variant antigens across stages

All *Plasmodium* stages present in the human host are potentially exposed to immunity and thus need to develop means to circumvent recognition and clearance, such as the expression of variant antigens (Ferreira et al. 2004). In the IE, the role of PfEMP1 is well characterized in this respect (Chen 2007; Flick and Chen 2004; Gamain et al. 2007). An implication of RIFINs is largely accepted (Abdel-Latif et al. 2003; Abdel-Latif et al. 2002; Fernandez et al. 1999; Kyes et al. 1999). However, the significance of polymorphic gene families in other stages is only slowly emerging both as multistage and multifunctional antigens.

Polymorphic protein families described in the context of merozoites as well as asexual parasites include for example the *P. yoelii* Py235 family, the *P. falciparum* SURFIN and Pf60 families. Initially shown to code for proteins located in the apical complex of the merozoite and shown to be important for invasion, members of the Py235 family were later found not only to be expressed in merozoites but also in sporozoites and in hepatic schizonts (Preiser et al. 1999; Preiser et al. 2002). Similarly, SURFINs were detected not only on the surface of IE, but also in an amorphous cap at the merozoite apex (Winter et al. 2005). Pf60, initially characterized as a rhoptry protein (Grellier et al. 1994), was later discovered to be member of a functionally and structurally highly diverse protein family, variants of which share sequence homologies to PfEMP1, the rhoptry protein RAP1 or even a nuclear protein (Bischoff et al. 2000; Bonnefoy et al. 1997). The multistage expression previously revealed for Py235, SURFINs, STEVORs and in this study for RIFINs, is highly supportive of a model whereby the parasite adapts rapidly evolving members of highly variable subtelomeric multigene families to fulfill distinct functions in various life cycle stages, rather than developing single copy molecules for each purpose (McRobert et al. 2004; Preiser et al. 2002; Winter et al. 2005).

Gametocytes persist in the human host for several days, yet it is unknown how they evade immune clearance in this period. The function of variant antigens in the sexual stages of *Plasmodium* parasites is still controversially discussed. Members of the PfEMP1 family have been only located at the surface of very early stage I and II gametocytes (Hayward et al. 1999), while variants belonging to STEVORs have been allocated to the host cell membrane till maturity of gametocytes (McRobert et al. 2004). Immature gametocytes are capable of sequestering in the bone marrow and the spleen (Talman et al. 2004), however, PfEMP1 is only considered as a major ligand mediating the interaction with host cell receptors in stage I and II gametocytes. A parasite ligand mediating cytoadhesion of more mature stages is still unknown. In view of their dominant expression in stage III and IV gametocytes, RIFINs might be involved in immune evasion of these stages.

It is tempting to speculate that RIFIN variants share a function in the cytoadhesion of the asexual or sexual IE as well as in the initial binding of merozoites to uninfected erythrocytes, analogous to that postulated for SURFINs (Winter et al. 2005). RIFIN molecules exposed at these two attachment sites are likely to be under strong immunological pressure, a fact that would explain why these molecules are highly variable in nature. However, invasion inhibition assays performed with anti-$B_{RIF\Delta NC}$ antiserum have failed to show an inhibitory action, at least for B-type RIFINs (Khattab et al., unpublished). Since RIFINs are present in young ring IE, they might alternatively be important very soon after invasion of the erythrocyte, similar to the single copy protein RESA (Ring-infected erythrocyte surface antigen) (Culvenor et al. 1991) or to Clag9 (cytoadherence linked asexual gene 9) which have both been shown to be exported to the erythrocyte shortly after formation of the PVM (Ling et al. 2004). In conclusion, however, the roles of RIFINs in asexual and sexual IE and in the merozoite remain speculative, and further analysis of the two RIFIN subgroups is needed to establish their functional relevance.

4.4 RIFIN expression dynamics

Several aspects of antigenic variation such as monoallelic and clonal expression have been defined on the basis of data generated for PfEMP1. Monoallelic (or mutually exclusive) expression refers to the restriction of *var* gene expression to a single variant in each cell (Chen et al. 1998; Dzikowski et al. 2006a; Freitas-Junior et al. 2005; Scherf et al. 1998; Voss et al. 2006). Clonal expression describes the phenomenon of synchronized production of only one type of protein in a population of parasites during an infection (Scherf et al. 2001). Both

contribute to controlled economy with respect to presentation of PfEMP1 to the immune system. However, to successfully escape immunity, the parasite eventually needs to be capable of switching expression during an infection, and switching and stage specific expression are subject to strict regulation as far as *var* genes are concerned (reviewed in (Kyes et al. 2007)). In the following paragraphs, the results from this thesis concerning regulation of *rif* gene expression will be discussed.

4.4.1 Polyallelic expression in individual cells

Double staining with anti-A and anti-B antisera provide evidence that A-type and B-type variants are both expressed in individual cells at the same time. In contrast to *var* genes, this rules out both monoallelic and clonal expression for *rif* genes. This striking coexpression was observed in asexual and sexual IE as well as in merozoites.

It was previously suggested that RIFIN expression is not clonally restricted, as a number of different protein bands were detected after immunoprecipitation with RIFIN-specific antibodies in patient isolates carrying only a single parasite genotype (Fernandez et al. 1999). This lack of clonal expression was further documented by an in vivo transcriptome analysis, comparing transcript levels in patient isolates and the laboratory adapted strain 3D7 (Daily et al. 2005). The same study showed expression of a large repertoire of transcripts encoded by both the *stevor* and the *rif* families in the isolates, while *var* gene expression was limited. Similarly, the *Plasmodium vivax vir* gene family has recently been described to encode several subfamilies, variants of which are expressed in parallel during a clonal infection, thereby challenging antigenic variation in the classical sense (Fernandez-Becerra et al. 2005). Thus, data from other multigene families substantiate the finding of non-clonal expression. However, the description of polyallelic expression in single cells for members of a multigene family as shown here for RIFINs is novel and adds an additional level of complexity to the phenomenon of antigenic variation.

4.4.2 Differences in developmental regulation

When analyzing A- and B-type expression in different stages during the *P. falciparum* life cycle, distinct patterns of developmental regulation became apparent. Western blot analysis in trophozoites, merozoites and schizonts showed that the repertoires of A-type RIFINs were subject to changes, whereas the expression of B-type RIFINs remained largely stable. While anti-A_{RIF29} only detected proteins in asexual parasites, anti-A_{565}, anti-B_{562} and anti-$B_{RIF\Delta NC}$ reacted with proteins in both trophozoites and merozoites. Similarly, both the A-type specific

antiserum anti-RIF40 and the B-type specific antiserum anti-$B_{RIF\Delta NC}$ detected variants in both trophozoites as well as in gametocytes, whereas a third anti-RIFIN antiserum, anti-RIF44, revealed two distinctly regulated variants, one of which was upregulated during gametocytogenesis whereas the expression of the other ceased.

This result of variant-dependent stage specific regulation was confirmed and further specified on the RNA level in RT-PCR experiments. Interestingly, when analyzing the transcripts in immature and mature gametocytes as well as in asexual parasites, B-type RIFINs showed a similar pattern of dominant variants at all time points under investigation. In contrast, the repertoire of A-type variants changed significantly, exhibiting different dominant variants between asexual and early sexual parasites. Moreover, in mature gametocytes A-type RIFIN expression was totally random. In comparison to results obtained from a recent study in which *var* and *stevor* expression dynamics were characterized, it intriguingly crystallized that A-type variants seem to follow similar dynamics as *var* genes, whereas B-type *rif* genes are transcribed in a fashion comparable to *stevor* genes (Sharp et al. 2006). More specifically, *var* and A-type *rif* transcripts differed in trophozoites as opposed to gametocytes, while *stevor* and B-type *rif* transcript patterns remained largely the same between asexual and sexual parasites. Considering that both PfEMP1 and A-type RIFINs are thought to be exposed at the erythrocyte surface (Baruch et al. 1995; Fernandez et al. 1999; Kyes et al. 1999; Su et al. 1995), a change in the expression pattern during transition from the asexual to the sexual period (or from trophozoite to merozoite in the case of RIFINs), might reflect an adaption to their specific functions in the different stages. Similarly, the lack of evidence for surface exposure of both STEVORs (McRobert et al. 2004) and B-type RIFINs (as shown in this thesis) might mirror the absence of external pressure for switching expression between the different developmental phases.

Identification of common and distinctive elements involved in the regulation of *rif* variants belonging to each rups group might help to understand the observed expression patterns. So far, only one study has addressed regulatory elements in the 5'-UTRs of a single *rif* gene (Tham et al. 2007). According to the novel classification presented here, the respective *rif* variant belongs to the rupsA1 group organized head to head with an adjacent *var* gene. Both activating and silencing elements were identified. Interestingly, a search of these elements in the rups sequence groups defined here could confirm both silencing elements as group specific features. Notably, expression of the *rif* gene under investigation appeared to be uncoupled from expression of the adjacent *var* gene in asexual IE (Tham et al. 2007), as was

also shown for *stevor* gene expression in gametocytes (Sharp et al. 2006), indicating that distinct silencing or activating mechanisms apply for these multigene families.

The results presented here imply a more pronounced expression of rupsA2 than of rupsA1 related variants in asexual, and especially in immature sexual stages. Northern blot analysis revealed two pools of A-type *rif* transcripts, which possibly represent the two subclusters. The intensities of the bands in the different stages with respect to the data obtain from RT-PCR might suggest the upper band to represent the rupsA2 pool and the lower band the rupsA1 pool, but this remains speculative until more specific probes for each type are available.

Analysis of available mass spectrometric data identified peptides of neither of the two A-type groups, which is conceivable considering that mature gametocytes were used for that study (Florens et al. 2002). Thus, the data coincide with our finding of downregulation of A-type RIFIN expression at the end of gametocytogenesis on the protein level, as shown by fluorescence rates and in western blots.

4.5 Conclusion

Although the aspects of RIFIN physiology highlighted in this thesis are merely small pieces in the large puzzle of understanding function and significance of this variant antigen family, the results presented here have opened important new perspectives for malaria research. Differences uncovered in the topology as well as in subcellular and developmental expression patterns of individual variants urge caution against generalizing results obtained for single RIFIN members. Moreover, the classification of RIFINs into subgroups based on structural differences in coding and non-coding regions may in the future serve as a basis for analyzing disease related expression patterns, helping to elucidate their biological roles in the interplay with the human host. To conceive what roles variant antigens play in disease pathology means a major step for designing new measures against *P. falciparum,* the most dreadful of protozoan killers.

5 LITERATURE

Abdel-Latif MS, Dietz K, Issifou S, Kremsner PG and Klinkert MQ (2003). Antibodies to *Plasmodium falciparum* rifin proteins are associated with rapid parasite clearance and asymptomatic infections. *Infect Immun* **71** (11): 6229-33.

Abdel-Latif MS, Khattab A, Lindenthal C, Kremsner PG and Klinkert MQ (2002). Recognition of variant Rifin antigens by human antibodies induced during natural *Plasmodium falciparum* infections. *Infect Immun* **70** (12): 7013-21.

Abhiman S and Sonnhammer EL (2005a). FunShift: a database of function shift analysis on protein subfamilies. *Nucleic Acids Res* **33** (Database issue): D197-200.

Abhiman S and Sonnhammer EL (2005b). Large-scale prediction of function shift in protein families with a focus on enzymatic function. *Proteins* **60** (4): 758-68.

Adisa A, Albano FR, Reeder J, Foley M and Tilley L (2001). Evidence for a role for a *Plasmodium falciparum* homologue of Sec31p in the export of proteins to the surface of malaria parasite-infected erythrocytes. *J Cell Sci* **114** (Pt 18): 3377-86.

Aikawa M, Torii M, Sjolander A, Berzins K, Perlmann P and Miller LH (1990). Pf155/RESA antigen is localized in dense granules of *Plasmodium falciparum* merozoites. *Exp Parasitol* **71** (3): 326-9.

Alano P, Premawansa S, Bruce MC and Carter R (1991). A stage specific gene expressed at the onset of gametocytogenesis in *Plasmodium falciparum*. *Mol Biochem Parasitol* **46** (1): 81-8.

Albano FR, Berman A, La Greca N, Hibbs AR, Wickham M, Foley M and Tilley L (1999). A homologue of Sar1p localises to a novel trafficking pathway in malaria-infected erythrocytes. *Eur J Cell Biol* **78** (7): 453-62.

Albrecht L, Merino EF, Hoffmann EH, Ferreira MU, de Mattos Ferreira RG, Osakabe AL, Dalla Martha RC, Ramharter M, Durham AM, Ferreira JE, Del Portillo HA and Wunderlich G (2006). Extense variant gene family repertoire overlap in Western Amazon *Plasmodium falciparum* isolates. *Mol Biochem Parasitol* **150** (2): 157-65.

Amino R, Thiberge S, Martin B, Celli S, Shorte S, Frischknecht F and Menard R (2006). Quantitative imaging of *Plasmodium* transmission from mosquito to mammal. *Nat Med* **12** (2): 220-4.

Andrews KT, Pirrit LA, Przyborski JM, Sanchez CP, Sterkers Y, Ricken S, Wickert H, Lepolard C, Avril M, Scherf A, Gysin J and Lanzer M (2003). Recovery of adhesion to chondroitin-4-sulphate in *Plasmodium falciparum* varCSA disruption mutants by antigenically similar PfEMP1 variants. *Mol Microbiol* **49** (3): 655-69.

Ansorge I, Benting J, Bhakdi S and Lingelbach K (1996). Protein sorting in *Plasmodium falciparum*-infected red blood cells permeabilized with the pore-forming protein streptolysin O. *Biochem J* **315 (Pt 1)**: 307-14.

Ansorge I, Paprotka K, Bhakdi S and Lingelbach K (1997). Permeabilization of the erythrocyte membrane with streptolysin O allows access to the vacuolar membrane of *Plasmodium falciparum* and a molecular analysis of membrane topology. *Mol Biochem Parasitol* **84** (2): 259-61.

Atkinson CT, Aikawa M, Perry G, Fujino T, Bennett V, Davidson EA and Howard RJ (1988). Ultrastructural localization of erythrocyte cytoskeletal and integral membrane proteins in *Plasmodium falciparum*-infected erythrocytes. *Eur J Cell Biol* **45** (2): 192-9.

Baker DA, Daramola O, McCrossan MV, Harmer J and Targett GA (1994). Subcellular localization of Pfs16, a *Plasmodium falciparum* gametocyte antigen. *Parasitology* **108 (Pt 2)**: 129-37.

Bannister LH, Hopkins JM, Fowler RE, Krishna S and Mitchell GH (2000). A brief illustrated guide to the ultrastructure of *Plasmodium falciparum* asexual blood stages. *Parasitol Today* **16** (10): 427-33.

Bannister LH, Hopkins JM, Margos G, Dluzewski AR and Mitchell GH (2004). Three-dimensional ultrastructure of the ring stage of *Plasmodium falciparum*: evidence for export pathways. *Microsc Microanal* **10** (5): 551-62.

Baruch DI, Pasloske BL, Singh HB, Bi X, Ma XC, Feldman M, Taraschi TF and Howard RJ (1995). Cloning the *P. falciparum* gene encoding PfEMP1, a malarial variant antigen and adherence receptor on the surface of parasitized human erythrocytes. *Cell* **82** (1): 77-87.

Beaumelle BD, Vial HJ and Philippot JR (1987). Reevaluation, using marker enzymes, of the ability of saponin and ammonium chloride to free *Plasmodium* from infected erythrocytes. *J Parasitol* **73** (4): 743-8.

Bhakdi S, Tranum-Jensen J and Sziegoleit A (1985). Mechanism of membrane damage by streptolysin-O. *Infect Immun* **47** (1): 52-60.

Biggs BA, Kemp DJ and Brown GV (1989). Subtelomeric chromosome deletions in field isolates of *Plasmodium falciparum* and their relationship to loss of cytoadherence in vitro. *Proc Natl Acad Sci U S A* **86** (7): 2428-32.

Bischoff E, Guillotte M, Mercereau-Puijalon O and Bonnefoy S (2000). A member of the *Plasmodium falciparum* Pf60 multigene family codes for a nuclear protein expressed by readthrough of an internal stop codon. *Mol Microbiol* **35** (5): 1005-16.

Blackman MJ, Heidrich HG, Donachie S, McBride JS and Holder AA (1990). A single fragment of a malaria merozoite surface protein remains on the parasite during red cell invasion and is the target of invasion-inhibiting antibodies. *J Exp Med* **172** (1): 379-82.

Blisnick T, Morales Betoulle ME, Barale JC, Uzureau P, Berry L, Desroses S, Fujioka H, Mattei D and Braun Breton C (2000). Pfsbp1, a Maurer's cleft *Plasmodium falciparum* protein, is associated with the erythrocyte skeleton. *Mol Biochem Parasitol* **111** (1): 107-21.

Blisnick T, Vincensini L, Barale JC, Namane A and Braun Breton C (2005). LANCL1, an erythrocyte protein recruited to the Maurer's clefts during *Plasmodium falciparum* development. *Mol Biochem Parasitol* **141** (1): 39-47.

Bolad A and Berzins K (2000). Antigenic diversity of *Plasmodium falciparum* and antibody-mediated parasite neutralization. *Scand J Immunol* **52** (3): 233-9.

Bonnefoy S, Bischoff E, Guillotte M and Mercereau-Puijalon O (1997). Evidence for distinct prototype sequences within the *Plasmodium falciparum* Pf60 multigene family. *Mol Biochem Parasitol* **87** (1): 1-11.

Bradley PJ, Ward C, Cheng SJ, Alexander DL, Coller S, Coombs GH, Dunn JD, Ferguson DJ, Sanderson SJ, Wastling JM and Boothroyd JC (2005). Proteomic analysis of rhoptry organelles reveals many novel constituents for host-parasite interactions in *Toxoplasma gondii*. *J Biol Chem* **280** (40): 34245-58.

Bray RS and Sinden RE (1979). The sequestration of *Plasmodium falciparum* infected erythrocytes in the placenta. *Trans R Soc Trop Med Hyg* **73** (6): 716-9.

Bruce MC, Alano P, Duthie S and Carter R (1990). Commitment of the malaria parasite *Plasmodium falciparum* to sexual and asexual development. *Parasitology* **100 Pt 2**: 191-200.

Bruce MC, Carter RN, Nakamura K, Aikawa M and Carter R (1994). Cellular location and temporal expression of the *Plasmodium falciparum* sexual stage antigen Pfs16. *Mol Biochem Parasitol* **65** (1): 11-22.

Bruce-Chwatt LJ (1963). A Longitudinal Survey of Natural Malaria Infection in a Group of West African Adults. *West Afr Med J* **12**: 199-217.

Buffet PA, Gamain B, Scheidig C, Baruch D, Smith JD, Hernandez-Rivas R, Pouvelle B, Oishi S, Fujii N, Fusai T, Parzy D, Miller LH, Gysin J and Scherf A (1999). *Plasmodium falciparum* domain mediating adhesion to chondroitin sulfate A: a receptor for human placental infection. *Proc Natl Acad Sci U S A* **96** (22): 12743-8.

Bull PC, Berriman M, Kyes S, Quail MA, Hall N, Kortok MM, Marsh K and Newbold CI (2005). *Plasmodium falciparum* variant surface antigen expression patterns during malaria. *PLoS Pathog* **1** (3): e26.

Bull PC, Lowe BS, Kortok M, Molyneux CS, Newbold CI and Marsh K (1998). Parasite antigens on the infected red cell surface are targets for naturally acquired immunity to malaria. *Nat Med* **4** (3): 358-60.

Carlson J, Helmby H, Hill AV, Brewster D, Greenwood BM and Wahlgren M (1990). Human cerebral malaria: association with erythrocyte rosetting and lack of anti-rosetting antibodies. *Lancet* **336** (8729): 1457-60.

Carter R, Graves PM, Creasey A, Byrne K, Read D, Alano P and Fenton B (1989). *Plasmodium falciparum*: an abundant stage-specific protein expressed during early gametocyte development. *Exp Parasitol* **69** (2): 140-9.

Carter R and Miller LH (1979). Evidence for environmental modulation of gametocytogenesis in *Plasmodium falciparum* in continuous culture. *Bull World Health Organ* **57 Suppl 1**: 37-52.

Chamberlain LH (2004). Detergents as tools for the purification and classification of lipid rafts. *FEBS Lett* **559** (1-3): 1-5.

Chen Q (2007). The naturally acquired immunity in severe malaria and its implication for a PfEMP-1 based vaccine. *Microbes Infect* **9** (6): 777-83.

Chen Q, Fernandez V, Sundstrom A, Schlichtherle M, Datta S, Hagblom P and Wahlgren M (1998). Developmental selection of var gene expression in *Plasmodium falciparum*. *Nature* **394** (6691): 392-5.

Chen Q, Schlichtherle M and Wahlgren M (2000). Molecular aspects of severe malaria. *Clin Microbiol Rev* **13** (3): 439-50.

Cheng Q, Cloonan N, Fischer K, Thompson J, Waine G, Lanzer M and Saul A (1998). stevor and rif are *Plasmodium falciparum* multicopy gene families which potentially encode variant antigens. *Mol Biochem Parasitol* **97** (1-2): 161-76.

Chia YS, Badaut C, Tuikue Ndam NG, Khattab A, Igonet S, Fievet N, Bentley GA, Deloron P and Klinkert MQ (2005). Functional and immunological characterization of a duffy binding-like-gamma domain from *Plasmodium falciparum* erythrocyte membrane protein-1 expressed by a placental isolate. *J Infect Dis* **192** (7): 1284-93.

Collins WE, Pye D, Crewther PE, Vandenberg KL, Galland GG, Sulzer AJ, Kemp DJ, Edwards SJ, Coppel RL, Sullivan JS and et al. (1994). Protective immunity induced in squirrel monkeys with recombinant apical membrane antigen-1 of *Plasmodium fragile*. *Am J Trop Med Hyg* **51** (6): 711-9.

Cooke BM, Buckingham DW, Glenister FK, Fernandez KM, Bannister LH, Marti M, Mohandas N and Coppel RL (2006). A Maurer's cleft-associated protein is essential for expression of the major malaria virulence antigen on the surface of infected red blood cells. *J Cell Biol* **172** (6): 899-908.

Cooke BM, Lingelbach K, Bannister LH and Tilley L (2004). Protein trafficking in *Plasmodium falciparum*-infected red blood cells. *Trends Parasitol* **20** (12): 581-9.

Cowman AF and Crabb BS (2006). Invasion of red blood cells by malaria parasites. *Cell* **124** (4): 755-66.

Crabb BS, Cooke BM, Reeder JC, Waller RF, Caruana SR, Davern KM, Wickham ME, Brown GV, Coppel RL and Cowman AF (1997). Targeted gene disruption shows that knobs enable malaria-infected red cells to cytoadhere under physiological shear stress. *Cell* **89** (2): 287-96.

Culvenor JG, Day KP and Anders RF (1991). *Plasmodium falciparum* ring-infected erythrocyte surface antigen is released from merozoite dense granules after erythrocyte invasion. *Infect Immun* **59** (3): 1183-7.

Daily JP, Le Roch KG, Sarr O, Ndiaye D, Lukens A, Zhou Y, Ndir O, Mboup S, Sultan A, Winzeler EA and Wirth DF (2005). In vivo transcriptome of *Plasmodium falciparum* reveals overexpression of transcripts that encode surface proteins. *J Infect Dis* **191** (7): 1196-203.

Day KP, Hayward RE, Smith D and Culvenor JG (1998). CD36-dependent adhesion and knob expression of the transmission stages of *Plasmodium falciparum* is stage specific. *Mol Biochem Parasitol* **93** (2): 167-77.

Diouf I, Fievet N, Doucoure S, Ngom M, Gaye A, Dumont A, Ndao CT, Le Hesran JY, Chaouat G and Deloron P (2004). Monocyte activation and T cell inhibition in *Plasmodium falciparum*-infected placenta. *J Infect Dis* **189** (12): 2235-42.

Dzikowski R, Frank M and Deitsch K (2006a). Mutually exclusive expression of virulence genes by malaria parasites is regulated independently of antigen production. *PLoS Pathog* **2** (3): e22.

Dzikowski R, Templeton TJ and Deitsch K (2006b). Variant antigen gene expression in malaria. *Cell Microbiol* **8** (9): 1371-81.

Eksi S, Stump A, Fanning SL, Shenouda MI, Fujioka H and Williamson KC (2002). Targeting and sequestration of truncated Pfs230 in an intraerythrocytic compartment during *Plasmodium falciparum* gametocytogenesis. *Mol Microbiol* **44** (6): 1507-16.

Elmendorf HG and Haldar K (1993). Secretory transport in Plasmodium. *Parasitol Today* **9** (3): 98-102.

Elmendorf HG and Haldar K (1994). *Plasmodium falciparum* exports the Golgi marker sphingomyelin synthase into a tubovesicular network in the cytoplasm of mature erythrocytes. *J Cell Biol* **124** (4): 449-62.

Fernandez V, Hommel M, Chen Q, Hagblom P and Wahlgren M (1999). Small, clonally variant antigens expressed on the surface of the *Plasmodium falciparum*-infected erythrocyte are encoded by the rif gene family and are the target of human immune responses. *J Exp Med* **190** (10): 1393-404.

Fernandez-Becerra C, Pein O, de Oliveira TR, Yamamoto MM, Cassola AC, Rocha C, Soares IS, de Braganca Pereira CA and del Portillo HA (2005). Variant proteins of *Plasmodium vivax* are not clonally expressed in natural infections. *Mol Microbiol* **58** (3): 648-58.

Ferreira MU, da Silva Nunes M and Wunderlich G (2004). Antigenic diversity and immune evasion by malaria parasites. *Clin Diagn Lab Immunol* **11** (6): 987-95.

Fischer K, Marti T, Rick B, Johnson D, Benting J, Baumeister S, Helmbrecht C, Lanzer M and Lingelbach K (1998). Characterization and cloning of the gene encoding the vacuolar membrane protein EXP-2 from *Plasmodium falciparum*. *Mol Biochem Parasitol* **92** (1): 47-57.

Fivelman QL, McRobert L, Sharp S, Taylor CJ, Saeed M, Swales CA, Sutherland CJ and Baker DA (2007). Improved synchronous production of *Plasmodium falciparum* gametocytes in vitro. *Mol Biochem Parasitol* **154** (1): 119-23.

Flick K and Chen Q (2004). var genes, PfEMP1 and the human host. *Mol Biochem Parasitol* **134** (1): 3-9.

Florens L, Washburn MP, Raine JD, Anthony RM, Grainger M, Haynes JD, Moch JK, Muster N, Sacci JB, Tabb DL, Witney AA, Wolters D, Wu Y, Gardner MJ, Holder AA, Sinden RE, Yates JR and Carucci DJ (2002). A proteomic view of the *Plasmodium falciparum* life cycle. *Nature* **419** (6906): 520-6.

Foley M, Tilley L, Sawyer WH and Anders RF (1991). The ring-infected erythrocyte surface antigen of *Plasmodium falciparum* associates with spectrin in the erythrocyte membrane. *Mol Biochem Parasitol* **46** (1): 137-47.

Francis SE, Sullivan DJ, Jr. and Goldberg DE (1997). Hemoglobin metabolism in the malaria parasite *Plasmodium falciparum*. *Annu Rev Microbiol* **51**: 97-123.

Frankland S, Adisa A, Horrocks P, Taraschi TF, Schneider T, Elliott SR, Rogerson SJ, Knuepfer E, Cowman AF, Newbold CI and Tilley L (2006). Delivery of the malaria virulence protein PfEMP1 to the erythrocyte surface requires cholesterol-rich domains. *Eukaryot Cell* **5** (5): 849-60.

Freitas-Junior LH, Bottius E, Pirrit LA, Deitsch KW, Scheidig C, Guinet F, Nehrbass U, Wellems TE and Scherf A (2000). Frequent ectopic recombination of virulence factor genes in telomeric chromosome clusters of *P. falciparum*. *Nature* **407** (6807): 1018-22.

Freitas-Junior LH, Hernandez-Rivas R, Ralph SA, Montiel-Condado D, Ruvalcaba-Salazar OK, Rojas-Meza AP, Mancio-Silva L, Leal-Silvestre RJ, Gontijo AM, Shorte S and Scherf A (2005). Telomeric heterochromatin propagation and histone acetylation control mutually exclusive expression of antigenic variation genes in malaria parasites. *Cell* **121** (1): 25-36.

Fremount HN and Rossan RN (1974). The sites of sequestration of the Uganda-Palo Alto strain of *plasmodium falciparum*-infected red blood cells in the squirrel monkey, Samimiri sciureus. *J Parasitol* **60** (3): 534-6.

Fried M, Domingo GJ, Gowda CD, Mutabingwa TK and Duffy PE (2006). *Plasmodium falciparum*: chondroitin sulfate A is the major receptor for adhesion of parasitized erythrocytes in the placenta. *Exp Parasitol* **113** (1): 36-42.

Fried M and Duffy PE (1996). Adherence of *Plasmodium falciparum* to chondroitin sulfate A in the human placenta. *Science* **272** (5267): 1502-4.

Fried M and Duffy PE (2002). Two DBLgamma subtypes are commonly expressed by placental isolates of *Plasmodium falciparum*. *Mol Biochem Parasitol* **122** (2): 201-10.

Frischknecht F, Baldacci P, Martin B, Zimmer C, Thiberge S, Olivo-Marin JC, Shorte SL and Menard R (2004). Imaging movement of malaria parasites during transmission by Anopheles mosquitoes. *Cell Microbiol* **6** (7): 687-94.

Galinski MR, Medina CC, Ingravallo P and Barnwell JW (1992). A reticulocyte-binding protein complex of *Plasmodium vivax* merozoites. *Cell* **69** (7): 1213-26.

Gamain B, Smith JD, Viebig NK, Gysin J and Scherf A (2007). Pregnancy-associated malaria: parasite binding, natural immunity and vaccine development. *Int J Parasitol* **37** (3-4): 273-83.

Gardner MJ, Hall N, Fung E, White O, Berriman M, Hyman RW, Carlton JM, Pain A, Nelson KE, Bowman S, Paulsen IT, James K, Eisen JA, Rutherford K, Salzberg SL, Craig A, Kyes S, Chan MS, Nene V, Shallom SJ, Suh B, Peterson J, Angiuoli S, Pertea M, Allen J, Selengut J, Haft D, Mather MW, Vaidya AB, Martin DM, Fairlamb AH, Fraunholz MJ, Roos DS, Ralph SA, McFadden GI, Cummings LM, Subramanian GM, Mungall C, Venter JC, Carucci DJ, Hoffman SL, Newbold C, Davis RW, Fraser CM and Barrell B (2002). Genome sequence of the human malaria parasite *Plasmodium falciparum*. *Nature* **419** (6906): 498-511.

Gaur D, Mayer DC and Miller LH (2004). Parasite ligand-host receptor interactions during invasion of erythrocytes by *Plasmodium* merozoites. *Int J Parasitol* **34** (13-14): 1413-29.

Gilberger TW, Thompson JK, Triglia T, Good RT, Duraisingh MT and Cowman AF (2003). A novel erythrocyte binding antigen-175 paralogue from *Plasmodium falciparum* defines a new trypsin-resistant receptor on human erythrocytes. *J Biol Chem* **278** (16): 14480-6.

Golding GB and Dean AM (1998). The structural basis of molecular adaptation. *Mol Biol Evol* **15** (4): 355-69.

Grellier P, Precigout E, Valentin A, Carcy B and Schrevel J (1994). Characterization of a new 60 kDa apical protein of *Plasmodium falciparum* merozoite expressed in late schizogony. *Biol Cell* **82** (2-3): 129-38.

Gruenberg J, Allred DR and Sherman IW (1983). Scanning electron microscope-analysis of the protrusions (knobs) present on the surface of *Plasmodium falciparum*-infected erythrocytes. *J Cell Biol* **97** (3): 795-802.

Gunther K, Tummler M, Arnold HH, Ridley R, Goman M, Scaife JG and Lingelbach K (1991). An exported protein of *Plasmodium falciparum* is synthesized as an integral membrane protein. *Mol Biochem Parasitol* **46** (1): 149-57.

Haeggstrom M, A VONE, Kironde F, Fernandez V and Wahlgren M (2007). Characterization of Maurer's clefts in *Plasmodium falciparum*-infected erythrocytes. *Am J Trop Med Hyg* **76** (1): 27-32.

Haeggstrom M, Kironde F, Berzins K, Chen Q, Wahlgren M and Fernandez V (2004). Common trafficking pathway for variant antigens destined for the surface of the *Plasmodium falciparum*-infected erythrocyte. *Mol Biochem Parasitol* **133** (1): 1-14.

Haldar K, Kamoun S, Hiller NL, Bhattacharje S and van Ooij C (2006). Common infection strategies of pathogenic eukaryotes. *Nat Rev Microbiol* **4** (12): 922-31.

Hayward RE, Tiwari B, Piper KP, Baruch DI and Day KP (1999). Virulence and transmission success of the malarial parasite *Plasmodium falciparum*. *Proc Natl Acad Sci U S A* **96** (8): 4563-8.

Heidrich HG, Strych W and Mrema JE (1983). Identification of surface and internal antigens from spontaneously released *Plasmodium falciparum* merozoites by radio-iodination and metabolic labelling. *Z Parasitenkd* **69** (6): 715-25.

Helmby H, Cavelier L, Pettersson U and Wahlgren M (1993). Rosetting *Plasmodium falciparum*-infected erythrocytes express unique strain-specific antigens on their surface. *Infect Immun* **61** (1): 284-8.

Heussler V and Doerig C (2006). In vivo imaging enters parasitology. *Trends Parasitol* **22** (5): 192-5; discussion 195-6.

Higy M, Junne T and Spiess M (2004). Topogenesis of membrane proteins at the endoplasmic reticulum. *Biochemistry* **43** (40): 12716-22.

Hiller NL, Bhattacharjee S, van Ooij C, Liolios K, Harrison T, Lopez-Estrano C and Haldar K (2004). A host-targeting signal in virulence proteins reveals a secretome in malarial infection. *Science* **306** (5703): 1934-7.

Hinterberg K, Scherf A, Gysin J, Toyoshima T, Aikawa M, Mazie JC, da Silva LP and Mattei D (1994). *Plasmodium falciparum*: the Pf332 antigen is secreted from the parasite by a brefeldin A-dependent pathway and is translocated to the erythrocyte membrane via the Maurer's clefts. *Exp Parasitol* **79** (3): 279-91.

Holder AA, Freeman RR, Uni S and Aikawa M (1985). Isolation of a *Plasmodium falciparum* rhoptry protein. *Mol Biochem Parasitol* **14** (3): 293-303.

Holder AA, Guevara Patino JA, Uthaipibull C, Syed SE, Ling IT, Scott-Finnigan T and Blackman MJ (1999). Merozoite surface protein 1, immune evasion, and vaccines against asexual blood stage malaria. *Parassitologia* **41** (1-3): 409-14.

Hviid L (2007). Development of vaccines against *Plasmodium falciparum* malaria: taking lessons from naturally acquired protective immunity. *Microbes Infect* **9** (6): 772-6.

Ikeda M, Arai M, Lao DM and Shimizu T (2002). Transmembrane topology prediction methods: a re-assessment and improvement by a consensus method using a dataset of experimentally-characterized transmembrane topologies. *In Silico Biol* **2** (1): 19-33.

Janssen CS, Phillips RS, Turner CM and Barrett MP (2004). *Plasmodium* interspersed repeats: the major multigene superfamily of malaria parasites. *Nucleic Acids Res* **32** (19): 5712-20.

Jeffares DC, Pain A, Berry A, Cox AV, Stalker J, Ingle CE, Thomas A, Quail MA, Siebenthall K, Uhlemann AC, Kyes S, Krishna S, Newbold C, Dermitzakis ET and Berriman M (2007). Genome variation and evolution of the malaria parasite *Plasmodium falciparum*. *Nat Genet* **39** (1): 120-5.

Jegga AG, Sherwood SP, Carman JW, Pinski AT, Phillips JL, Pestian JP and Aronow BJ (2002). Detection and visualization of compositionally similar cis-regulatory element clusters in orthologous and coordinately controlled genes. *Genome Res* **12** (9): 1408-17.

Jensen AT, Magistrado P, Sharp S, Joergensen L, Lavstsen T, Chiucchiuini A, Salanti A, Vestergaard LS, Lusingu JP, Hermsen R, Sauerwein R, Christensen J, Nielsen MA, Hviid L, Sutherland C, Staalsoe T and Theander TG (2004). *Plasmodium falciparum* associated with severe childhood malaria preferentially expresses PfEMP1 encoded by group A var genes. *J Exp Med* **199** (9): 1179-90.

Kaestli M, Cockburn IA, Cortes A, Baea K, Rowe JA and Beck HP (2006). Virulence of malaria is associated with differential expression of *Plasmodium falciparum* var gene subgroups in a case-control study. *J Infect Dis* **193** (11): 1567-74.

Kall L, Krogh A and Sonnhammer EL (2004). A combined transmembrane topology and signal peptide prediction method. *J Mol Biol* **338** (5): 1027-36.

Kass L, Willerson D, Jr., Rieckmann KH, Carson PE and Becker RP (1971). *Plasmodium falciparum* gametocytes. Electron microscopic observations on material obtained by a new method. *Am J Trop Med Hyg* **20** (2): 187-94.

Kats LM, Black CG, Proellocks NI and Coppel RL (2006). *Plasmodium* rhoptries: how things went pear-shaped. *Trends Parasitol* **22** (6): 269-76.

Kaviratne M, Khan SM, Jarra W and Preiser PR (2002). Small variant STEVOR antigen is uniquely located within Maurer's clefts in *Plasmodium falciparum*-infected red blood cells. *Eukaryot Cell* **1** (6): 926-35.

Khan SM, Jarra W and Preiser PR (2001). The 235 kDa rhoptry protein of *Plasmodium (yoelii) yoelii*: function at the junction. *Mol Biochem Parasitol* **117** (1): 1-10.

Khattab A and Klinkert MQ (2006). Maurer's clefts-restricted localization, orientation and export of a *Plasmodium falciparum* RIFIN. *Traffic* **7** (12): 1654-65.

Khattab A, Kremsner PG and Klinkert MQ (2003). Common surface-antigen var genes of limited diversity expressed by *Plasmodium falciparum* placental isolates separated by time and space. *J Infect Dis* **187** (3): 477-83.

Khattab A, Kun J, Deloron P, Kremsner PG and Klinkert MQ (2001). Variants of *Plasmodium falciparum* erythrocyte membrane protein 1 expressed by different placental parasites are closely related and adhere to chondroitin sulfate A. *J Infect Dis* **183** (7): 1165-9.

Khattab A, Reinhardt C, Staalsoe T, Fievet N, Kremsner PG, Deloron P, Hviid L and Klinkert MQ (2004). Analysis of IgG with specificity for variant surface antigens expressed by placental *Plasmodium falciparum* isolates. *Malar J* **3**: 21.

Kidgell C, Volkman SK, Daily J, Borevitz JO, Plouffe D, Zhou Y, Johnson JR, Le Roch K, Sarr O, Ndir O, Mboup S, Batalov S, Wirth DF and Winzeler EA (2006). A systematic map of genetic variation in *Plasmodium falciparum*. *PLoS Pathog* **2** (6): e57.

Knuepfer E, Rug M and Cowman AF (2005). Function of the *plasmodium* export element can be blocked by green fluorescent protein. *Mol Biochem Parasitol* **142** (2): 258-62.

Kocken CH, van der Wel AM, Dubbeld MA, Narum DL, van de Rijke FM, van Gemert GJ, van der Linde X, Bannister LH, Janse C, Waters AP and Thomas AW (1998). Precise timing of expression of a *Plasmodium falciparum*-derived transgene in *Plasmodium berghei* is a critical determinant of subsequent subcellular localization. *J Biol Chem* **273** (24): 15119-24.

Kraemer SM, Kyes SA, Aggarwal G, Springer AL, Nelson SO, Christodoulou Z, Smith LM, Wang W, Levin E, Newbold CI, Myler PJ and Smith JD (2007). Patterns of gene recombination shape var gene repertoires in *Plasmodium falciparum*: comparisons of geographically diverse isolates. *BMC Genomics* **8**: 45.

Kraemer SM and Smith JD (2003). Evidence for the importance of genetic structuring to the structural and functional specialization of the *Plasmodium falciparum* var gene family. *Mol Microbiol* **50** (5): 1527-38.

Kriek N, Tilley L, Horrocks P, Pinches R, Elford BC, Ferguson DJ, Lingelbach K and Newbold CI (2003). Characterization of the pathway for transport of the cytoadherence-mediating protein, PfEMP1, to the host cell surface in malaria parasite-infected erythrocytes. *Mol Microbiol* **50** (4): 1215-27.

Kumar S, Tamura K and Nei M (2004). MEGA3: Integrated software for Molecular Evolutionary Genetics Analysis and sequence alignment. *Brief Bioinform* **5** (2): 150-63.

Kyes S, Pinches R and Newbold C (2000). A simple RNA analysis method shows var and rif multigene family expression patterns in *Plasmodium falciparum*. *Mol Biochem Parasitol* **105** (2): 311-5.

Kyes SA, Christodoulou Z, Raza A, Horrocks P, Pinches R, Rowe JA and Newbold CI (2003). A well-conserved *Plasmodium falciparum* var gene shows an unusual stage-specific transcript pattern. *Mol Microbiol* **48** (5): 1339-48.

Kyes SA, Kraemer SM and Smith JD (2007). Antigenic Variation in *Plasmodium falciparum*: Gene Organization and Regulation of the var Multigene Family. *Eukaryot Cell*.

Kyes SA, Rowe JA, Kriek N and Newbold CI (1999). Rifins: a second family of clonally variant proteins expressed on the surface of red cells infected with *Plasmodium falciparum*. *Proc Natl Acad Sci U S A* **96** (16): 9333-8.

Kyriacou HM, Stone GN, Challis RJ, Raza A, Lyke KE, Thera MA, Kone AK, Doumbo OK, Plowe CV and Rowe JA (2006). Differential var gene transcription in *Plasmodium falciparum* isolates from patients with cerebral malaria compared to hyperparasitaemia. *Mol Biochem Parasitol* **150** (2): 211-8.

Langreth SG and Peterson E (1985). Pathogenicity, stability, and immunogenicity of a knobless clone of *Plasmodium falciparum* in Colombian owl monkeys. *Infect Immun* **47** (3): 760-6.

Lanzer M, Wickert H, Krohne G, Vincensini L and Braun Breton C (2006). Maurer's clefts: a novel multi-functional organelle in the cytoplasm of *Plasmodium falciparum*-infected erythrocytes. *Int J Parasitol* **36** (1): 23-36.

Lauer S, VanWye J, Harrison T, McManus H, Samuel BU, Hiller NL, Mohandas N and Haldar K (2000). Vacuolar uptake of host components, and a role for cholesterol and sphingomyelin in malarial infection. *Embo J* **19** (14): 3556-64.

Lauer SA, Rathod PK, Ghori N and Haldar K (1997). A membrane network for nutrient import in red cells infected with the malaria parasite. *Science* **276** (5315): 1122-5.

Lavazec C, Sanyal S and Templeton TJ (2006). Hypervariability within the Rifin, Stevor and Pfmc-2TM superfamilies in *Plasmodium falciparum*. *Nucleic Acids Res* **34** (22): 6696-707.

Lavstsen T, Salanti A, Jensen AT, Arnot DE and Theander TG (2003). Sub-grouping of *Plasmodium falciparum* 3D7 var genes based on sequence analysis of coding and non-coding regions. *Malar J* **2**: 27.

Le Roch KG, Zhou Y, Blair PL, Grainger M, Moch JK, Haynes JD, De La Vega P, Holder AA, Batalov S, Carucci DJ and Winzeler EA (2003). Discovery of gene function by expression profiling of the malaria parasite life cycle. *Science* **301** (5639): 1503-8.

Lindenthal C and Klinkert MQ (2002). Identification and biochemical characterisation of a protein phosphatase 5 homologue from *Plasmodium falciparum*. *Mol Biochem Parasitol* **120** (2): 257-68.

Lindenthal C, Kremsner PG and Klinkert MQ (2003). Commonly recognised *Plasmodium falciparum* parasites cause cerebral malaria. *Parasitol Res* **91** (5): 363-8.

Ling IT, Florens L, Dluzewski AR, Kaneko O, Grainger M, Yim Lim BY, Tsuboi T, Hopkins JM, Johnson JR, Torii M, Bannister LH, Yates JR, 3rd, Holder AA and Mattei D (2004). The *Plasmodium falciparum* clag9 gene encodes a rhoptry protein that is transferred to the host erythrocyte upon invasion. *Mol Microbiol* **52** (1): 107-18.

Marsh K, Otoo L, Hayes RJ, Carson DC and Greenwood BM (1989). Antibodies to blood stage antigens of *Plasmodium falciparum* in rural Gambians and their relation to protection against infection. *Trans R Soc Trop Med Hyg* **83** (3): 293-303.

Marti M, Baum J, Rug M, Tilley L and Cowman AF (2005). Signal-mediated export of proteins from the malaria parasite to the host erythrocyte. *J Cell Biol* **171** (4): 587-92.

Marti M, Good RT, Rug M, Knuepfer E and Cowman AF (2004). Targeting malaria virulence and remodeling proteins to the host erythrocyte. *Science* **306** (5703): 1930-3.

McBride JS and Heidrich HG (1987). Fragments of the polymorphic Mr 185,000 glycoprotein from the surface of isolated *Plasmodium falciparum* merozoites form an antigenic complex. *Mol Biochem Parasitol* **23** (1): 71-84.

McGregor IA (1974). Mechanisms of acquired immunity and epidemiological patterns of antibody responses in malaria in man. *Bull World Health Organ* **50** (3-4): 259-66.

McRobert L, Preiser P, Sharp S, Jarra W, Kaviratne M, Taylor MC, Renia L and Sutherland CJ (2004). Distinct trafficking and localization of STEVOR proteins in three stages of the *Plasmodium falciparum* life cycle. *Infect Immun* **72** (11): 6597-602.

Meijer HA and Thomas AA (2002). Control of eukaryotic protein synthesis by upstream open reading frames in the 5'-untranslated region of an mRNA. *Biochem J* **367** (Pt 1): 1-11.

Merino EF, Fernandez-Becerra C, Durham AM, Ferreira JE, Tumilasci VF, d'Arc-Neves J, da Silva-Nunes M, Ferreira MU, Wickramarachchi T, Udagama-Randeniya P, Handunnetti SM and

Del Portillo HA (2006). Multi-character population study of the vir subtelomeric multigene superfamily of *Plasmodium vivax*, a major human malaria parasite. *Mol Biochem Parasitol* **149** (1): 10-6.

Miller LH (1969). Distribution of mature trophozoites and schizonts of *Plasmodium falciparum* in the organs of Aotus trivirgatus, the night monkey. *Am J Trop Med Hyg* **18** (6): 860-5.

Mills JP, Diez-Silva M, Quinn DJ, Dao M, Lang MJ, Tan KS, Lim CT, Milon G, David PH, Mercereau-Puijalon O, Bonnefoy S and Suresh S (2007). Effect of plasmodial RESA protein on deformability of human red blood cells harboring *Plasmodium falciparum*. *Proc Natl Acad Sci U S A* **104** (22): 9213-7.

Moll K, Chene A, Ribacke U, Kaneko O, Nilsson S, Winter G, Haeggstrom M, Pan W, Berzins K, Wahlgren M and Chen Q (2007). A novel DBL-domain of the *P. falciparum* 332 molecule possibly involved in erythrocyte adhesion. *PLoS ONE* **2**: e477.

Mota MM, Hafalla JC and Rodriguez A (2002). Migration through host cells activates *Plasmodium* sporozoites for infection. *Nat Med* **8** (11): 1318-22.

Mu J, Awadalla P, Duan J, McGee KM, Keebler J, Seydel K, McVean GA and Su XZ (2007). Genome-wide variation and identification of vaccine targets in the *Plasmodium falciparum* genome. *Nat Genet* **39** (1): 126-30.

Murphy SC, Samuel BU, Harrison T, Speicher KD, Speicher DW, Reid ME, Prohaska R, Low PS, Tanner MJ, Mohandas N and Haldar K (2004). Erythrocyte detergent-resistant membrane proteins: their characterization and selective uptake during malarial infection. *Blood* **103** (5): 1920-8.

Nagao E, Seydel KB and Dvorak JA (2002). Detergent-resistant erythrocyte membrane rafts are modified by a *Plasmodium falciparum* infection. *Exp Parasitol* **102** (1): 57-9.

Newbold C, Craig A, Kyes S, Rowe A, Fernandez-Reyes D and Fagan T (1999). Cytoadherence, pathogenesis and the infected red cell surface in *Plasmodium falciparum*. *Int J Parasitol* **29** (6): 927-37.

Oh SS, Voigt S, Fisher D, Yi SJ, LeRoy PJ, Derick LH, Liu S and Chishti AH (2000). *Plasmodium falciparum* erythrocyte membrane protein 1 is anchored to the actin-spectrin junction and knob-associated histidine-rich protein in the erythrocyte skeleton. *Mol Biochem Parasitol* **108** (2): 237-47.

Pain A, Ferguson DJ, Kai O, Urban BC, Lowe B, Marsh K and Roberts DJ (2001). Platelet-mediated clumping of *Plasmodium falciparum*-infected erythrocytes is a common adhesive phenotype and is associated with severe malaria. *Proc Natl Acad Sci U S A* **98** (4): 1805-10.

Papakrivos J, Newbold CI and Lingelbach K (2005). A potential novel mechanism for the insertion of a membrane protein revealed by a biochemical analysis of the *Plasmodium falciparum* cytoadherence molecule PfEMP-1. *Mol Microbiol* **55** (4): 1272-84.

Pei X, An X, Guo X, Tarnawski M, Coppel R and Mohandas N (2005). Structural and functional studies of interaction between *Plasmodium falciparum* knob-associated histidine-rich protein (KAHRP) and erythrocyte spectrin. *J Biol Chem* **280** (35): 31166-71.

Pei X, Guo X, Coppel R, Bhattacharjee S, Haldar K, Gratzer W, Mohandas N and An X (2007). The ring-infected erythrocyte surface antigen (RESA) of *Plasmodium falciparum* stabilizes spectrin tetramers and suppresses further invasion. *Blood* **110** (3): 1036-42.

Petter M, Haeggström M, Khattab A, Fernandez V, Klinkert MQ, Wahlgren M (2007). Variant proteins of the *Plasmodium falciparum* RIFIN family show distinct subcellular localization and developmental expression patterns. *Mol Biochem Parasitol* (in press).

Pologe LG and Ravetch JV (1986). A chromosomal rearrangement in a *P. falciparum* histidine-rich protein gene is associated with the knobless phenotype. *Nature* **322** (6078): 474-7.

Ponnudurai T, Lensen AH, Leeuwenberg AD and Meuwissen JH (1982). Cultivation of fertile *Plasmodium falciparum* gametocytes in semi-automated systems. 1. Static cultures. *Trans R Soc Trop Med Hyg* **76** (6): 812-8.

Pradel G, Hayton K, Aravind L, Iyer LM, Abrahamsen MS, Bonawitz A, Mejia C and Templeton TJ (2004). A multidomain adhesion protein family expressed in *Plasmodium falciparum* is essential for transmission to the mosquito. *J Exp Med* **199** (11): 1533-44.

Pradel G, Wagner C, Mejia C and Templeton TJ (2006). *Plasmodium falciparum*: Co-dependent expression and co-localization of the PfCCp multi-adhesion domain proteins. *Exp Parasitol* **112** (4): 263-8.

Preiser P, Kaviratne M, Khan S, Bannister L and Jarra W (2000). The apical organelles of malaria merozoites: host cell selection, invasion, host immunity and immune evasion. *Microbes Infect* **2** (12): 1461-77.

Preiser PR, Jarra W, Capiod T and Snounou G (1999). A rhoptry-protein-associated mechanism of clonal phenotypic variation in rodent malaria. *Nature* **398** (6728): 618-22.

Preiser PR, Khan S, Costa FT, Jarra W, Belnoue E, Ogun S, Holder AA, Voza T, Landau I, Snounou G and Renia L (2002). Stage-specific transcription of distinct repertoires of a multigene family during *Plasmodium* life cycle. *Science* **295** (5553): 342-5.

Przyborski JM, Miller SK, Pfahler JM, Henrich PP, Rohrbach P, Crabb BS and Lanzer M (2005). Trafficking of STEVOR to the Maurer's clefts in *Plasmodium falciparum*-infected erythrocytes. *Embo J* **24** (13): 2306-17.

Quakyi IA, Matsumoto Y, Carter R, Udomsangpetch R, Sjolander A, Berzins K, Perlmann P, Aikawa M and Miller LH (1989). Movement of a falciparum malaria protein through the erythrocyte cytoplasm to the erythrocyte membrane is associated with lysis of the erythrocyte and release of gametes. *Infect Immun* **57** (3): 833-9.

Rabilloud T (1996). Solubilization of proteins for electrophoretic analyses. *Electrophoresis* **17** (5): 813-29.

Rasti N, Wahlgren M and Chen Q (2004). Molecular aspects of malaria pathogenesis. *FEMS Immunol Med Microbiol* **41** (1): 9-26.

Rayner JC, Galinski MR, Ingravallo P and Barnwell JW (2000). Two *Plasmodium falciparum* genes express merozoite proteins that are related to *Plasmodium vivax* and *Plasmodium yoelii* adhesive proteins involved in host cell selection and invasion. *Proc Natl Acad Sci U S A* **97** (17): 9648-53.

Reeder JC, Cowman AF, Davern KM, Beeson JG, Thompson JK, Rogerson SJ and Brown GV (1999). The adhesion of *Plasmodium falciparum*-infected erythrocytes to chondroitin sulfate A is mediated by *P. falciparum* erythrocyte membrane protein 1. *Proc Natl Acad Sci U S A* **96** (9): 5198-202.

Reynolds ES (1963). The use of lead citrate at high pH as an electron-opaque stain in electron microscopy. *J Cell Biol* **17**: 208-12.

Roberts DJ, Pain A, Kai O, Kortok M and Marsh K (2000). Autoagglutination of malaria-infected red blood cells and malaria severity. *Lancet* **355** (9213): 1427-8.

Rogers NJ, Daramola O, Targett GA and Hall BS (1996a). CD36 and intercellular adhesion molecule 1 mediate adhesion of developing *Plasmodium falciparum* gametocytes. *Infect Immun* **64** (4): 1480-3.

Rogers NJ, Hall BS, Obiero J, Targett GA and Sutherland CJ (2000). A model for sequestration of the transmission stages of *Plasmodium falciparum*: adhesion of gametocyte-infected erythrocytes to human bone marrow cells. *Infect Immun* **68** (6): 3455-62.

Rogers NJ, Targett GA and Hall BS (1996b). *Plasmodium falciparum* gametocyte adhesion to C32 cells via CD36 is inhibited by antibodies to modified band 3. *Infect Immun* **64** (10): 4261-8.

Rogerson SJ, Hviid L, Duffy PE, Leke RF and Taylor DW (2007). Malaria in pregnancy: pathogenesis and immunity. *Lancet Infect Dis* **7** (2): 105-17.

Rottmann M, Lavstsen T, Mugasa JP, Kaestli M, Jensen AT, Muller D, Theander T and Beck HP (2006). Differential expression of var gene groups is associated with morbidity caused by *Plasmodium falciparum* infection in Tanzanian children. *Infect Immun* **74** (7): 3904-11.

Rowe A, Obeiro J, Newbold CI and Marsh K (1995). *Plasmodium falciparum* rosetting is associated with malaria severity in Kenya. *Infect Immun* **63** (6): 2323-6.

Rowe JA, Moulds JM, Newbold CI and Miller LH (1997). *P. falciparum* rosetting mediated by a parasite-variant erythrocyte membrane protein and complement-receptor 1. *Nature* **388** (6639): 292-5.

Rug M, Prescott SW, Fernandez KM, Cooke BM and Cowman AF (2006). The role of KAHRP domains in knob formation and cytoadherence of P falciparum-infected human erythrocytes. *Blood* **108** (1): 370-8.

Rug M, Wickham ME, Foley M, Cowman AF and Tilley L (2004). Correct promoter control is needed for trafficking of the ring-infected erythrocyte surface antigen to the host cytosol in transfected malaria parasites. *Infect Immun* **72** (10): 6095-105.

Salanti A, Staalsoe T, Lavstsen T, Jensen AT, Sowa MP, Arnot DE, Hviid L and Theander TG (2003). Selective upregulation of a single distinctly structured var gene in chondroitin sulphate A-adhering *Plasmodium falciparum* involved in pregnancy-associated malaria. *Mol Microbiol* **49** (1): 179-91.

Sam-Yellowe TY, Florens L, Johnson JR, Wang T, Drazba JA, Le Roch KG, Zhou Y, Batalov S, Carucci DJ, Winzeler EA and Yates JR, 3rd (2004). A *Plasmodium* gene family encoding Maurer's cleft membrane proteins: structural properties and expression profiling. *Genome Res* **14** (6): 1052-9.

Scherf A, Hernandez-Rivas R, Buffet P, Bottius E, Benatar C, Pouvelle B, Gysin J and Lanzer M (1998). Antigenic variation in malaria: in situ switching, relaxed and mutually exclusive transcription of var genes during intra-erythrocytic development in *Plasmodium falciparum*. *Embo J* **17** (18): 5418-26.

Scherf A, Pouvelle B, Buffet PA and Gysin J (2001). Molecular mechanisms of *Plasmodium falciparum* placental adhesion. *Cell Microbiol* **3** (3): 125-31.

Schneider TD and Stephens RM (1990). Sequence logos: a new way to display consensus sequences. *Nucleic Acids Res* **18** (20): 6097-100.

Schofield L, Bushell GR, Cooper JA, Saul AJ, Upcroft JA and Kidson C (1986). A rhoptry antigen of *Plasmodium falciparum* contains conserved and variable epitopes recognized by inhibitory monoclonal antibodies. *Mol Biochem Parasitol* **18** (2): 183-95.

Schreiber N, Brattig N, Evans J, Tsiri A, Horstmann RD, May J and Klinkert MQ (2006). Cerebral malaria is associated with IgG2 and IgG4 antibody responses to recombinant *Plasmodium falciparum* RIFIN antigen. *Microbes Infect* **8** (5): 1269-76.

Sharp S, Lavstsen T, Fivelman QL, Saeed M, McRobert L, Templeton TJ, Jensen AT, Baker DA, Theander TG and Sutherland CJ (2006). Programmed transcription of the var gene family, but not of stevor, in *Plasmodium falciparum* gametocytes. *Eukaryot Cell* **5** (8): 1206-14.

Sherman IW, Eda S and Winograd E (2003). Cytoadherence and sequestration in *Plasmodium falciparum*: defining the ties that bind. *Microbes Infect* **5** (10): 897-909.

Silvestrini F, Alano P and Williams JL (2000). Commitment to the production of male and female gametocytes in the human malaria parasite *Plasmodium falciparum*. *Parasitology* **121 Pt 5**: 465-71.

Simmons D, Woollett G, Bergin-Cartwright M, Kay D and Scaife J (1987). A malaria protein exported into a new compartment within the host erythrocyte. *Embo J* **6** (2): 485-91.

Sinden RE (1982). Gametocytogenesis of *Plasmodium falciparum* in vitro: an electron microscopic study. *Parasitology* **84** (1): 1-11.

Smalley ME, Abdalla S and Brown J (1981). The distribution of *Plasmodium falciparum* in the peripheral blood and bone marrow of Gambian children. *Trans R Soc Trop Med Hyg* **75** (1): 103-5.

Smith JD, Kyes S, Craig AG, Fagan T, Hudson-Taylor D, Miller LH, Baruch DI and Newbold CI (1998). Analysis of adhesive domains from the A4VAR *Plasmodium falciparum* erythrocyte membrane protein-1 identifies a CD36 binding domain. *Mol Biochem Parasitol* **97** (1-2): 133-48.

Smith JD, Subramanian G, Gamain B, Baruch DI and Miller LH (2000a). Classification of adhesive domains in the *Plasmodium falciparum* erythrocyte membrane protein 1 family. *Mol Biochem Parasitol* **110** (2): 293-310.

Smith TG, Lourenco P, Carter R, Walliker D and Ranford-Cartwright LC (2000b). Commitment to sexual differentiation in the human malaria parasite, *Plasmodium falciparum*. *Parasitology* **121 (Pt 2)**: 127-33.

Spielmann T, Fergusen DJ and Beck HP (2003). etramps, a new *Plasmodium falciparum* gene family coding for developmentally regulated and highly charged membrane proteins located at the parasite-host cell interface. *Mol Biol Cell* **14** (4): 1529-44.

Spielmann T, Hawthorne PL, Dixon MW, Hannemann M, Klotz K, Kemp DJ, Klonis N, Tilley L, Trenholme KR and Gardiner DL (2006). A cluster of ring stage-specific genes linked to a locus implicated in cytoadherence in *Plasmodium falciparum* codes for PEXEL-negative and PEXEL-positive proteins exported into the host cell. *Mol Biol Cell* **17** (8): 3613-24.

Sturm A, Amino R, van de Sand C, Regen T, Retzlaff S, Rennenberg A, Krueger A, Pollok JM, Menard R and Heussler VT (2006). Manipulation of host hepatocytes by the malaria parasite for delivery into liver sinusoids. *Science* **313** (5791): 1287-90.

Sturm A and Heussler V (2007). Live and let die: manipulation of host hepatocytes by exoerythrocytic *Plasmodium* parasites. *Med Microbiol Immunol* **196** (3): 127-33.

Su XZ, Heatwole VM, Wertheimer SP, Guinet F, Herrfeldt JA, Peterson DS, Ravetch JA and Wellems TE (1995). The large diverse gene family var encodes proteins involved in cytoadherence and antigenic variation of *Plasmodium falciparum*-infected erythrocytes. *Cell* **82** (1): 89-100.

Su XZ, Wu Y, Sifri CD and Wellems TE (1996). Reduced extension temperatures required for PCR amplification of extremely A+T-rich DNA. *Nucleic Acids Res* **24** (8): 1574-5.

Talman AM, Domarle O, McKenzie FE, Ariey F and Robert V (2004). Gametocytogenesis: the puberty of *Plasmodium falciparum*. *Malar J* **3**: 24.

Taylor HM, Kyes SA and Newbold CI (2000). Var gene diversity in *Plasmodium falciparum* is generated by frequent recombination events. *Mol Biochem Parasitol* **110** (2): 391-7.

Tham WH, Payne PD, Brown GV and Rogerson SJ (2007). Identification of basic transcriptional elements required for rif gene transcription. *Int J Parasitol* **37** (6): 605-15.

Thomson JG and Robertson A (1935). The structure and development of *plasmodium falciparum* gametocytes in the internal organs and peripheral circulation. *Trans R Soc Trop Med Hyg* **29**: 31-40.

Torii M, Adams JH, Miller LH and Aikawa M (1989). Release of merozoite dense granules during erythrocyte invasion by *Plasmodium knowlesi. Infect Immun* **57** (10): 3230-3.

Trager W, Rozario C, Shio H, Williams J and Perkins ME (1992). Transfer of a dense granule protein of *Plasmodium falciparum* to the membrane of ring stages and isolation of dense granules. *Infect Immun* **60** (11): 4656-61.

Udomsangpetch R, Wahlin B, Carlson J, Berzins K, Torii M, Aikawa M, Perlmann P and Wahlgren M (1989). *Plasmodium falciparum*-infected erythrocytes form spontaneous erythrocyte rosettes. *J Exp Med* **169** (5): 1835-40.

Uhlemann AC, Staalsoe T, Klinkert MQ and Hviid L (2000). Analysis of *Plasmodium falciparum*-infected red blood cells. *MACS&more Miltenyi Biotec* **4** (2): 7-8.

Vazquez-Macias A, Martinez-Cruz P, Castaneda-Patlan MC, Scheidig C, Gysin J, Scherf A and Hernandez-Rivas R (2002). A distinct 5' flanking var gene region regulates *Plasmodium falciparum* variant erythrocyte surface antigen expression in placental malaria. *Mol Microbiol* **45** (1): 155-67.

Viebig NK, Gamain B, Scheidig C, Lepolard C, Przyborski J, Lanzer M, Gysin J and Scherf A (2005). A single member of the *Plasmodium falciparum* var multigene family determines cytoadhesion to the placental receptor chondroitin sulphate A. *EMBO Rep* **6** (8): 775-81.

Volkman SK, Sabeti PC, DeCaprio D, Neafsey DE, Schaffner SF, Milner DA, Jr., Daily JP, Sarr O, Ndiaye D, Ndir O, Mboup S, Duraisingh MT, Lukens A, Derr A, Stange-Thomann N, Waggoner S, Onofrio R, Ziaugra L, Mauceli E, Gnerre S, Jaffe DB, Zainoun J, Wiegand RC, Birren BW, Hartl DL, Galagan JE, Lander ES and Wirth DF (2007). A genome-wide map of diversity in *Plasmodium falciparum*. *Nat Genet* **39** (1): 113-9.

Voss TS, Healer J, Marty AJ, Duffy MF, Thompson JK, Beeson JG, Reeder JC, Crabb BS and Cowman AF (2006). A var gene promoter controls allelic exclusion of virulence genes in *Plasmodium falciparum* malaria. *Nature* **439** (7079): 1004-8.

Voss TS, Thompson JK, Waterkeyn J, Felger I, Weiss N, Cowman AF and Beck HP (2000). Genomic distribution and functional characterisation of two distinct and conserved *Plasmodium falciparum* var gene 5' flanking sequences. *Mol Biochem Parasitol* **107** (1): 103-15.

Waller KL, Cooke BM, Nunomura W, Mohandas N and Coppel RL (1999). Mapping the binding domains involved in the interaction between the *Plasmodium falciparum* knob-associated histidine-rich protein (KAHRP) and the cytoadherence ligand *P. falciparum* erythrocyte membrane protein 1 (PfEMP1). *J Biol Chem* **274** (34): 23808-13.

Ward CP, Clottey GT, Dorris M, Ji DD and Arnot DE (1999). Analysis of *Plasmodium falciparum* PfEMP-1/var genes suggests that recombination rearranges constrained sequences. *Mol Biochem Parasitol* **102** (1): 167-77.

Ward GE, Miller LH and Dvorak JA (1993). The origin of parasitophorous vacuole membrane lipids in malaria-infected erythrocytes. *J Cell Sci* **106 (Pt 1)**: 237-48.

Waterkeyn JG, Wickham ME, Davern KM, Cooke BM, Coppel RL, Reeder JC, Culvenor JG, Waller RF and Cowman AF (2000). Targeted mutagenesis of *Plasmodium falciparum* erythrocyte membrane protein 3 (PfEMP3) disrupts cytoadherence of malaria-infected red blood cells. *Embo J* **19** (12): 2813-23.

Weber JL (1988). Interspersed repetitive DNA from *Plasmodium falciparum*. *Mol Biochem Parasitol* **29** (2-3): 117-24.

WHO (2000). Severe falciparum malaria. World Health Organization, Communicable Diseases Cluster. *Trans R Soc Trop Med Hyg* **94 Suppl 1**: S1-90.

WHO (2005). World Malaria Report.

Wickert H, Gottler W, Krohne G and Lanzer M (2004). Maurer's cleft organization in the cytoplasm of *plasmodium falciparum*-infected erythrocytes: new insights from three-dimensional reconstruction of serial ultrathin sections. *Eur J Cell Biol* **83** (10): 567-82.

Wickert H, Wissing F, Andrews KT, Stich A, Krohne G and Lanzer M (2003). Evidence for trafficking of PfEMP1 to the surface of *P. falciparum*-infected erythrocytes via a complex membrane network. *Eur J Cell Biol* **82** (6): 271-84.

Wickham ME, Rug M, Ralph SA, Klonis N, McFadden GI, Tilley L and Cowman AF (2001). Trafficking and assembly of the cytoadherence complex in *Plasmodium falciparum*-infected human erythrocytes. *Embo J* **20** (20): 5636-49.

Wilkie GS, Dickson KS and Gray NK (2003). Regulation of mRNA translation by 5'- and 3'-UTR-binding factors. *Trends Biochem Sci* **28** (4): 182-8.

Winter G, Kawai S, Haeggstrom M, Kaneko O, von Euler A, Kawazu S, Palm D, Fernandez V and Wahlgren M (2005). SURFIN is a polymorphic antigen expressed on *Plasmodium falciparum* merozoites and infected erythrocytes. J Exp Med 201 (11): 1853-63.

6 SUPPLEMENTARY FIGURES

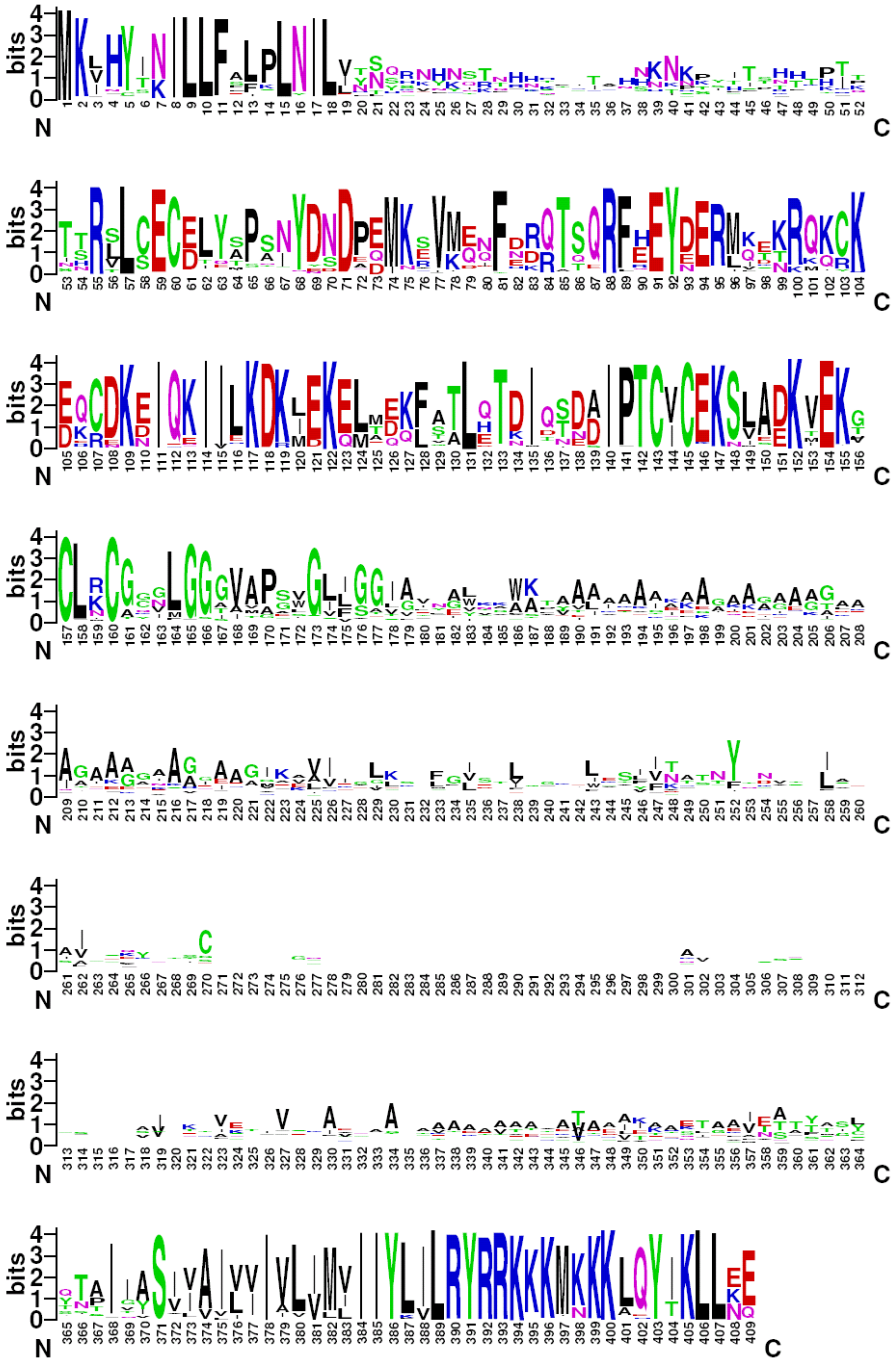

Supplementary Fig. S1 LOGOs of A- and B-type RIFINs
Graphical representation of amino acid frequencies at certain positions in the alignment of all RIFINs.

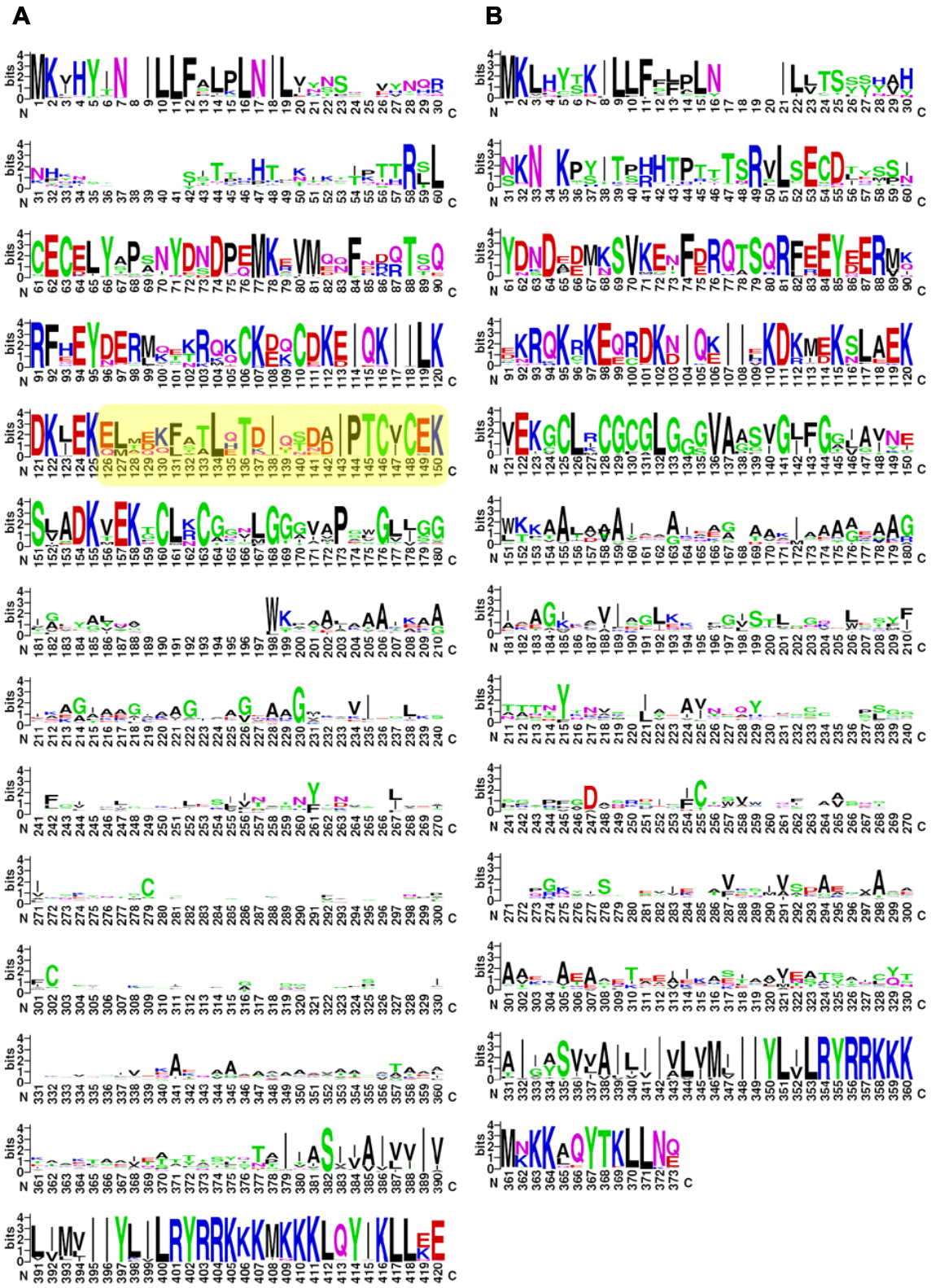

Supplementary Fig. S2 LOGOs of A- and B-type RIFINs
Graphical representation of amino acid frequencies at certain positions in the alignment of **A:** A- and **B:** B-type RIFINs. The yellow area labels the distinctive 25 amino acid peptide present only in A-type variants.

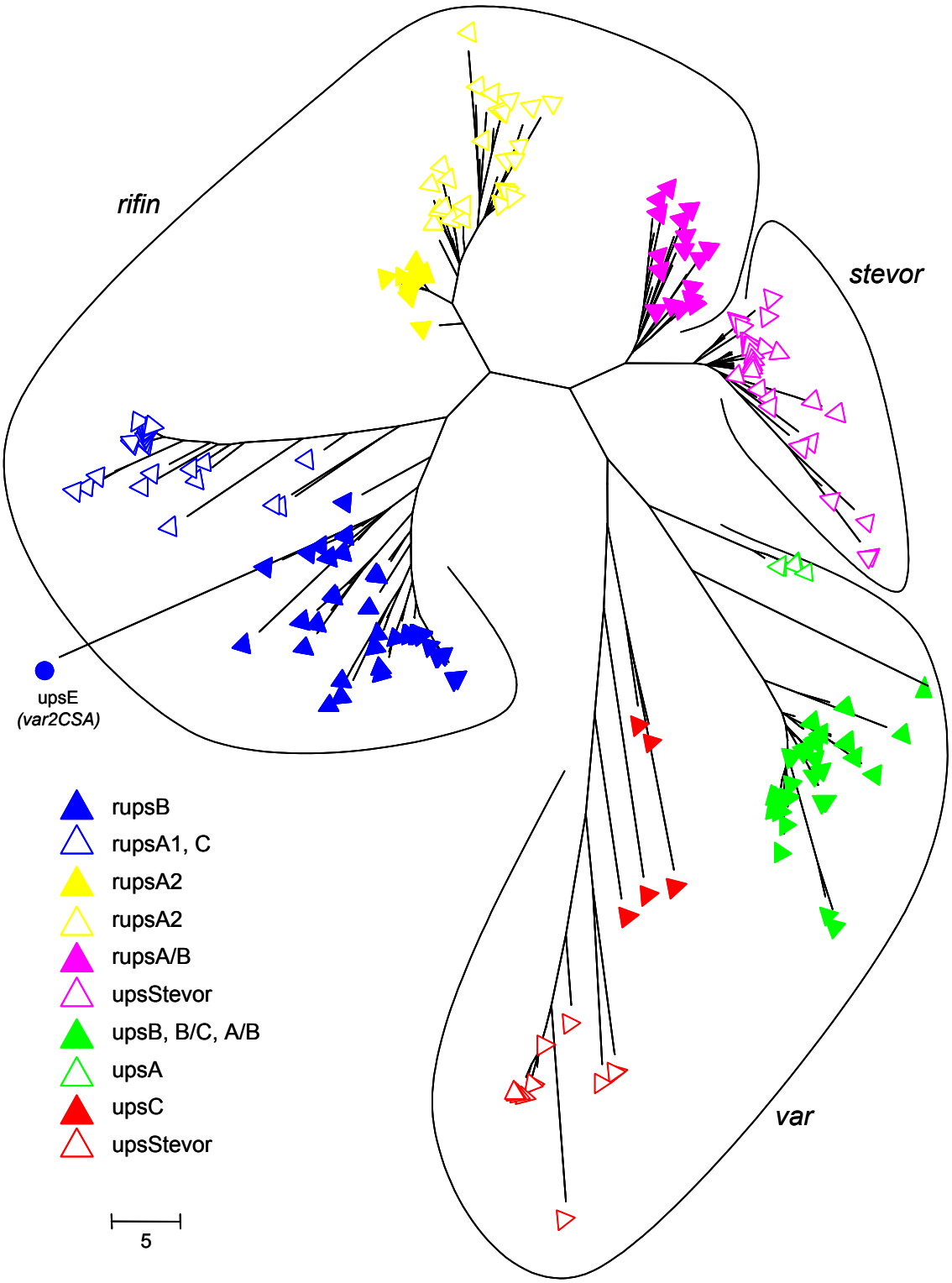

Supplementary Fig. S3 Distance tree of 5'-upstream regions of *rif*, *stevor* and *var* genes
Sequences 1000 bp upstream of the *rif*, *stevor* and *var* genes were analyzed with the p-distance/Neighbor-Joining method.

ACKNOWLEDGEMENTS

I want to express my deepest gratitude to the many people who have in one or the other way significantly contributed to this thesis: Thank you!

In particular, I would like to acknowledge

Mo-Quen Klinkert for introducing me to this interesting research topic, for supervision of my work, for her support and encouragement and her faith in my ideas.

Iris Bruchhaus for introducing me to Northern blotting and for evaluating my thesis.

All past and present colleagues in the lab, especially:
Insa Bonow for helping out with a lot of experiments and for her mental support.
Ayman Khattab and Yu-Shan Chia for many interesting discussions on science and beyond.
Nadine Schreiber for a brilliant teamwork in spell-checking manuscripts and theses.

Kathrin Schuldt and Claudia Esser for last-minute proof reading and substantially helping to clear my mind over cryptic results.

Mats Wahlgren for providing antisera and for giving me the opportunity to go to Uganda.
Malin Haeggström for the productive collaboration on merozoites.
Nicolas Joannin for pointing out „the gap“, and many inspiring discussions.

T.W. Gilberger, K. Lingelbach, C. Braun-Breton, A.A. Holder, A.W. Thomas, P. Alano, G. Pradel and A. Saul for providing antisera.

Christel Schmetz for performing the electron microscopy.

The “Vereinigung der Freunde des Tropeninstitutes“ and Prof. Rolf D. Horstmann for their financial support.

The Party Team and all other friends from BNI and abroad.

My family, and especially my mother: for boundless assistance and the freedom to realize my ideas and dreams.

Last but not least a very big thank you goes to Lars Tögel, for all his love and encouragement, for his patience with me - and for being the music in my life.

The linguistic correctness of the present work was verified by Dr. Rebecca Stanway.

Dr. Rebecca Stanway
Bernhard-Nocht-Institute for Tropical Medicine
Bernhard-Nocht-Str. 74
20359 Hamburg